UNIVERSITAT POLITÈCNICA DE VALÈNCIA

ETS INGENIEROS DE CAMINOS, CANALES Y PUERTOS

TRABAJO DE FIN DE MASTER

A proposal of design fire curves for I-girder bridges. Application to an overpass on U.S. Route 1 in Trenton, New Jersey, USA.

Presentado por

Howard, Jethro David

Para la obtención del

Master en Ingeniería de Caminos, Canales y Puertos

Curso: *2018/2019*

Fecha: *4 de septiembre de 2019*

Tutor: *Payá Zaforteza, Ignacio Javier*

Cotutor: *Peris Sayol, Guillem*

GENERAL INDEX

DOCUMENT No. 1:
REPORT

Titulación: Máster en Ingeniería de Caminos, Canales y Puertos
Autor: Jethro David Howard
Tutor: Payá Zaforteza, Ignacio Javier
Cotutor: Guillem Peris Sayol
Curso: 2018/2019
Fecha: 04 de septiembre de 2019

INDEX

LIST OF TABLES

LIST OF FIGURES

1. INTRODUCTION

The importance of bridges within national transportation systems is unquantifiable, given the socioeconomical impact that just one single structure can have on its surrounding area. As such, a bridges design is heavily regulated by codes that define the loads that should be considered to guarantee the long-term integrity of these critical structures. These loads aren't limited to everyday occurrences, such as traffic or wind loads, but also contemplate the inclusion of extraordinary events, such as earthquakes, vehicle impacts, flooding, explosions or fires.

Whilst some extraordinary actions have been widely researched and included in design codes, such as earthquakes, others like fires have been practically ignored, even though there are numerous examples of the importance of bridge fires.

One of the major obstacles in developing a specific code for bridge fires is the complexity of the numerical models involved in analysing and obtaining the adiabatic temperatures a bridge is exposed to during a fire.

Through the analysis of the influence of different parameters on the temperatures reached by a bridge's superstructure, such as a bridges vertical clearance, width, span or substructure configuration, or the fires location and magnitude, the following report develops a proposal of design fire curves, based on the statistical analysis of each parameters significance on adiabatic temperatures.

These design fire curves are then validated by comparing the structural response of a bridge on U.S. Route 1, in Trenton, New Jersey, USA using the temperatures obtained in an FDS analysis and the temperatures predicted using the fire curves.

2. OBJECTIVE AND SCOPE

The main objective of the present project is the development of design fire curves capable of predicting the adiabatic temperatures which a bridge is subjected to, based on independent parameters that depend on the bridge's geometry (vertical clearance, width, span or substructure configuration) and the fire scenario (location and magnitude).

The design fire curves will be developed following an initial analysis of the influence of these independent parameters, based on the results of sixty-four FDS analyses for an orthogonal array of bridge configurations.

Once the significant parameters have been identified, multiple linear regression techniques will be employed to find the best fit equation for adiabatic temperatures, for each of the relative positions of a bridge's superstructure. When these equations for individual positions are represented together, they represent the proposal of design fire curves.

In order to validate the design fire curves obtained, they will be applied to an existing bridge on U.S. Route 1, in Trenton, New Jersey, U.S.A., comparing the adiabatic temperatures obtained with those measured in the corresponding FDS models developed for the present case study.

3. METHODOLOGY

This section will offer an overview of the proposed methodology for the development of design fire curves for I-girder bridges. This process can be divided into the following parts:

- The initial experiment design, including an evaluation of the parameters to be studied and the total number of configurations needed in order to guarantee the statistical significance of any observed effects.
- The definition of the Fire Dynamics Simulator (FDS) models needed to perform the computational fluid dynamics simulations and obtain the adiabatic temperatures of the gasses in contact with the I-girders for each configuration.
- A description of the statistical analysis carried out to determine the significance of each parameter on the adiabatic temperatures (Analysis of Variance, ANOVA), and the statistical technique used to obtain a predictive model of adiabatic temperatures based on the significant parameters (multiple linear regression). The combination of different models for various points along the bridges span will provide the design fire curves.
- Finally, these design fire curves will be contrasted using a case study of a bridge located on U.S. Route 1 in Trenton, New Jersey, USA, comparing the thermomechanical response of the bridge when subjected to the temperatures provided by a FDS analysis and those predicted by the fire design curves.

3.1. EXPERIMENT DESIGN AND PARAMETER DEFINITION

The number of parameters to be studied as a fundamental impact on the experiment design, as it determines the number of different configurations required in order to guarantee the statistical significance of the results.

The current report will analyse the influence of six parameters, four relating to the bridges geometry (bridge substructure configuration, width, span and vertical clearance) and two related to the design fire (fire position and heat release rate), to determine their effect on the adiabatic temperatures (both maximum temperatures and longitudinal temperatures along the whole span) of the central beam of I-girder bridges, based on the methodology of Peris-Sayol et al. [1].

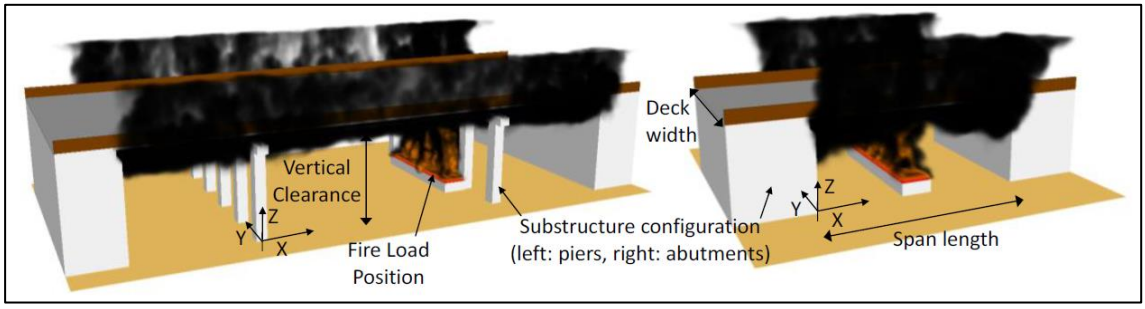

Figure 1. Graphical definition of the model parameters. Source: Peris-Sayol et al. [1]

Other parameters such as the production of smoke (soot), the production of carbon monoxide (CO yield), the position and number of cross beams/diaphragms and the separation between the main I-girders have not been analysed in order to reduce the total number of configurations to be simulated, as stated in Peris-Sayol et al. [1].

The experiment will be configured using a standard 2^k factorial design, where each of the six parameters has two levels, allowing their impact on the dependant variable, in this case adiabatic temperatures, to be assessed. **Error! Reference source not found.** defines the levels for each parameter considered for the current report (the lower level of vertical clearance has been reduced from six metres, proposed in Peris-Sayol et al. [1], to five metres, taking into account the minimum vertical clearance set by the Federal Highway Administration, of between 4.3 and 4.9 metres [X - https://www.dot.state.al.us/dsweb/pdf/A%20Policy%20on%20Design%20Standards%20-%20Interstate%20System%20May%202016.pdf]).

Level	Position	Bridge Substructure Configuration	Width	Span	Vertical Clearance	Heat Release Rate (HRR)
–	Mid-Span	Piers	13 m	16 m	5 m	1800 kW/m²
+	Abutment	Abutments	23.4 m	24 m	9 m	2400 kW/m²

Table 1. Definition of parameter levels.

When dealing with 2^k factorial designs with a high number of factors (generally six or more), the total number of configurations needed to cover all possible parameter combinations is very high (six factors, 2^6=64 configurations; eight factors, 2^8=256 configurations; etc.), and often it is not practical or possible to carry out so many experiments.

In these cases, it is common to perform fractional factorial designs (2^{k-1}, …, 2^{k-p}), reducing the total number of configurations needed, such as the one proposed in Peris-Sayol et al. [1]. The total number of configurations needed for six parameters were reduced from sixty-four

(corresponding to a standard 2^k factorial design, $2^6 = 64$ configurations) to thirty-two thanks to the use of a fractional factorial design ($2^{6-1} = 32$ configurations).

For this report, in order to allow the development of individual fire curves based on fire position, either adjacent to abutment/piers or located mid-span, a fractional factorial design cannot be used, due to an insufficient number of degrees of freedom for the corresponding Analysis of Variance, as explained in *Section 5. Statistical analysis of the influence of different parameters on the adiabatic temperatures generated in I-girder bridge fires.*

Therefore, following a standard 2^k factorial experimental design, the sixty-four scenarios proposed for the following report are defined in Table 2 and Table 3.

Model	Position	Bridge Substructure Config.	Width	Span	Vertical Clearance	Heat Release Rate (HRR)
1	Abutment	Piers	23.4 m	24 m	5 m	2400 kW/m2
2	Abutment	Piers	23.4 m	24 m	5 m	1800 kW/m2
3	Mid-Span	Piers	23.4 m	24 m	5 m	2400 kW/m2
4	Mid-Span	Piers	23.4 m	24 m	5 m	1800 kW/m2
5	Abutment	Piers	23.4 m	24 m	9 m	2400 kW/m2
6	Abutment	Piers	23.4 m	24 m	9 m	1800 kW/m2
7	Mid-Span	Piers	23.4 m	24 m	9 m	2400 kW/m2
8	Mid-Span	Piers	23.4 m	24 m	9 m	1800 kW/m2
9	Abutment	Piers	23.4 m	16 m	5 m	2400 kW/m2
10	Abutment	Piers	23.4 m	16 m	5 m	1800 kW/m2
11	Mid-Span	Piers	23.4 m	16 m	5 m	2400 kW/m2
12	Mid-Span	Piers	23.4 m	16 m	5 m	1800 kW/m2
13	Abutment	Piers	23.4 m	16 m	9 m	2400 kW/m2
14	Abutment	Piers	23.4 m	16 m	9 m	1800 kW/m2
15	Mid-Span	Piers	23.4 m	16 m	9 m	2400 kW/m2
16	Mid-Span	Piers	23.4 m	16 m	9 m	1800 kW/m2
17	Abutment	Piers	13.0 m	24 m	5 m	2400 kW/m2
18	Abutment	Piers	13.0 m	24 m	5 m	1800 kW/m2
19	Mid-Span	Piers	13.0 m	24 m	5 m	2400 kW/m2
20	Mid-Span	Piers	13.0 m	24 m	5 m	1800 kW/m2
21	Abutment	Piers	13.0 m	24 m	9 m	2400 kW/m2
22	Abutment	Piers	13.0 m	24 m	9 m	1800 kW/m2
23	Mid-Span	Piers	13.0 m	24 m	9 m	2400 kW/m2
24	Mid-Span	Piers	13.0 m	24 m	9 m	1800 kW/m2
25	Abutment	Piers	13.0 m	16 m	5 m	2400 kW/m2
26	Abutment	Piers	13.0 m	16 m	5 m	1800 kW/m2
27	Mid-Span	Piers	13.0 m	16 m	5 m	2400 kW/m2
28	Mid-Span	Piers	13.0 m	16 m	5 m	1800 kW/m2
29	Abutment	Piers	13.0 m	16 m	9 m	2400 kW/m2
30	Abutment	Piers	13.0 m	16 m	9 m	1800 kW/m2

31	Mid-Span	Piers	13.0 m	16 m	9 m	2400 kW/m2
32	Mid-Span	Piers	13.0 m	16 m	9 m	1800 kW/m2

Table 2. Models 1-32 of the proposed experimental design.

Model	Position	Bridge Substructure Config.	Width	Span	Vertical Clearance	Heat Release Rate (HRR)
33	Abutment	Abutments	23.4 m	24 m	5 m	2400 kW/m2
34	Abutment	Abutments	23.4 m	24 m	5 m	1800 kW/m2
35	Mid-Span	Abutments	23.4 m	24 m	5 m	2400 kW/m2
36	Mid-Span	Abutments	23.4 m	24 m	5 m	1800 kW/m2
37	Abutment	Abutments	23.4 m	24 m	9 m	2400 kW/m2
38	Abutment	Abutments	23.4 m	24 m	9 m	1800 kW/m2
39	Mid-Span	Abutments	23.4 m	24 m	9 m	2400 kW/m2
40	Mid-Span	Abutments	23.4 m	24 m	9 m	1800 kW/m2
41	Abutment	Abutments	23.4 m	16 m	5 m	2400 kW/m2
42	Abutment	Abutments	23.4 m	16 m	5 m	1800 kW/m2
43	Mid-Span	Abutments	23.4 m	16 m	5 m	2400 kW/m2
44	Mid-Span	Abutments	23.4 m	16 m	5 m	1800 kW/m2
45	Abutment	Abutments	23.4 m	16 m	9 m	2400 kW/m2
46	Abutment	Abutments	23.4 m	16 m	9 m	1800 kW/m2
47	Mid-Span	Abutments	23.4 m	16 m	9 m	2400 kW/m2
48	Mid-Span	Abutments	23.4 m	16 m	9 m	1800 kW/m2
49	Abutment	Abutments	13.0 m	24 m	5 m	2400 kW/m2
50	Abutment	Abutments	13.0 m	24 m	5 m	1800 kW/m2
51	Mid-Span	Abutments	13.0 m	24 m	5 m	2400 kW/m2
52	Mid-Span	Abutments	13.0 m	24 m	5 m	1800 kW/m2
53	Abutment	Abutments	13.0 m	24 m	9 m	2400 kW/m2
54	Abutment	Abutments	13.0 m	24 m	9 m	1800 kW/m2
55	Mid-Span	Abutments	13.0 m	24 m	9 m	2400 kW/m2
56	Mid-Span	Abutments	13.0 m	24 m	9 m	1800 kW/m2
57	Abutment	Abutments	13.0 m	16 m	5 m	2400 kW/m2
58	Abutment	Abutments	13.0 m	16 m	5 m	1800 kW/m2
59	Mid-Span	Abutments	13.0 m	16 m	5 m	2400 kW/m2
60	Mid-Span	Abutments	13.0 m	16 m	5 m	1800 kW/m2
61	Abutment	Abutments	13.0 m	16 m	9 m	2400 kW/m2
62	Abutment	Abutments	13.0 m	16 m	9 m	1800 kW/m2
63	Mid-Span	Abutments	13.0 m	16 m	9 m	2400 kW/m2
64	Mid-Span	Abutments	13.0 m	16 m	9 m	1800 kW/m2

Table 3. Models 33-64 of the proposed experimental design.

3.2. FDS ANALYSIS

In order to obtain the adiabatic temperatures reached for each of the sixty-four scenarios defined in Table 2 and Table 3, an equal number of models must be setup and run using the Fire

Dynamics Simulator (FDS, version 6.6.0), which applies computational fluid dynamics (CFD) techniques to fire engineering.

According to Peris-Sayol et al. [1], the following must be defined for each FDS model:

- a control volume (with its corresponding boundary conditions).
- the geometrical definition of a bridge for the corresponding scenario.
- a mesh or discretization of the control volume.
- the material properties (in the case of non-adiabatic surfaces).
- the fire source or sources.
- a combustion model.
- sensors or other elements capable of recording the model's outputs (adiabatic temperatures).

The definition of each of these properties is explained in detail in *Section 4.2. FDS Models* of this report, as well as the software and calculation cluster used to run the FDS models.

The FDS analysis of each model provides the adiabatic temperatures recorded by the sensors placed by the centre of the bottom flange and on either side of the web, which after being processed (removing the fire growth stage, calculating the average temperature for the web, etc.), provide a longitudinal fire curve (of adiabatic temperatures) of the central I-girder, for both the bottom flange and web.

3.3. STATISTICAL ANALYSIS

The adiabatic temperature curves obtained for each of the sixty-four configurations, for both the bottom flange and web, are analysed using ANOVA tests to determine the significance of each of the six parameters (fire position, bridge substructure configuration, width, span, vertical clearance and HRR), as well as their second order interactions.

Numerous ANOVA tests have been carried out, based on the adiabatic temperature analysed (maximum or by position) and the model subset considered (global analysis of all models or individual analyses for each fire position). A summary of the analyses performed is shown in

Table 4 (the number of ANOVA tests includes those carried out for both the bottom flange and the web)

ADIABATIC TEMPERATURES	MODELS SUBSET	No. ANOVA
Maximum	Global analysis (all models)	2
Maximum	Fire position located adjacent to abutm./piers	2
Maximum	Fire position located mid-span	2
By position (X/L)	Global analysis (all models)	22
By position (X/L)	Fire position located adjacent to abutm./piers	22
By position (X/L)	Fire position located mid-span	22

Table 4. Summary of statistical analyses performed.

The parameters and interactions which are found to be statistically significant for each of the ANOVA tests are used in the corresponding multiple linear regression models, with the objective of obtaining an expression capable of predicting the adiabatic temperatures for each individual analysis.

Peris-Sayol et al. [1] concludes that there is a linear relation between a bridges vertical clearance and the superstructures adiabatic temperatures, and based on the results of the following report, the same can be said for the HRR, and therefore both can be estimated using linear regression models. Whilst both the bridges width and spans relation with the superstructures adiabatic temperatures is unclear (linear or non-linear), their effect on the latter is significantly smaller than the rest of parameters.

In the case of fire position and bridge substructure configuration, which are categorical parameters (they only have two configurations, the parameters aren't continuous like the case of vertical clearance, HRR, span and width) both can be estimated using linear regression models, by determining the average effect between each of the parameters two levels (as the levels are considered to have values of either 0 or 1, known as "dummy variables", the effect can be quantified in the model).

The accuracy of each regression model is verified using the coefficient of determination (R^2), which indicates the proportion of the dependent variable (adiabatic temperatures) that is predictable from the independent parameters (and interactions), and by plotting the observed and predicted temperatures in order to graphically check if the model can be considered a "good fit".

In order to simplify the regression prediction models, an iterative calculation contrasting the of number of parameters and interactions versus the coefficient of determination (R^2) for each calculation is carried out. Where parameters or interactions are identified that have little effect on the overall coefficient of determination, they are removed from that predictive regression model, even if found to have been to be "significant" in the corresponding ANOVA test.

The final result is a series of predictive formulas for the maximum or by position adiabatic temperatures, that in the case of the latter, when plotted together, leads to the representation of a design fire curve, for either the bottom flange or web, and for any of the scenarios considered: global analysis or individual fire position analyses.

3.3.1. STATGRAPHICS

Although *Section 5.1.1 anova example* includes a manual calculation of a three parameter ANOVA test, in order to understand the concept behind this statistical technique, due to the size of the configurations that need to be analysed (either sixty-four or thirty-two models, corresponding with six or five independent parameters respectively), it is impractical to perform ANOVA tests using manual calculations or spreadsheets for all analyses.

Therefore, the ANOVA tests have be performed using the program Statgraphics Centurion 18 (licensed to the *Universitat Politècnica de València* for academic uses), which is capable of carrying multifactorial ANOVA tests, and iterative multiple linear regression calculations.

3.4. THERMOMECHANICAL ANALYSIS

In order to validate the design fire curves obtained from the statistical analysis, *Section 7* compares the thermomechanical response of an overpass on US Route 1 in Trenton, New Jersey, U.S.A. for the adiabatic temperatures obtained from a FDS analysis and those predicted by the design fire curves.

The thermomechanical response of the bridge is obtained with SAFIR, version 2019.a.2, a computer program specifically written for modelling the behaviour of structures subjected to fire, for which the *Instituto de Ciencia y Tecnología del Hormigón (ICITECH)* of the *Universitat Politècnica de València* has a license.

Developed using the FORTRAN programming language, the software allows both two and three-dimensional models, using the finite element method (FEM) to find approximate solutions for very complex partial differential equations.

The response is calculated in two steps: the first, performs the heat transfer analysis, using the adiabatic temperatures from either the FDS model or the fire design curves, to obtain the temperature evolution of the I-girder beam taking into account the materials thermal conductivity properties; the second, uses the results of the heat transfer analysis to perform an iterative mechanical analysis, using the modified material properties for each time step corresponding with the calculated temperatures.

4. FDS ANALYSIS

4.1. DESCRIPTION

The adiabatic temperatures reached for each of the sixty-four scenarios defined in Table 2 and Table 3 have been calculated using the Fire Dynamics Simulator (FDS) computer program, version 6.6.0, developed by the *Building and Fire Research Laboratory del National Institute of Standards and Technology – NIST (USA)*, which uses specific computational fluid mechanics (CFD) techniques to perform fire simulations, and has undergone an extensive validation program (FDS Validation Guide [2]). Applying FDS to study bridge fires has been validated by Alos-Moya et al. [3] using FDS and Abaqus to analyse an overpass failure caused by a tanker fire.

It works by numerically solving, for a pre-defined meshed control volume, a large eddy simulation (LES) form of the Navier-Stokes equations appropriate for low-speed, thermally-driven flow, with an emphasis on smoke and heat transport from fires, to describe the evolution of fire.

4.2. FDS MODELS

As described in section 3.2, the following must be defined for each FDS model: a control volume (with its corresponding boundary conditions); the geometrical definition of a bridge for the corresponding scenario; a mesh or discretization of the control volume; the material properties (in the case of non-adiabatic surfaces); the fire source (or sources); a combustion model and sensors or other elements capable of recording the model's outputs (adiabatic temperatures).

4.2.1. CONTROL VOLUME, MESH AND GEOMETRY

As described by Peris-Sayol et al. [1], the control volume used for the FDS models is larger than the bridges geometry, as it includes part the approaches on either side. Its length measured along the x-axis (parallel to the I-girders) varies between 34 and 58 metres depending on the span length and configuration (central span with piers of individual span with abutments), whilst its width measured long the y-axis (perpendicular to the I-girders) varies between 30 and 46

metres, depending on the width of the bridge. The z-axis varies between 12 and 18 metres, depending on the vertical clearance considered.

The size of the hexahedral cells has been determined in accordance with the characteristic fire diameter (D*), based on reference technical specifications for the correct resolution of the fire zone (in the vicinity of the fire source). This zone, as indicated in the *"Fire Dynamics Simulator: User's Guide"*, is the most critical part when determining the model discretization:

> *"For simulations involving buoyant plumes, a measure of how well the flow field is resolved is given by the non-dimensional expression* D^*/δ_x*, where D* is a characteristic fire diameter:*
>
> $$D^* = \left(\frac{\dot{Q}}{\rho_\infty c_p T_\infty \sqrt{g}}\right)^{\frac{2}{5}}$$
>
> *And δx is the nominal size of a mesh cell. The quantity* D^*/δ_x *can be thought of as the number of computational cells spanning the characteristic (not necessarily the physical) diameter of the fire. The more cells spanning the fire, the better the resolution of the calculation. It is better to assess the quality of the mesh in terms of this non-dimensional parameter, rather than an absolute mesh cell size. For example, a cell size of 10 cm may be "adequate," in some sense, for evaluating the spread of smoke and heat through a building from a sizable fire, but may not be appropriate to study a very small, smoldering source. "*

In

Input			Output		
Q	59000	kW	**D***	4.90	m
ρ	1.2	kg/m3	**Size**	0.25	m
c_p	1.005	kJ/kgK			
T	20	ºC			
Mesh size	Fine	-			
D^*/δ_x	20	-			
g	9.81	m/s2			

Table 5, the calculations for determining the cell discretization size are shown:

Input			Output		
Q	59000	kW	**D***	4.90	m
ρ	1.2	kg/m3	**Size**	0.25	m
c_p	1.005	kJ/kgK			
T	20	ºC			

Mesh size	Fine	-
D*/δ_x	20	-
g	9.81	m/s2

Table 5. Discretization calculations

For the two types of fire scenario considered, with fire heat release rates of between 51.8 and 69 MW (1800 kW/m^2 and 2400 kW/m^2 respectively), and considering a fine mesh, by using a D^*/δ_x of 20, the cell size selected is of 0.2 metres (below the limit calculated in Table 5), and is coherent with the software verification and validation [2], as is considered adequate for the evaluation of sustainability conditions in the vicinity of the bridge.

The FDS models are therefore discretized into hexahedral cells (see Figure 2), with dimensions of 0.20 m x 0.20 m x 0.20 m, meaning that the total number of cells range from 1,260,000 to 6,003,000 depending on the model considered.

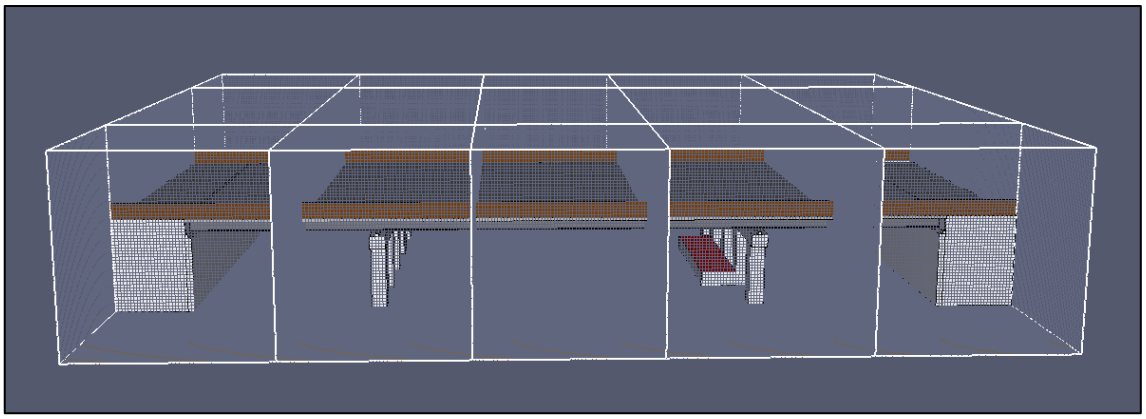

Figure 2. Cell discretization of FDS model 1.

The models control volume has been divided into smaller rectilinear volumes called meshes, which each contain cells with the same dimensions, in order to permit the parallel calculation on various CPU and therefore reduce calculation time (see Figure 3).

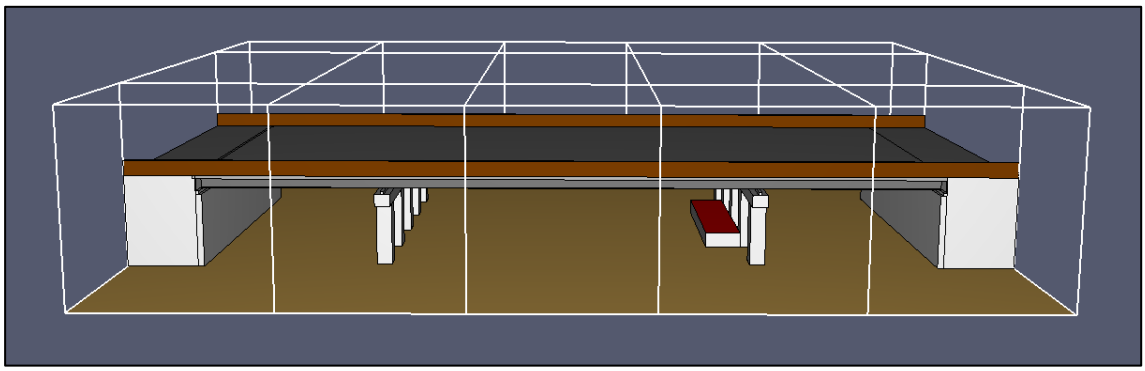

Figure 3. Mesh discretization of FDS model 1.

The discretization of the control volume into smaller meshes has been carried out respecting that the fire has to be contained into a single mesh and sufficiently far away from the meshes boundaries, in order to avoid numerical calculation problems.

4.2.2. FIRE SCENARIO

Each FDS model includes an area equivalent to a tanker trucks cistern, which has been modelled as a 28.8 m^2 horizontal surface (12 x 2.4 m) one metre above road level, in the models corresponding fire position (adjacent to an abutment/piers or located mid-span).

As stated in Peris-Sayol et al. [1], the carbon monoxide (CO) and soot yields have been set according to recommendations of the SPFE Handbook manual for hydrocarbon liquids and have values of 0.019 and 0.059 respectively.

4.2.3. BOUNDARY CONDITIONS AND MATERIAL PROPERTIES

There are two main types of boundary conditions in the FDS models: the adiabatic surfaces, such as the bridges superstructure (I-girders, diaphragms, etc.) and deck; and the nonadiabatic surfaces, as in the case of the abutments and/or piers.

The adiabatic surface temperatures (developed by Wickström et al. [4]) are a fictitious temperature obtained by FDS considering that the structural element is a perfect insulator, and is used to transfer the information calculated by the fire model to the thermal model, for both convective and radiative heat transfer. Essentially, it means the temperature is not influenced by the material of the bridges substructure and can therefore be used as the input for a thermomechanical analysis.

By defining adiabatic surfaces for the bridge superstructure, the temperatures obtained in the FDS analyses are independent of the type of superstructure analysed (steel, concrete, composite, etc.), and therefore, they can be used to perform a thermomechanical analysis of a bridges superstructure, for both steel or concrete girders (or other material types).

In the case of the nonadiabatic surfaces, the materials are defined within the FDS model, and therefore these surfaces "absorb" part of the heat emitted by the fire source. The reason for including these nonadiabatic surfaces in the analysis is so that the adiabatic temperatures obtained in the model for the bridge girders/beams take into account the influence of the bridge substructures (abutments and/or piers), as these are not included in the thermomechanical analysis.

4.2.4. OUTPUT

In order to obtain the results of the adiabatic temperatures along the central I-girder, for both the bottom flange and either side of the web (see Figure 4), the user has to define a series of sensors. These sensors have been placed in the FDS models with a separation of 20 cm, as shown in Figure 5.

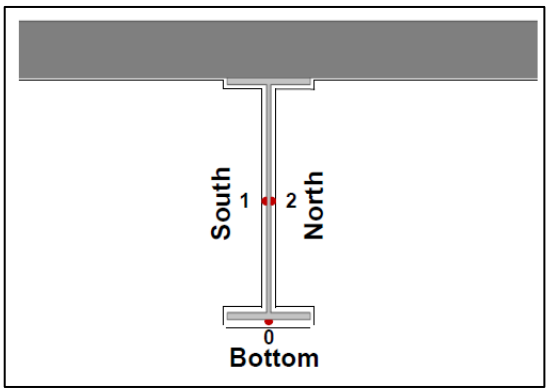

Figure 4. Cross section sensor placement in the FDS models to monitor adiabatic temperatures. Source: Peris-Sayol et al. [1]

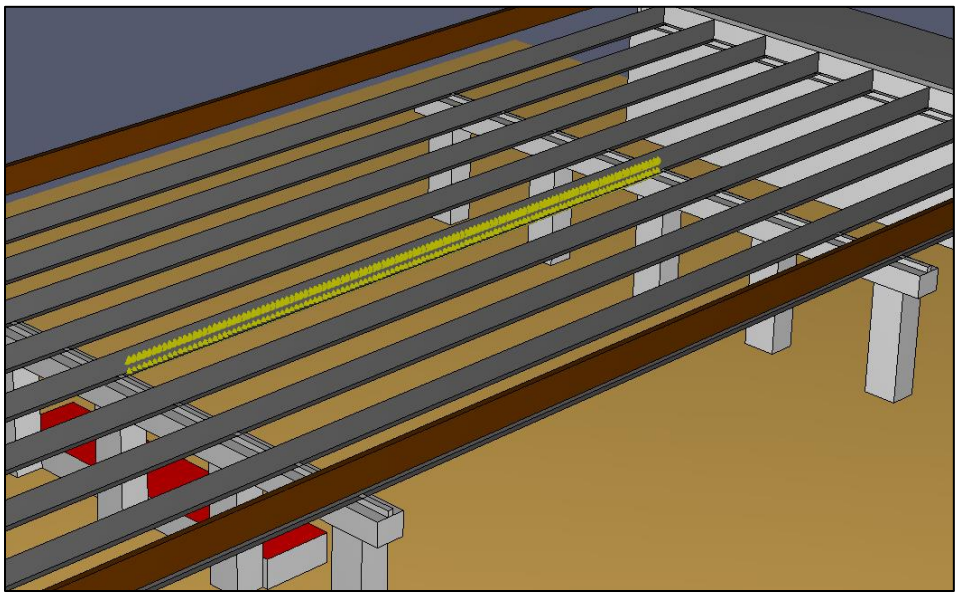

Figure 5. Longitudinal sensor placement in the FDS models to monitor adiabatic temperatures

4.3. FDS CALCULATIONS

All the FDS models were run using version 6.6.0, as an MPI parallel job on a the *Universitat Politècnica de València (UPV)* calculation cluster, Rigel. Each model had between three and fifteen cores assigned for the calculations, with 8 GB of RAM per core. Total calculation times for each model varied between eight and thirty-two hours.

4.4. RESULTS

In order to obtain the temperatures for each of the sixty-four FDS models, it is necessary to process a Comma Separated Values file (.csv) provided as at the end of the FDS analyses.

These CSV files contain the temperatures registered by each of the sensors (bottom flange, left side of web and right side of web) located on the central I-girder (with a separation of 0.2 metres) for the duration of the simulation (approximately every 0.15 seconds, for a total of 150 seconds), resulting in a total of between 243243 and 363363 temperature readings for each model (depending on the span of each model, either 16 or 24 metres).

The average temperatures for each sensor are calculated without considering the first 30 seconds of data, due to this period being associated to the growth stage of the fire, as seen in Figure 6.

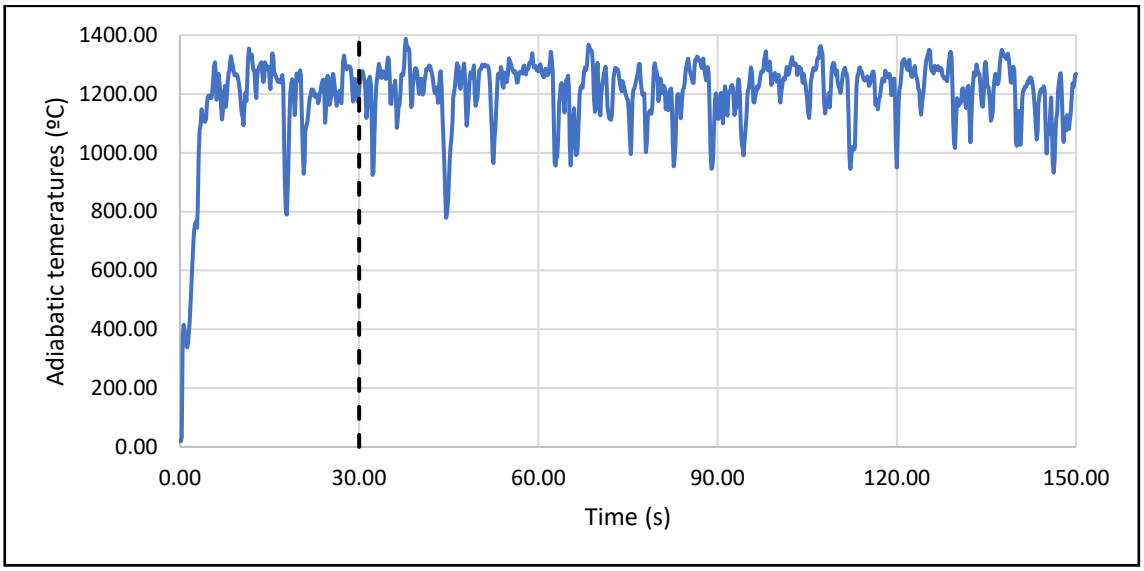

Figure 6. Adiabatic temperatures registered during the FDS analysis of model 3 at X/L=0.5.

The results of the average temperatures of each sensor for all of the 64 models can be found in *APPENDIX 1: FDS average temperatures*, in both tabular and graphical formats.

4.4.1. GRAPHICAL COMPARISON

The following pages contain a graphical comparison of various model pairings, with the objective of analysing the effect of each of the six parameters' (in the case of fire position, either mid-span or adjacent to an abutment, the effect is clear) influence on the temperatures measured along the central I-girder, both for the bottom flange and web.

This graphical analysis will provide an initial estimation of which parameters appear to be most significant in affecting the adiabatic temperatures a bridge is subjected to during a fire, although it is likely that more complicated two-way interactions between parameters are difficult to identify. Either way, these initial estimations will be subsequently contrasted with the results obtained from the statistical analysis.

i. Bridge substructure configuration

The following pairs of bridge configuration models share the same characteristics for each parameter (one pair, models 1 and 33, with the fire located adjacent to an abutment/pier, X/L=1; another pair , models 3 and 35, with the fire located mid-span, X/L=0.5), except for the nature of their substructure configurations, which are either piers or abutments.

Model	Position	Bridge Substructure Configuration	Width	Span	Vertical Clearance	Heat Release Rate (HRR)
1	Abutment	*Piers*	23.4 m	24 m	5 m	2400 kW/m²
33	Abutment	*Abutments*	23.4 m	24 m	5 m	2400 kW/m²
3	Mid-Span	*Piers*	23.4 m	24 m	5 m	2400 kW/m²
35	Mid-Span	*Abutments*	23.4 m	24 m	5 m	2400 kW/m²

Table 6. Bridge substructure configuration comparison 1 – model parameters

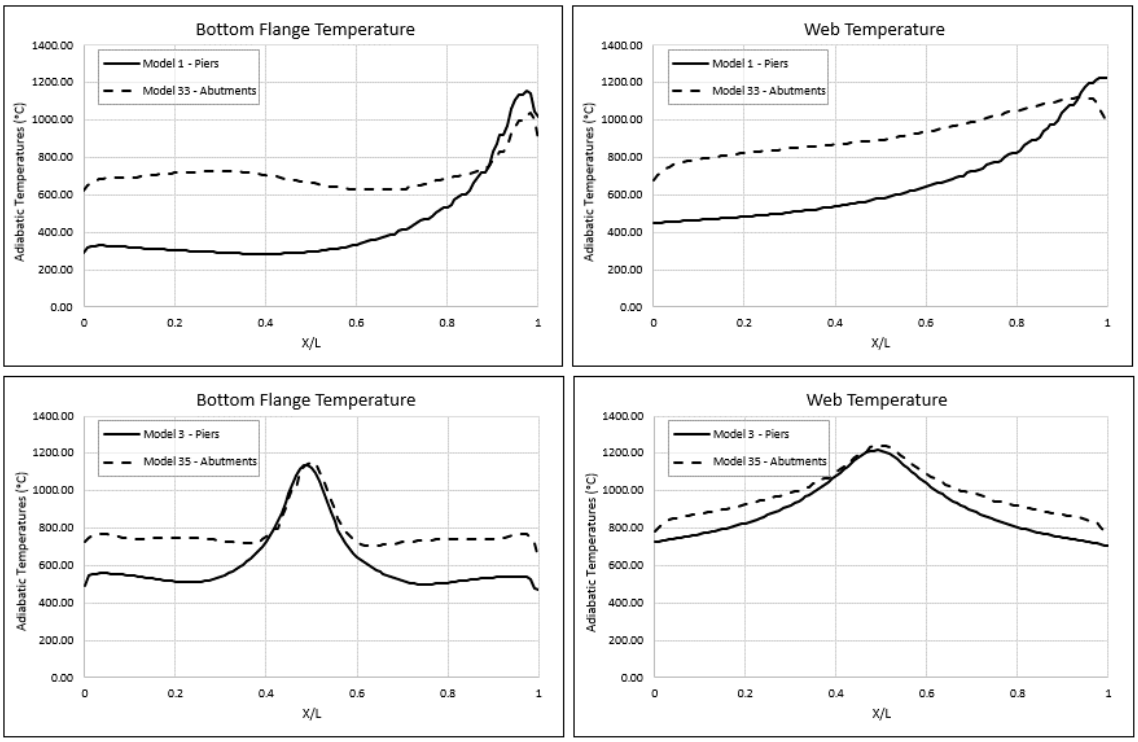

Figure 7. Bridge substructure configuration comparison 1

The most noticeable difference is that the models with abutments at each end of the span maintain higher temperatures compared with the models with piers the further we are from the source of the fire, with this being more pronounced for the bottom flange temperatures than the for the web temperatures. This is due to there being a larger body of air under the bridge for models with a central span with piers at either end, as well as the potential for greater entry of air, and therefore there is less build-up of heat and smoke under the superstructure.

Another phenomenon that can be observed is the slightly higher temperatures of models with piers when the fire is located adjacent to the bridge substructure, which seems counterintuitive considering the existence of the Coandă effect, which should have a bigger influence for the larger flat surface, as is the case of abutments in comparison to piers.

The reason higher temperatures are achieved in the models with piers in these positions is due to the fact that the bridge substructures (either piers or abutments), in contrast to the bridge superstructure, have been modelled as non-adiabatic surfaces, meaning that they absorb part of the heat produced by the fire. It stands to reason that as abutments present a much larger surface compared to piers that they would absorb more heat, and therefore reduce the temperatures in their proximity.

The following pairs are similar to the two analysed above, but in the case for bridges with a smaller width and span, and a larger vertical clearance.

Model	Position	Bridge Substructure Configuration	Width	Span	Vertical Clearance	Heat Release Rate (HRR)
29	Abutment	*Piers*	13.0 m	16 m	9 m	2400 kW/m²
61	Abutment	*Abutments*	13.0 m	16 m	9 m	2400 kW/m²
31	Mid-Span	*Piers*	13.0 m	16 m	9 m	2400 kW/m²
63	Mid-Span	*Abutments*	13.0 m	16 m	9 m	2400 kW/m²

Table 7. Bridge substructure configuration comparison 2 – model parameters

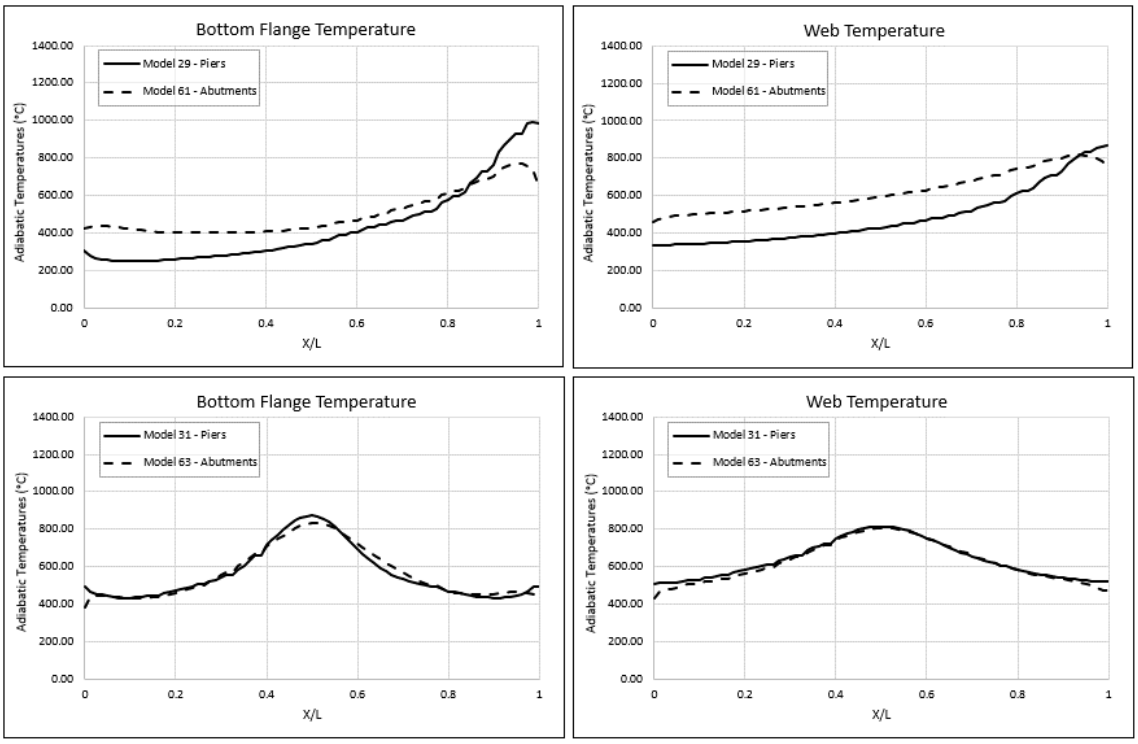

Figure 8. Bridge substructure configuration comparison 2

The differences in temperatures between the models in each pair are significantly smaller than those analysed before, especially in the case of models 31 and 63, where the temperatures are practically identical along the whole of the span. In this case, the smaller body of air under the

bridge due to the reduced span, as well as the diminished potential for entry of air, cause a larger build-up of heat and smoke under the superstructure compared to bridges with larger spans.

These models show that, although it is clear that bridge substructure configurations (abutments or piers) have an effect on the adiabatic temperatures, it is not always a straight-forward affair, as their influence can be amplified or nullified by other parameters, suggesting there are multiparameter interactions at play.

ii. Width

As before, the following pairs of bridge configuration models share the same characteristics for each parameter, except for the bridges' total width (in this case, considering piers at each end).

Model	Position	Bridge Substructure Configuration	Width	Span	Vertical Clearance	Heat Release Rate (HRR)
1	Abutment	Piers	*23.4 m*	24 m	5 m	2400 kW/m²
17	Abutment	Piers	*13.0 m*	24 m	5 m	2400 kW/m²
3	Mid-Span	Piers	*23.4 m*	24 m	5 m	2400 kW/m²
19	Mid-Span	Piers	*13.0 m*	24 m	5 m	2400 kW/m²

Table 8. Width comparison 1 – model parameters

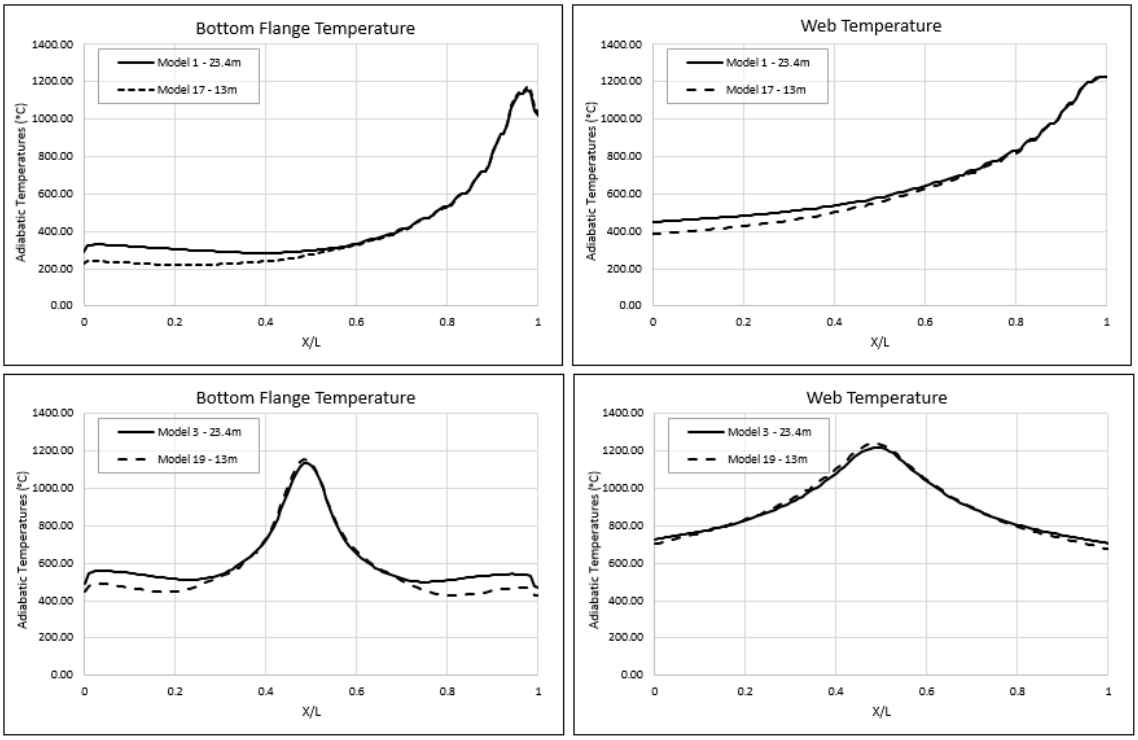

Figure 9. Width comparison 1

In this case, the adiabatic temperatures furthest from the fire source are slightly higher for the models with a bigger width, but it appears to have no effect on the maximum temperatures registered in the vicinity of the fire. Either way, it seems to be less significant than the differences observed when comparing bridge substructure configurations.

The following pairs are similar to the two analysed above, but in the case for bridges with abutments at each end of the span.

Model	Position	Bridge Substructure Configuration	Width	Span	Vertical Clearance	Heat Release Rate (HRR)
33	Abutment	Abutments	*23.4 m*	24 m	5 m	2400 kW/m²
49	Abutment	Abutments	*13.0 m*	24 m	5 m	2400 kW/m²
35	Mid-Span	Abutments	*23.4 m*	24 m	5 m	2400 kW/m²
51	Mid-Span	Abutments	*13.0 m*	24 m	5 m	2400 kW/m²

Table 9. Width comparison 2 – model parameters

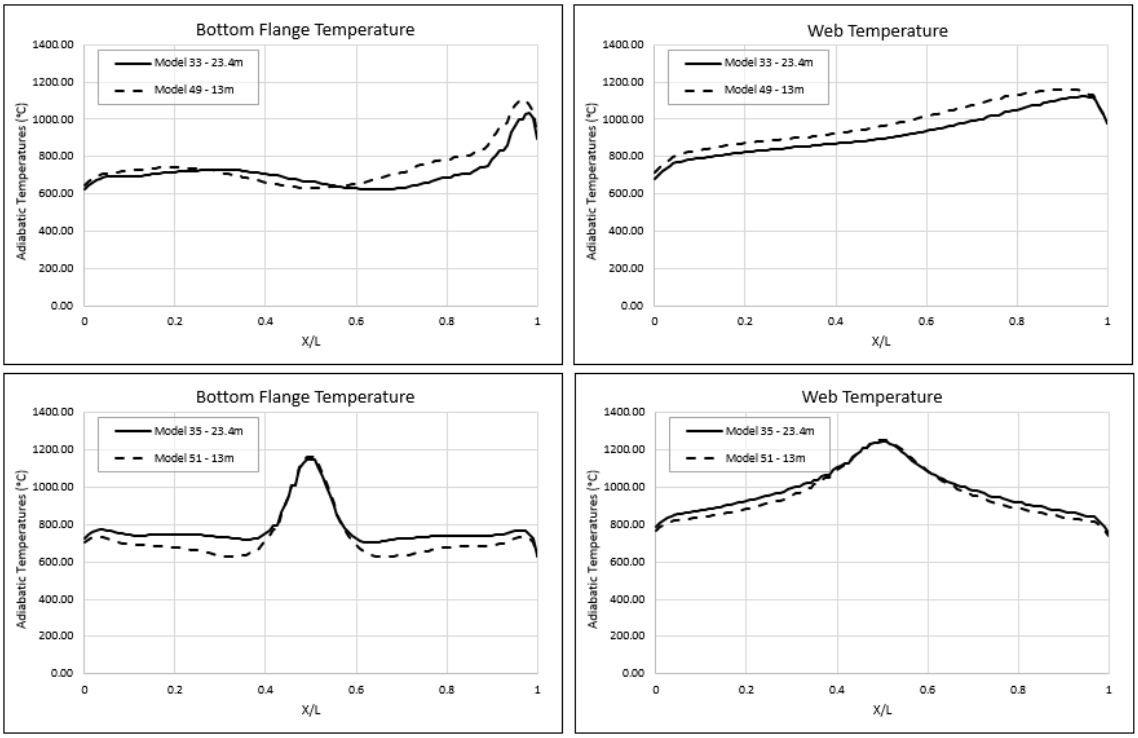

Figure 10. Width comparison 2

As before, it seems that the width of the bridges has little effect on the adiabatic temperatures registered for both the bottom flange and the web, with minor differences observed along the whole span.

It should be noted that this project is analysing the adiabatic temperatures of the central I-girder/beam, and therefore it would seem plausible that this parameter would have greater significance on the temperatures the outlying I-girders/beams are subjected to, due to the relative distance between each of these and the fire source.

iii. Span

The next parameter to be compared is the bridges span, which has been analysed for lengths of 16 and 24 metres. The following models have piers supporting the superstructure.

Model	Position	Bridge Substructure Configuration	Width	Span	Vertical Clearance	Heat Release Rate (HRR)
1	Abutment	Piers	23.4 m	*24 m*	5 m	2400 kW/m²
9	Abutment	Piers	23.4 m	*16 m*	5 m	2400 kW/m²
3	Mid-Span	Piers	23.4 m	*24 m*	5 m	2400 kW/m²
11	Mid-Span	Piers	23.4 m	*16 m*	5 m	2400 kW/m²

Table 10. Span comparison 1 – model parameters

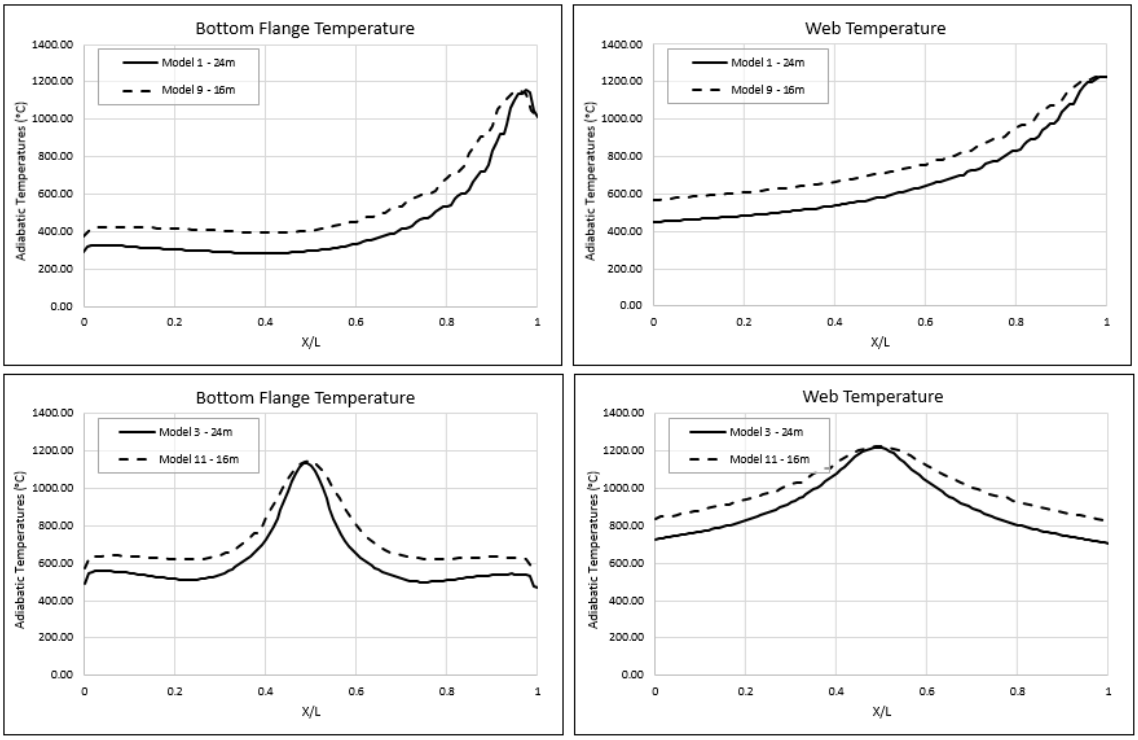

Figure 11. Span comparison 1 – relative distances

The influence of the span on the adiabatic temperatures of the bridge seems fairly straightforward: the temperatures are practically identical for both spans in the proximity of the fire source, whilst there is a clear difference for the points not in the vicinity of the flames, either at mid-span or adjacent to the bridge substructure.

The temperature difference seems to remain constant along the bridge and doesn't increase the further away the fire source is, as might be expected (when sufficiently separated from the source).

However, as these graphs are comparing relative positions for different span lengths, the larger drops in temperatures observed for the models with 24 metres are occurring at a larger absolute distance.

In Figure 12, the adiabatic temperatures are plotted for the absolute distances, measured from the right abutment for models 1 and 9 (meaning that the 8 metres furthest from the right abutment are truncated for model 1), and measured with respect to mid-span for models 3 and 11 (meaning that 4 metres are truncated at either end for model 3). This allows a direct comparison of adiabatic temperatures for the same absolute distances from the fire sources, for models with different spans.

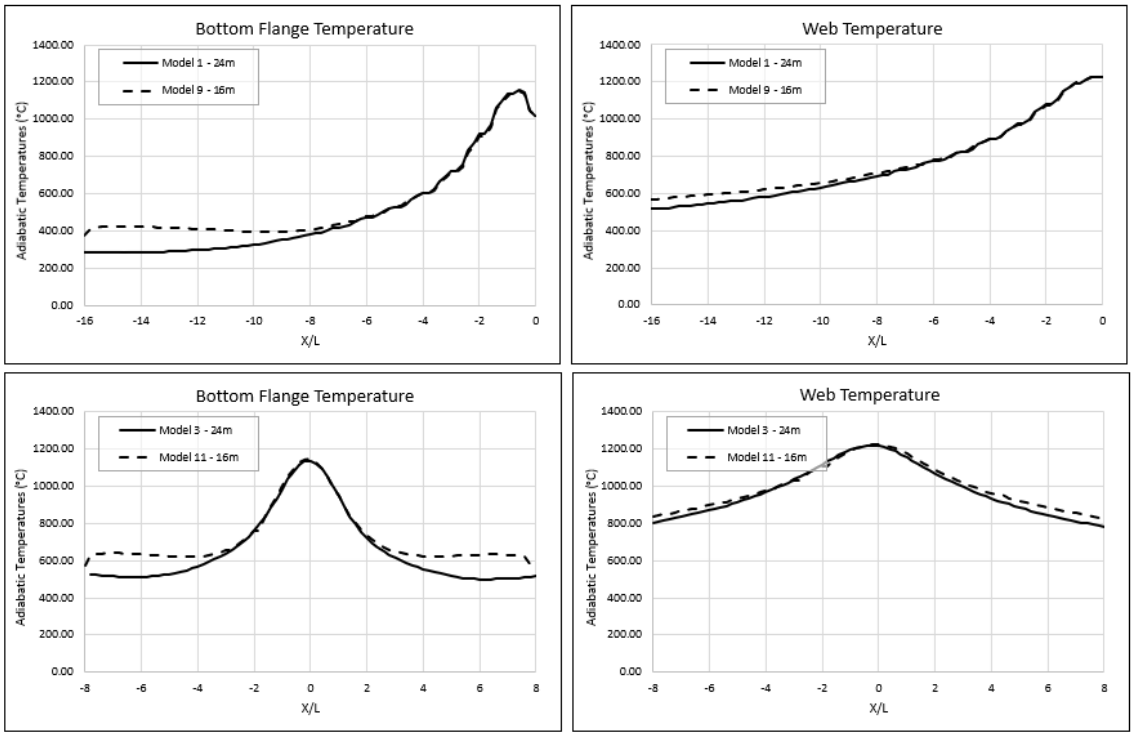

Figure 12. Span comparison 1 – absolute distances

Now the observed temperatures are practically identical for both models along most of the span, differing near the ends due to the influence of the bridge substructures.

In order to verify these initial findings also apply to bridges with abutments, the following models are also compared.

Model	Position	Bridge Substructure Configuration	Width	Span	Vertical Clearance	Heat Release Rate (HRR)
33	Abutment	Abutments	23.4 m	*24 m*	5 m	2400 kW/m²
41	Abutment	Abutments	23.4 m	*16 m*	5 m	2400 kW/m²
35	Mid-Span	Abutments	23.4 m	*24 m*	5 m	2400 kW/m²
43	Mid-Span	Abutments	23.4 m	*16 m*	5 m	2400 kW/m²

Table 11. Span comparison 2 – model parameters

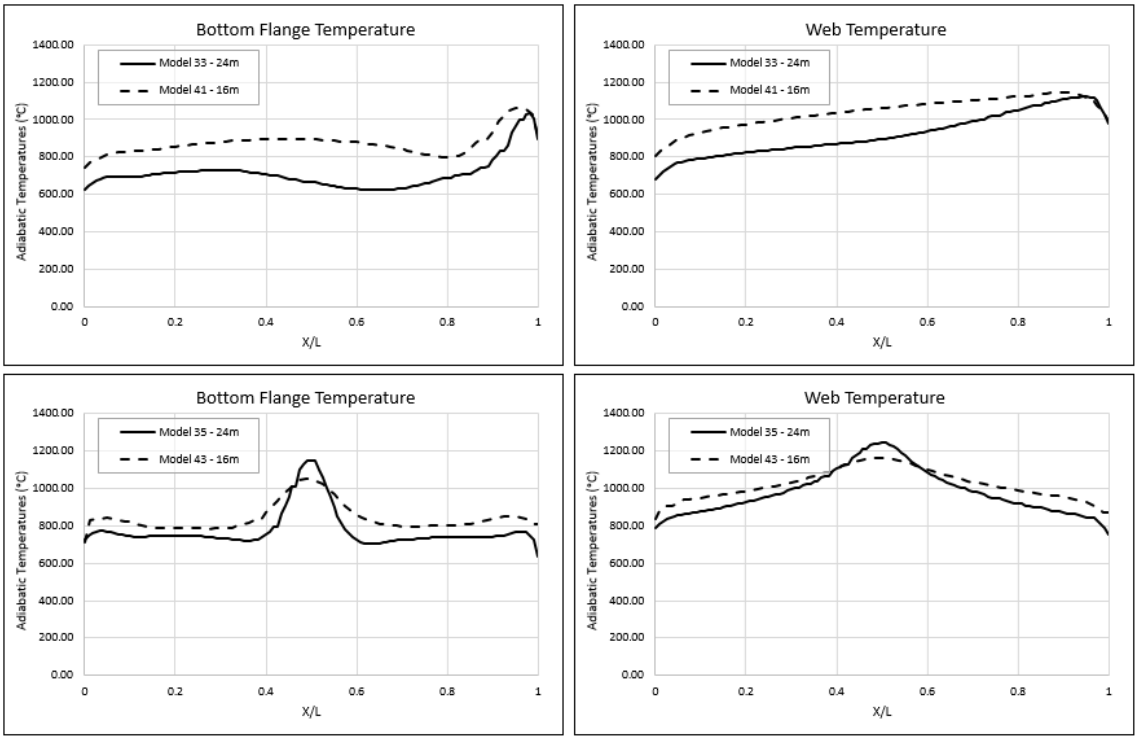

Figure 13. Span comparison 2

The significance of the parameter on the adiabatic temperatures appears to be similar, as the models with lower spans have higher temperatures at relative distances from the fire source, but with a more or less constant absolute difference, with no apparent linear increases.

The comparison between models 35 and 43 shows slight differences in maximum temperatures and seems to suggest that bridges with larger spans have higher maximum adiabatic temperatures. Conclusions shouldn't be drawn from analysing just one comparison, and there could be other factors at play, such as multiparameter interactions, or even slightly different conditions during the FDS analysis (such as the levels of oxygen in the vicinity of the fire, etc.).

iv. Vertical clearance

The models used to compare vertical clearance adopt values of either 5 or 9 metres, and as for the previous parameters analysed, the first two pairs have piers as the bridge substructure.

Model	Position	Bridge Substructure Configuration	Width	Span	Vertical Clearance	Heat Release Rate (HRR)
1	Abutment	Piers	23.4 m	24 m	*5 m*	2400 kW/m²
5	Abutment	Piers	23.4 m	24 m	*9 m*	2400 kW/m²
3	Mid-Span	Piers	23.4 m	24 m	*5 m*	2400 kW/m²
7	Mid-Span	Piers	23.4 m	24 m	*9 m*	2400 kW/m²

Table 12. Vertical clearance comparison 1 – model parameters

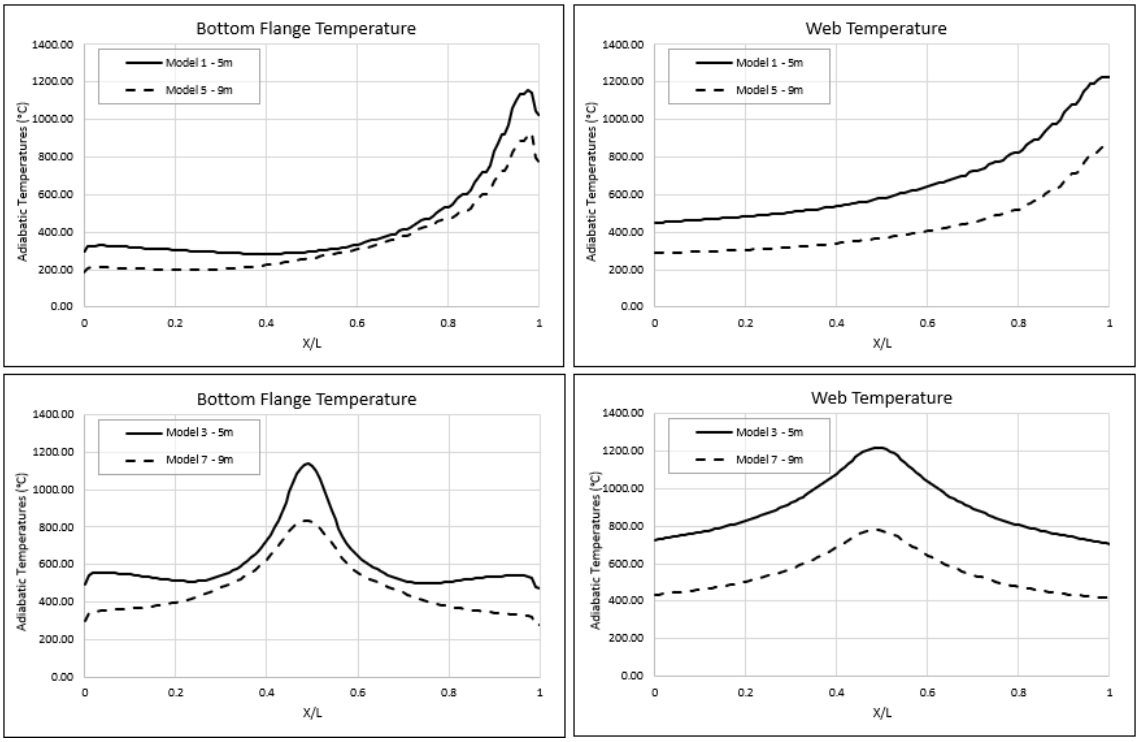

Figure 14. Vertical clearance comparison 1

The differences in adiabatic temperatures between the models with different vertical clearances is significant, with an almost constant variation in temperatures along the whole span, both in close proximity to the fire source and at the opposite ends. It appears that the difference between adiabatic temperatures is slightly larger in the case of web when compared to the bottom flange.

The next two pairs are identical to the previous two, but this time, considering abutments for the bridge substructure.

Model	Position	Bridge Substructure Configuration	Width	Span	Vertical Clearance	Heat Release Rate (HRR)
33	Abutment	Abutments	23.4 m	24 m	*5 m*	2400 kW/m²
37	Abutment	Abutments	23.4 m	24 m	*9 m*	2400 kW/m²
35	Mid-Span	Abutments	23.4 m	24 m	*5 m*	2400 kW/m²
39	Mid-Span	Abutments	23.4 m	24 m	*9 m*	2400 kW/m²

Table 13. Vertical clearance comparison 2 – model parameters

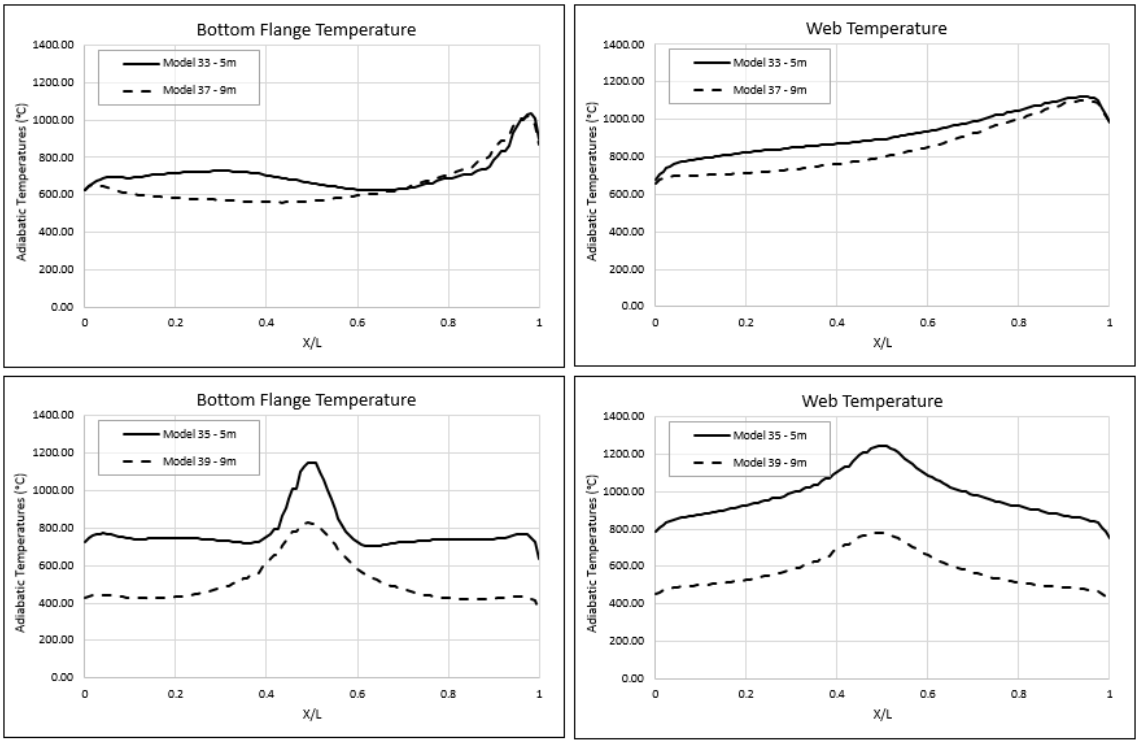

Figure 15. Vertical clearance comparison 2

In this case, the same constant difference seems to exist, with one noticeable exception: the adiabatic temperatures in the vicinity of the fire source when the latter is located adjacent to an abutment are practically identical for the bridges with different vertical clearance.

This could be as a result of the Coandă effect, in which the flames and/or hot gasses tend to stay attached to the flat surface of the abutment and help them reach larger heights as opposed to the flames being located mid-span, and therefore negate the difference of the vertical clearance between models 33 and 37.

v. HRR

Lastly, the following models will compare bridges exposed to different fire intensities, with Heat Release Rates (HRR) of either 2400 kW/m² or 1800 kW/m² (first for piers, and subsequently, for abutments).

Model	Position	Bridge Substructure Configuration	Width	Span	Vertical Clearance	Heat Release Rate (HRR)
1	Abutment	Piers	23.4 m	24 m	5 m	*2400 kW/m²*
2	Abutment	Piers	23.4 m	24 m	5 m	*1800 kW/m²*
3	Mid-Span	Piers	23.4 m	24 m	5 m	*2400 kW/m²*
4	Mid-Span	Piers	23.4 m	24 m	5 m	*1800 kW/m²*

Table 14. Heat Release Rate comparison 1 – model parameters

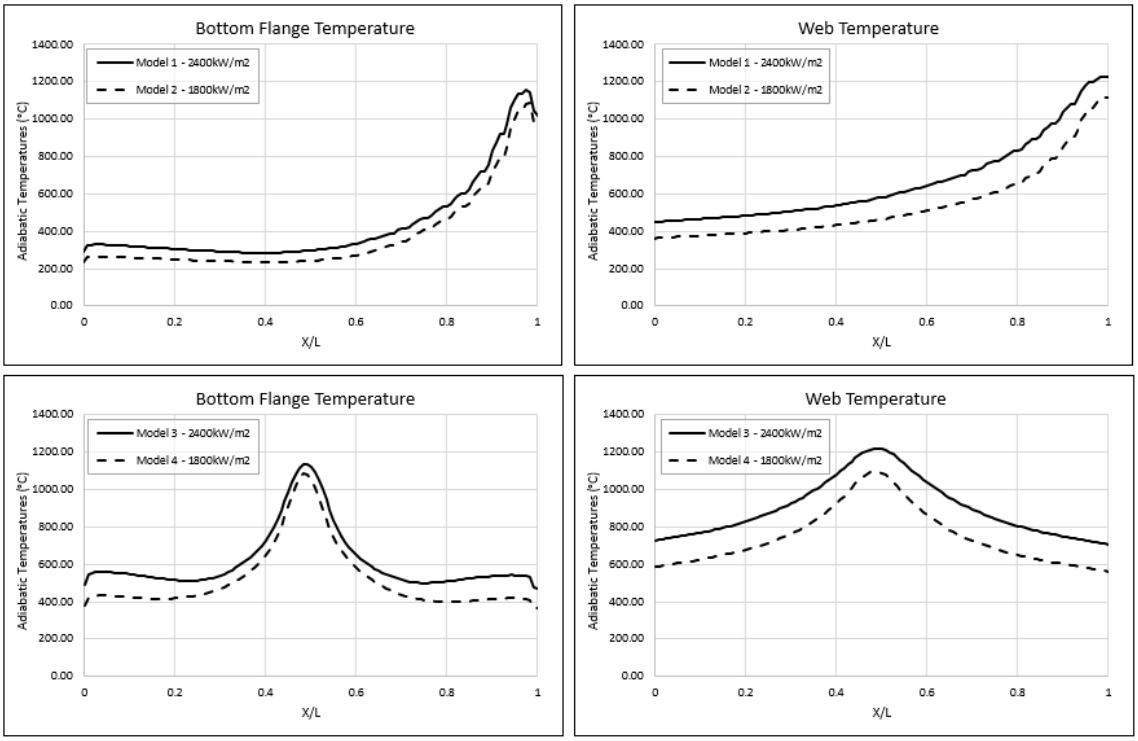

Figure 16. Heat Release Rate comparison 1

The effect of the HRR is similar to that observed with the different vertical clearances, although on a slightly smaller scale. The adiabatic temperatures have an almost constant difference along the whole of the bridges span when comparing the two values of HRR analysed, being slightly smaller in the vicinity of the fire in the case of the bottom flange, possibly due to the direct flame impingement on the I-girder.

The lower temperatures as a whole for a reduced HRR are to be expected, as a reduction in the heat generated is always going to cause the adiabatic temperatures to fall.

Model	Position	Bridge Substructure Configuration	Width	Span	Vertical Clearance	Heat Release Rate (HRR)
33	Abutment	Abutments	23.4 m	24 m	5 m	*2400 kW/m²*
34	Abutment	Abutments	23.4 m	24 m	5 m	*1800 kW/m²*
35	Mid-Span	Abutments	23.4 m	24 m	5 m	*2400 kW/m²*
36	Mid-Span	Abutments	23.4 m	24 m	5 m	*1800 kW/m²*

Table 15. Heat Release Rate comparison 2 – model parameters

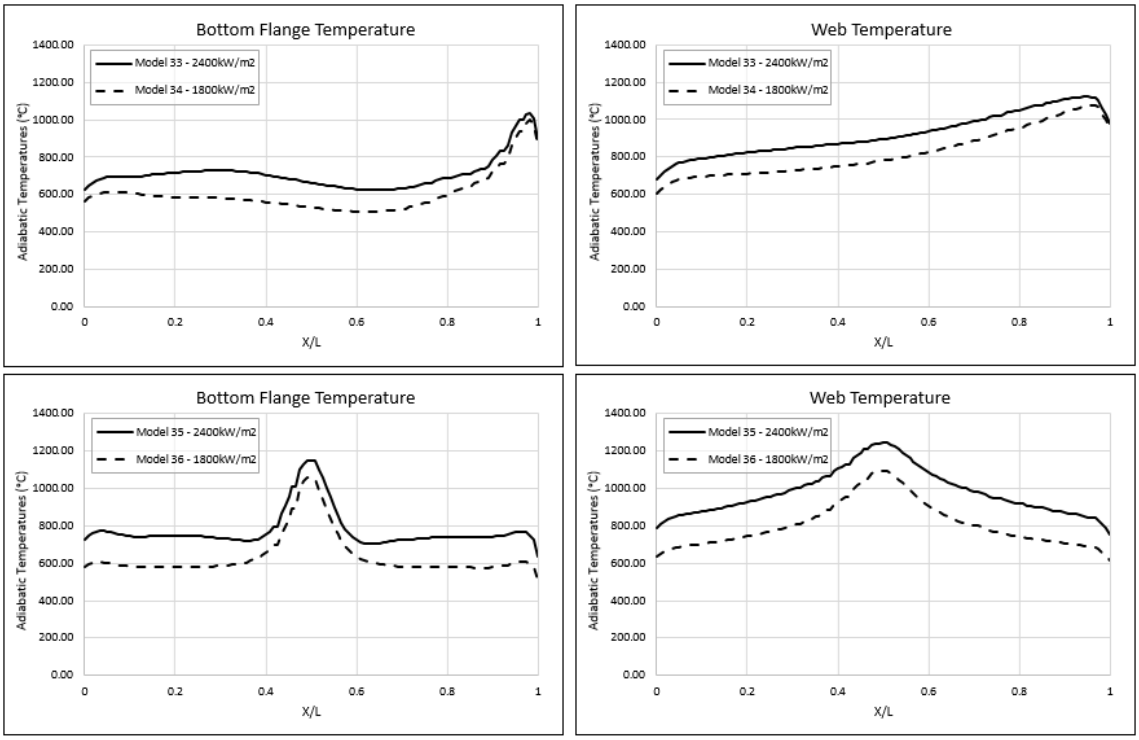

Figure 17. Heat Release Rate comparison 2

In the case of the comparison of models with abutments at each end of the span, the effect of the HRR on the adiabatic temperatures near to the fire source when this is located adjacent to the substructure is similar to that observed for the different vertical clearances. It appears that the lower HRR is possibly being nullified due to the Coandă effect, which facilitates the ascension of the flames and/or hot gasses to the superstructure.

Therefore, in conclusion, from the graphical comparison carried out, it appears that most parameters analysed have a significant effect on the adiabatic temperatures of both the bottom flange and the web of the bridges' beams (more significant in the case of vertical clearance and least significant in the case of the bridges' width).

A more thorough statistical analysis should confirm these initial assumptions and shed light on more complicated multiparameter interactions.

5. STATISTICAL ANALYSIS OF THE INFLUENCE OF DIFFERENT PARAMETERS ON THE ADIABATIC TEMPERATURES GENERATED IN I-GIRDER BRIDGE FIRES

Whilst the graphical comparison of results carried out in the previous section can lead to the identification of the parameters with the greatest influence on the models' adiabatic temperatures, it is unable to properly quantify if the differences observed between models in each pairing can be considered significant, due to the possibility of higher order multiparameter interactions taking place.

There are various statistical models/techniques that can determine if the effect of a given parameter/factor is significant on the mean of the dependent variable (in the case of this report, adiabatic temperature). This is performed by checking if the means of the dependent variable for the two subsets (one for each value of the parameter/factor) are equal, which can verified by checking if they fulfil the null hypothesis of certain distributions, such as the t-test or the F-test.

The main problem with these types of statistical models/techniques, which are known collectively as one-factor-at-a-time (OFAT) methods, is the amount of data required in order to guarantee the validity of the effect estimations provided. This would require a large number of models for each of the factors to be studied and would not allow the analysis of the significance of interactions between factors on the mean of the dependent variable.

In this case, the objective is to determine the influence or effect of various independent parameters on a single dependent variable (commonly known as a factorial experiment), including the significance of any of the interactions between these independent parameters, which can be obtained by performing Analysis of Variance (ANOVA) tests.

The present section will offer a description of ANOVA, with a practical example of its application to a simplified problem related to the current report (a 3-way-ANOVA, with three independent factors and one dependent variable, adiabatic temperatures), contrasting the results with some well-known exploratory tools for factorial experiments (main effects plots, interaction plots, Pareto plots, etc.). Subsequently, the results of the ANOVA tests for the 64 temperature curves, for both bottom flange and web, will be presented and discussed.

5.1. ANALYSIS OF VARIANCE DESCRIPTION

The Analysis of Variance (ANOVA) is a statistical technique which can determine the effect of one or more factors/parameters on the mean of a variable. Developed by R. A. Fisher during the 1920s, the ANOVA consists in breaking down the observed variance for a variable (for example, adiabatic temperatures) into different components attributable to different sources of variation, such as the studied factors (position, span, width, etc.) and their possible interactions (position-span, span-width, etc.), or the residual variance, associated with factors or interactions that are not included in the analysis, and which will serve as a benchmark to determine the significance of the ones that are included.

One of the main advantages of using ANOVA for factorial experiments is their efficiency when compared with OFAT methods, as they are able to analyse more factors, including their interactions, at no additional cost. The size of the sample required for a multifactorial ANOVA is no larger than that needed for a general OFAT analysis, thanks to the orthogonality of the 2^k factorial design used to select the 64 models.

For this report, a standard 2^k factorial design has been used, where each of the six parameters/factors has two levels/values, without replications, meaning the total number of configurations coincides with the total of number of simulations run, no configuration was run more than once.

Generally, replications are only required when carrying out 2^k factorial designs with four or less factors, or when higher order interactions want to be analysed (anything higher than a two-way interaction), as these have a reduce number of residual degrees of freedom, and this can lead to less precision when determining which effects are significant. Therefore, performing more than one run on each of the configurations increases the sample size, and with it, the residual degrees of freedom.

When dealing with 2^k factorial designs with a high number of factors (generally six or more), the problem is exactly the opposite, as the number of configurations needed is very high (six factors, 2^6=64 configurations; eight factors, 2^8=256 configurations; etc.), and often it is not practical or possible to carry out so many experiments.

In these cases, it is common to perform fractional factorial designs (2^{k-1}, …, 2^{k-p}), reducing the total number of configurations needed. This can be done without significantly affecting the precision of the analysis of significant effects, as generally only main effects and two-way interactions are analysed, meaning that degrees of freedom corresponding to higher order interactions (three-way, four-way, etc.) can be used as residual degrees of freedom.

As explained in Section 3 of this report, a fractional factorial design has not been carried out in this case even though a total of six parameters are studied, leading to a total of 64 models, in order to allow a partitioned analysis of the models based on fire position, either adjacent to abutment/piers or located mid-span.

In this case, the number of parameters for each subset is five, meaning that with a standard 2^k factorial design, 32 models are needed. If we were to use a fractional factorial design, such as a 2^{k-1}, a total of 16 configurations would be analysed.

In order to analyse the significance of the main effects and the two-way interactions, a total of 15 degrees of freedom would be needed (one for each of the five main effects and ten two-way interactions), leading to there being no residual degrees of freedom, as an ANOVA with 16 configurations, only has 15 degrees of freedom ($2^{5-1} - 1 = 15$).

5.1.1. ANOVA EXAMPLE

In order to understand the methodology of an ANOVA test, we are going to carry one out on a subset of our 64 models, analysing the effects of 3 parameters/factors (A: bridge substructure configuration, B: vertical clearance and C: HRR) on adiabatic temperatures.

I. Experiment design

In this case, if we were to use a 2^k factorial design without replications (each parameter has two configurations), we would have a total of 8 configurations, with a data set of the same size.

The total number of degrees of freedom is equal to size of the data set minus one:

$$df_{total} = 2^k - 1 = 2^3 - 1 = 7$$

The degrees of freedom for each of the main effects is equal to the levels of each factor (in the case of a 2^k factorial experiment, every factor has two levels) minus one:

$$df_{main\ effects} = 2 - 1 = 1$$

The degrees of freedom for each of the interactions are equal to the product of the degrees of freedom of the main effects for that interaction:

$$df_{interactions} = 1 \cdot 1 = 1$$

The residual degrees of freedom are equal to the total number of degrees of freedom minus the degrees of freedom of the main effects and interactions:

$$df_{residual} = 7 - 3 \cdot 1 - 3 \cdot 1 = 1$$

Therefore, if a standard 2^k factorial design without replications is used, there would only be one residual degree of freedom, and the capability of the ANOVA to determine the significance of the main effects and interactions with precision is reduced.

In order to increase the capability of ANOVA, we are going to use a 2^k factorial design with two replications, doubling the data set we had previously. The recalculated degrees of freedom are as follows:

$$df_{total} = r \cdot 2^k - 1 = 2 \cdot 2^3 - 1 = 15$$

$$df_{main\ effects} = 2 - 1 = 1$$

$$df_{interactions} = 1 \cdot 1 = 1$$

$$df_{residual} = 15 - 3 \cdot 1 - 3 \cdot 1 = 9$$

Having verified that the number of residual degrees of freedom is sufficient, we can conclude that the experiment has been adequately designed. The following table shows the configuration of the models to be run, each of which we will replicate in order to obtain two results.

Model	A: Subtr. Config.	B: Vert. Clearance	C: HRR
1	Piers	5 m	2400 kW/m²
2	Piers	5 m	1800 kW/m²
3	Piers	9 m	2400 kW/m²
4	Piers	9 m	1800 kW/m²
5	Abutment	5 m	2400 kW/m²
6	Abutment	5 m	1800 kW/m²
7	Abutment	9 m	2400 kW/m²
8	Abutment	9 m	1800 kW/m²

Table 16. Experiment design for ANOVA example.

II. Experiment results

The results for the models defined in the previous table have been taken from those obtained for the 64 models previously defined in this report (with matching configurations, considering fire position adjacent to abutment/piers, a span of 24 metres and a width of either 13 or 23.4 metres, in order to increase the subset size), for the bottom flange maximum adiabatic temperatures.

Model	A: Subtr. Config.	B: Vert. Clearance	C: HRR	Adiab. Temp. Subset 1	Adiab. Temp. Subset 2
1	Piers	5 m	1800 kW/m²	1088.44 ºC	1082.93 ºC
2	Piers	5 m	2400 kW/m²	1157.99 ºC	1147.73 ºC
3	Piers	9 m	1800 kW/m²	778.33 ºC	765.64 ºC
4	Piers	9 m	2400 kW/m²	926.81 ºC	902.53 ºC
5	Abutment	5 m	1800 kW/m²	1001.03 ºC	990.49 ºC
6	Abutment	5 m	2400 kW/m²	1035.91 ºC	1061.51 ºC
7	Abutment	9 m	1800 kW/m²	911.01 ºC	917.79 ºC
8	Abutment	9 m	2400 kW/m²	1019.55 ºC	1007.83 ºC

Table 17. Experiment results for the ANOVA example.

III. Estimated effects on the mean

The estimated effect of each factor on the mean can be calculated by comparing the differences between the means of the different levels:

$$A: Bridge\ Substr.Config.effect = \frac{\sum T_{piers}}{n} - \frac{\sum T_{abutments}}{n}$$

$$= \frac{1088.44 + 1082.93 + 1157.99 + 1147.73 + 778.33 + 765.64 + 926.81 + 902.53}{8}$$

$$- \frac{1001.03 + 990.49 + 1035.91 + 1061.51 + 911.01 + 917.79 + 1019.55 + 1007.83}{8}$$

$$= 981.30 - 993.14 = -11.84$$

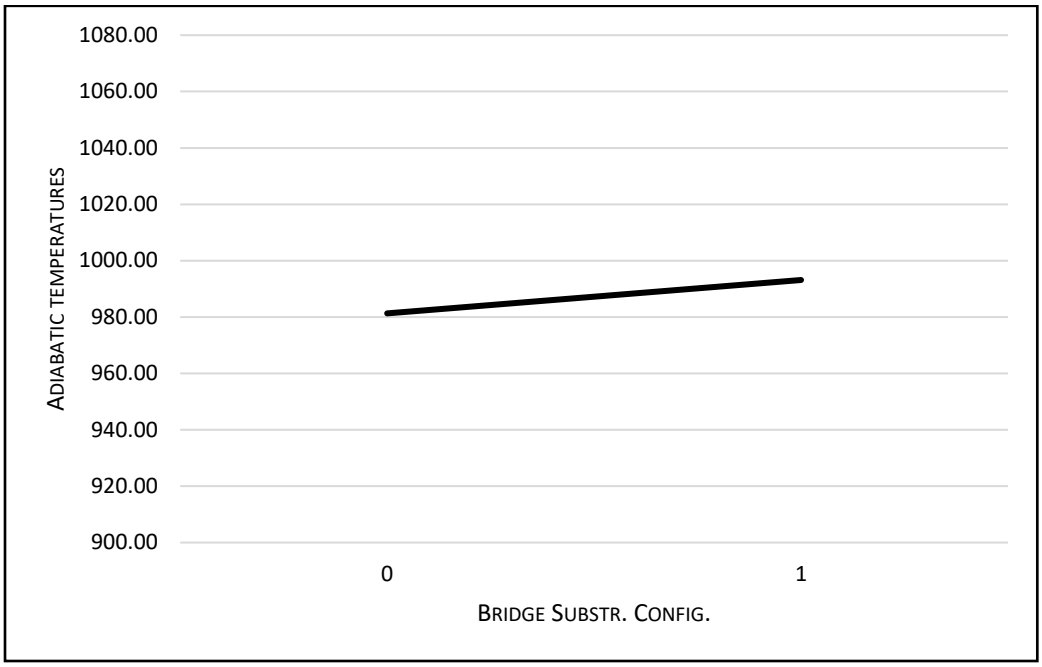

Figure 18. Main effect plot for bridge substructure configuration

$$B: Vert.clearance\ effect = \frac{\sum T_{5m}}{n} - \frac{\sum T_{9m}}{n}$$

$$= \frac{1088.44 + 1082.93 + 1157.99 + 1147.73 + 1001.03 + 990.49 + 1035.91 + 1061.51}{8}$$

$$- \frac{778.33 + 765.64 + 926.81 + 902.53 + 911.01 + 917.79 + 1019.55 + 1007.83}{8}$$

$$= 1070.75 - 903.68 = 167.07$$

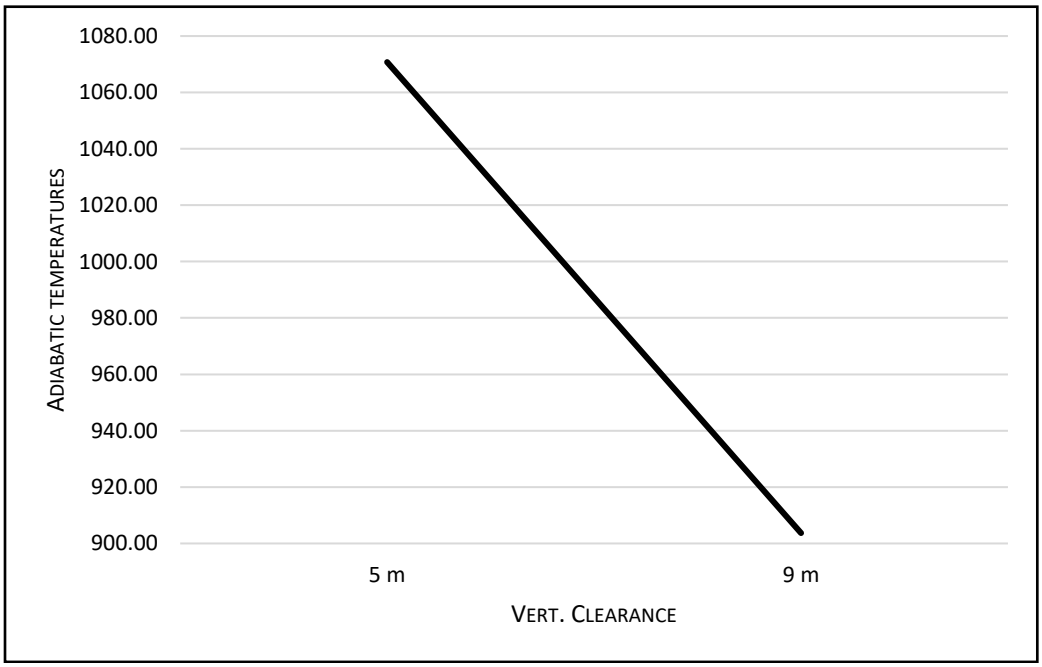

Figure 19. Main effect plot for vertical clearance

$$C\text{: } HRR\ effect = \frac{\sum T_{1800\ kW/m^2}}{n} - \frac{\sum T_{2400\ kW/m^2}}{n}$$

$$= \frac{1088.44 + 1082.93 + 778.33 + 765.64 + 1001.03 + 990.49 + 911.01 + 917.79}{8}$$

$$- \frac{1157.99 + 1147.73 + 926.81 + 902.53 + 1035.91 + 1061.51 + 1019.55 + 1007.83}{8}$$

$$= 941.96 - 1032.48 = -90.52$$

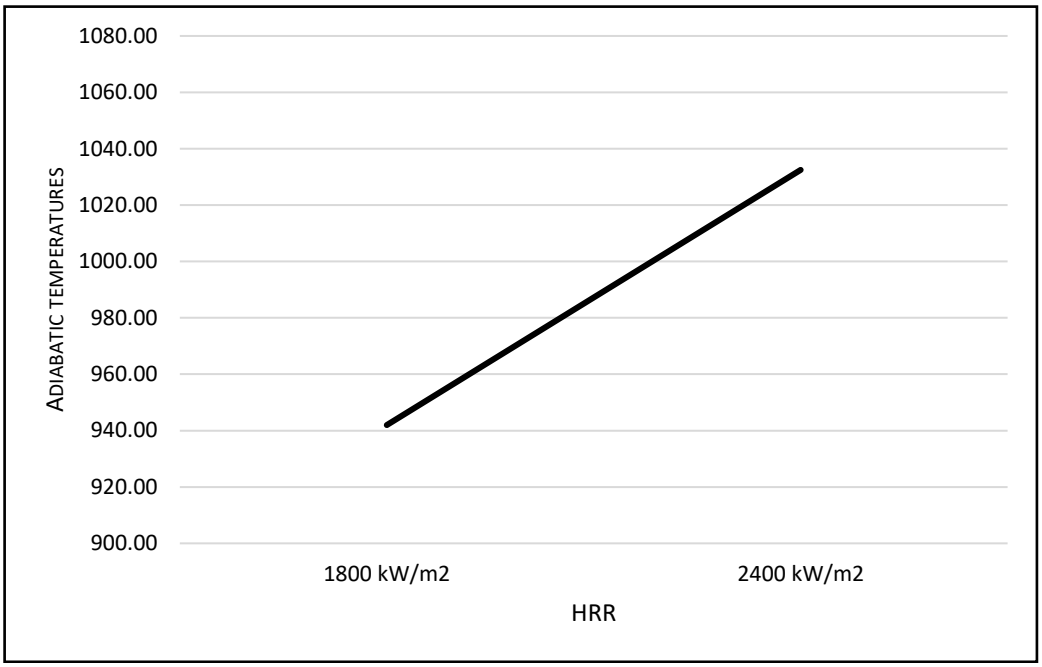

Figure 20. Main effect plot for HRR

The estimated effect of the interactions on the mean can be calculated as half the difference between the corresponding main effects on each of their two levels:

$$A \cdot B = \frac{1}{2}\left[\left(\frac{\sum T_{piers\cdot 5m}}{n} - \frac{\sum T_{piers\cdot 9m}}{n}\right) - \left(\frac{\sum T_{abutment\cdot 5m}}{n} - \frac{\sum T_{abutment\cdot 9m}}{n}\right)\right]$$

$$= \frac{1}{2}\left[\left(\frac{1088.44 + 1082.93 + 1157.99 + 1147.73}{4} - \frac{778.33 + 765.64 + 926.81 + 902.53}{4}\right) - \left(\frac{1001.03 + 990.49 + 1035.91 + 1061.51}{4} - \frac{911.01 + 917.79 + 1019.55 + 1007.83}{4}\right)\right]$$

$$= \frac{1}{2}[(1119.27 - 843.32) - (1022.23 - 964.04)] = 108.88$$

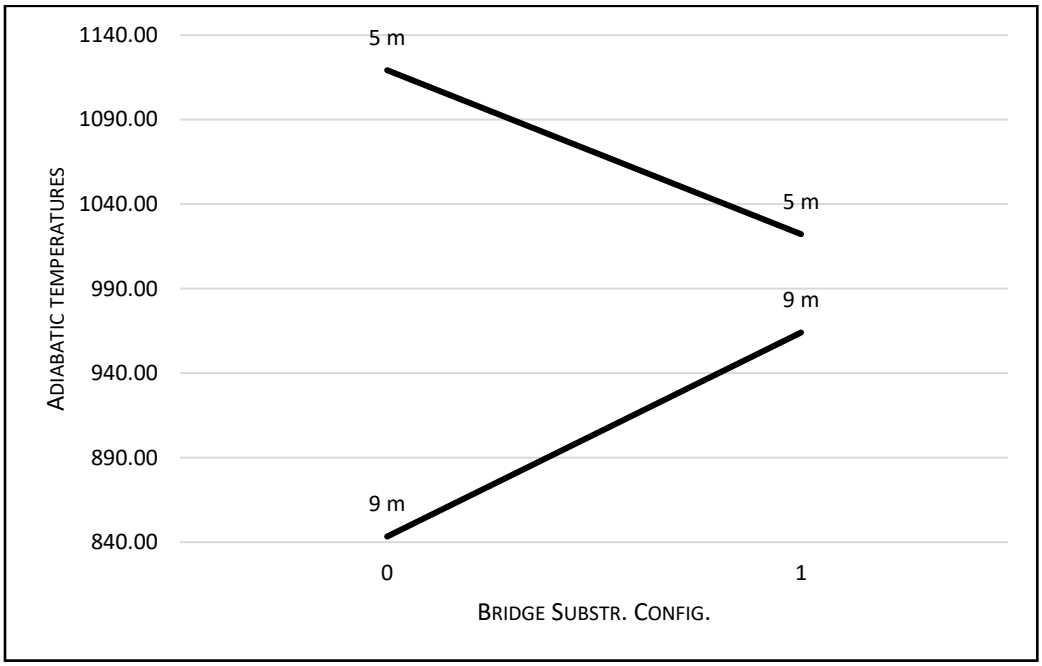

Figure 21. Interaction plot for bridge substructure configuration and vertical clearance

$$A \cdot C = \frac{1}{2}\left[\left(\frac{\sum T_{piers \cdot 1800\ kW/m^2}}{n} - \frac{\sum T_{piers \cdot 2400\ kW/m^2}}{n}\right) - \left(\frac{\sum T_{abutment \cdot 1800\ kW/m^2}}{n} - \frac{\sum T_{abutment \cdot 2400\ kW/m^2}}{n}\right)\right]$$

$$= \frac{1}{2}\left[\left(\frac{1088.44 + 1082.93 + 778.33 + 765.64}{4} - \frac{1157.99 + 1147.73 + 926.81 + 902.53}{4}\right) - \left(\frac{1001.03 + 990.49 + 911.01 + 917.79}{4} - \frac{1035.91 + 1061.51 + 1019.55 + 1007.83}{4}\right)\right]$$

$$= \frac{1}{2}[(928.83 - 1033.76) - (955.08 - 1031.20)] = -14.41$$

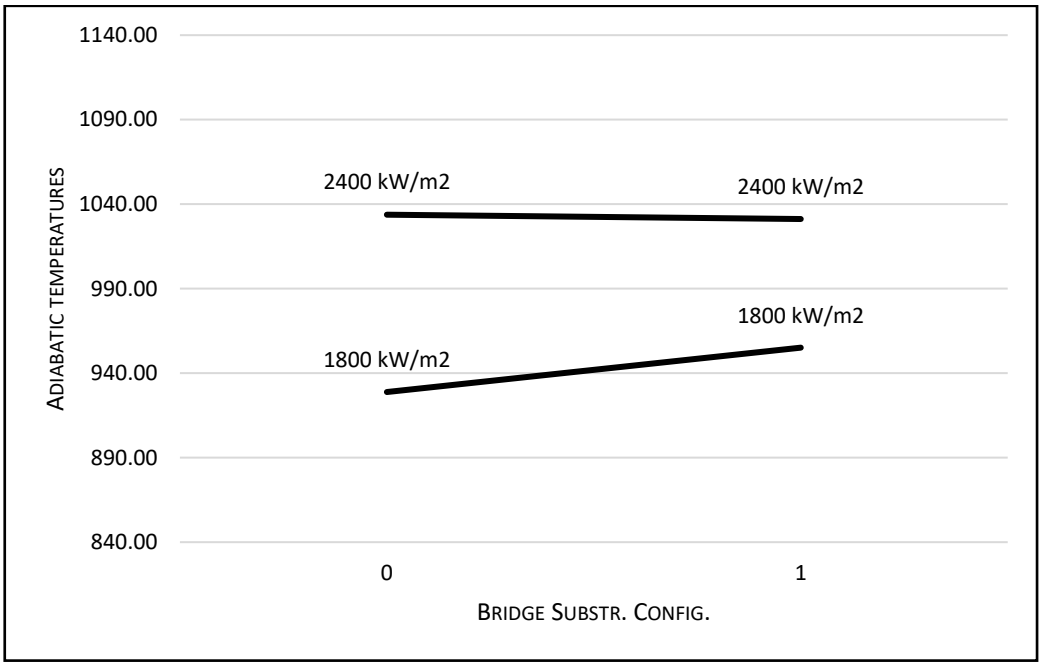

Figure 22. Interaction plot for bridge substructure configuration and HRR

$$B \cdot C = \frac{1}{2}\left[\left(\frac{\sum T_{5\ m\cdot 1800\ kW/m^2}}{n} - \frac{\sum T_{5\ m\cdot 2400\ kW/m^2}}{n}\right) - \left(\frac{\sum T_{9m\ \cdot 1800\ kW/m^2}}{n} - \frac{\sum T_{9\ m\cdot 2400\ kW/m^2}}{n}\right)\right]$$

$$= \frac{1}{2}\left[\left(\frac{1088.44 + 1082.93 + 1001.03 + 990.49}{4} - \frac{1157.99 + 1147.73 + 1035.91 + 1061.51}{4}\right) - \left(\frac{778.33 + 765.64 + 911.01 + 917.79}{4} - \frac{926.81 + 902.53 + 1019.55 + 1007.83}{4}\right)\right]$$

$$= \frac{1}{2}[(1040.72 - 1100.78) - (843.19 - 964.18)] = 30.46$$

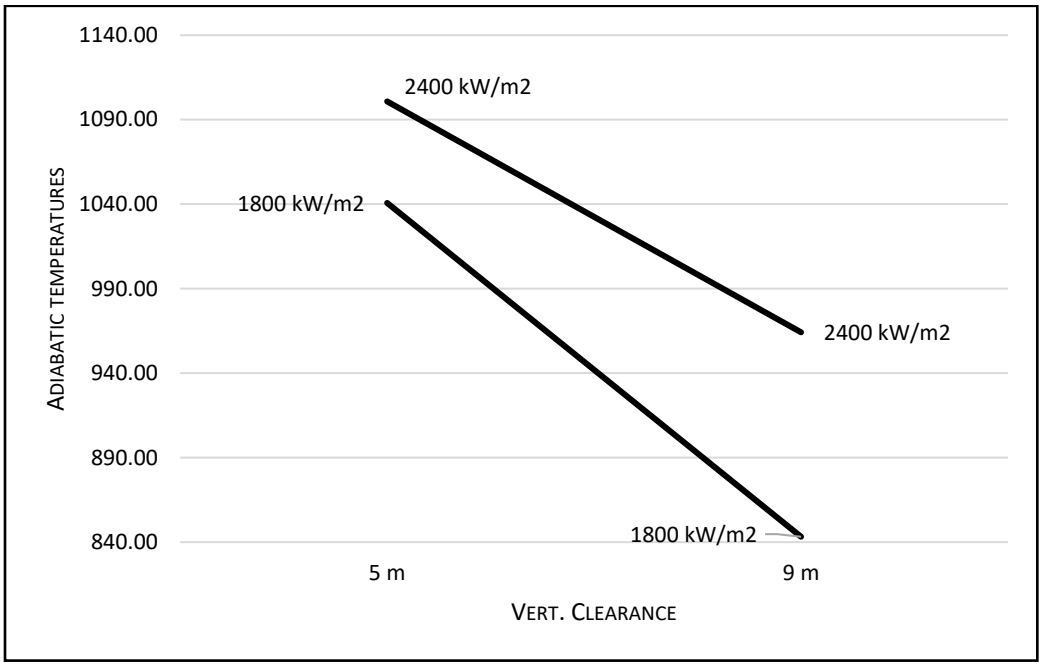

Figure 23. Interaction plot for vertical clearance and HRR

By analysing the main effect and interaction plots it can be determined that the most significant effects seem to be vertical clearance (B), HRR (C) and the interaction between bridge substructure configuration and vertical clearance (AB). This can be determined for main effects when their slope is clearly not horizontal and for interactions when the slopes of the two lines are not parallel to one another.

In the case of the interaction between bridge substructure configuration and vertical clearance (AB), it is a clear example of the Coandă effect, as the drop in adiabatic temperatures experienced due to a higher vertical clearance is significantly smaller when the bridge substructure is an abutment compared with when it is formed by piers.

Another way of estimating if main effects and/or interactions are significant on the mean of a variable is by representing the effects obtained above on a normal probability plot (either a full normal or half-normal plot).

The standardized effects are plotted in ascending order and compared with quantiles of a normal distribution. The effects that don't fall on a straight line (which must pass through the point 0, 50%) can be considered to be significant, whereas if the do approximately fall on the line, they can be considered to be non-significant.

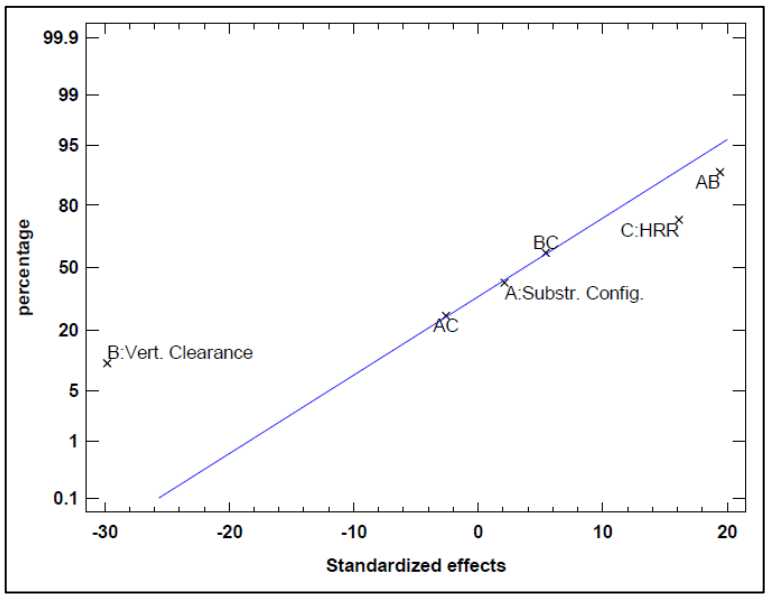

Figure 24. Normal probability plot of effects

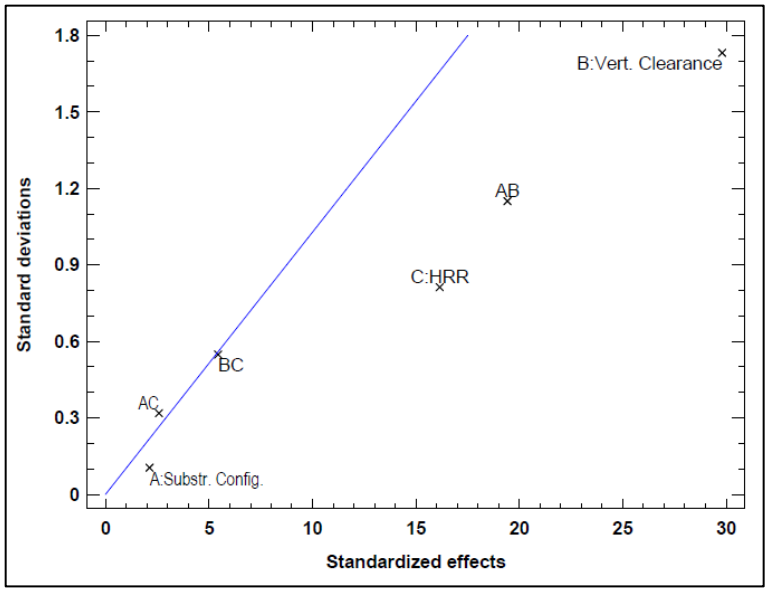

Figure 25. Half normal probability plot of effects.

By analysing the two normal probability plots (both full and half), it can be observed that the most significant effects seem to be vertical clearance (B), HRR (C) and the interaction between bridge substructure configuration and vertical clearance (AB), as was the case when studying the main effect and interaction plots. These conclusions will be contrasted with the results of the ANOVA.

Although it would also be possible to obtain the three-way interaction between the three main effects, they don't usually have any significance on the model and won't be calculated in this example.

IV. Analysis of Variance

As described before, the ANOVA breaks down the variance for a variable (adiabatic temperatures) into different components attributable to different sources of variation, such as the studied factors (A - bridge substructure configuration, B - vertical clearance and C - HRR), their possible interactions (AB, AC and BC), and the residual variance.

The total variance of a variable, in this case adiabatic temperatures, can be obtained by calculating the sum of squares of deviations of each data sample to the global mean of all the data:

$$SS_{total} = (1088.44^2 + 1082.93^2 + \cdots + 1007.83^2) - (1088.44 + 1082.93 + \cdots + 1007.83)^2/16 = 198075.9$$

The variance attributable to each of the main effects and the interactions can be obtained by calculating their corresponding sum of squares with the following simplified formula (in the case of 2^k factorial experiments):

$$SS_{effect} = \frac{No.\,data\ samples}{4} \cdot Effect^2$$

$$SS_A = \frac{16}{4} \cdot (-11.84)^2 = 560.74$$

$$SS_B = \frac{16}{4} \cdot (167.07)^2 = 111646.20$$

$$SS_C = \frac{16}{4} \cdot (-90.53)^2 = 32779.10$$

$$SS_{AB} = \frac{16}{4} \cdot (108.88)^2 = 474417.24$$

$$SS_{AC} = \frac{16}{4} \cdot (-14.41)^2 = 830.02$$

$$SS_{BC} = \frac{16}{4} \cdot (30.46)^2 = 3711.86$$

Finally, the variance attributable to the residual, represented by its sum of squares, can be calculated by subtraction, as the total sum of squares is equal to the sum of the sum of squares of the effects, the interactions and the residual:

$$SS_{res} = 198075.9 - 560.74 - 111646.20 - 32779.10 - 474417.24 - 830.02 - 3711.86 = 1130.70$$

In this case, as the degrees of freedom associated to each main effect and interaction is equal to one, the mean sum of squares is equal to the sum of squares calculated above. In the case of the residual, the mean sum of squares is obtained by dividing the residual sum of squares by the residual degrees of freedom:

$$MS_{res} = \frac{SS_{res}}{df_{residual}} = \frac{1130.70}{9} = 125.63$$

The F-Ratio of each effect and interaction can be obtained by dividing their mean sum of squares by the residual mean sum of squares:

$$F_{ratio} = \frac{SS_{effect}}{SS_{res}}$$

Once the F-Ratio has been obtained, in order to determine if an effect is significant or not, the P-value associated with the F-distribution of each effect, with 1 and 9 degrees of freedom (corresponding to the DOF of the effect and residual respectively), can be obtained. Generally, if given P-value is lower than the type I error rate (α = 0.05), than the effect or interaction can be considered to be significant.

Source	Sum of Squares	Degrees of freedom	Mean Square	F-Ratio	P-value
A (BSC)	560.74	1	560.74	4.46	0.0638
B (VC)	111646.20	1	111646.20	888.67	**0.0000**
C (HRR)	32779.10	1	32779.10	260.91	**0.0000**
AB	47417.24	1	47417.24	377.42	**0.0000**
AC	830.02	1	830.02	6.61	**0.0302**
BC	3711.86	1	3711.86	29.55	**0.0004**
Residual	1130.70	9	125.63		
Total	**198075.86**	**15**			

Figure 26. ANOVA results for the example (3 factor ANOVA)

The results obtained in the previous table indicate that virtually all factors and interactions are significant, although it is clear that the F-Ratio corresponding to vertical clearance, HRR and the

interaction between bridge substructure configuration and vertical clearance are noticeably more significant than the rest.

5.2. MAXIMUM TEMPERATURES

The following section provides the ANOVA tests of the maximum temperatures observed for each of the sixty-four bridge configurations analysed, using the statistical analytics software Statgraphics Centurion 18, due to the high number of factors (either 5 or 6 independent parameters, depending on whether it refers to the global analysis or the independent analysis for each fire location).

The data source used in the calculations, corresponding with the maximum adiabatic temperatures for each model, can be consulted in *APPENDIX 2: ANOVA INPUT DATA AND DETAILED RESULTS.*

5.2.1. GLOBAL ANALYSIS

In the global analysis, all sixty-four configurations are taken into account, with a total of six parameters and fifteen interactions (all two-way interactions) being studied, leading to there being forty-two residual degrees of freedom, meaning that the statistical significance of effects can be determined with high confidence.

The following table shows the results of the ANOVA test for the maximum adiabatic temperatures for the bottom flange of the central I-girder.

FLANGE TEMPERATURES	Sum of squares	Degrees of freedom	Mean Square	F-ratio	p-value
Main Effects					
A:Position	59911.7	1	59911.7	23.28	**0.0000**
B:Bridge Substructure Config.	38299	1	38299	14.88	**0.0004**
C:Width	830.809	1	830.809	0.32	0.5729
D:Span	128.397	1	128.397	0.05	0.8243
E:Vertical Clearance	1396020	1	1396020	542.48	**0.0000**
F:HRR	187034	1	187034	72.68	**0.0000**
Interactions					
AB	2028.04	1	2028.04	0.79	0.3797
AC	5290.2	1	5290.2	2.06	0.1590
AD	6528.44	1	6528.44	2.54	0.1187
AE	55735.5	1	55735.5	21.66	**0.0000**
AF	8672.96	1	8672.96	3.37	**0.0735**
BC	14142.9	1	14142.9	5.50	**0.0239**
BD	8574.99	1	8574.99	3.33	**0.0751**
BE	14571.8	1	14571.8	5.66	**0.0220**
BF	154.723	1	154.723	0.06	0.8075
CD	7727.07	1	7727.07	3.00	**0.0905**
CE	27526.5	1	27526.5	10.70	**0.0021**
CF	231.763	1	231.763	0.09	0.7656
DE	476.603	1	476.603	0.19	0.6691
DF	128.681	1	128.681	0.05	0.8241
EF	18219.3	1	18219.3	7.08	**0.0110**
Residual	108083	42	2573.41		
Total	1.96E+06	63			

Table 18. ANOVA of bottom flange maximum adiabatic temperatures for all configurations.

In order to compare the overall significance of each of the effects, the ANOVA results can be presented in graphical form using either the Standardized Pareto Chart or the Normal Probability Plot (in this case the half-normal version for easier comparison) seen in the ANOVA example from the previous section.

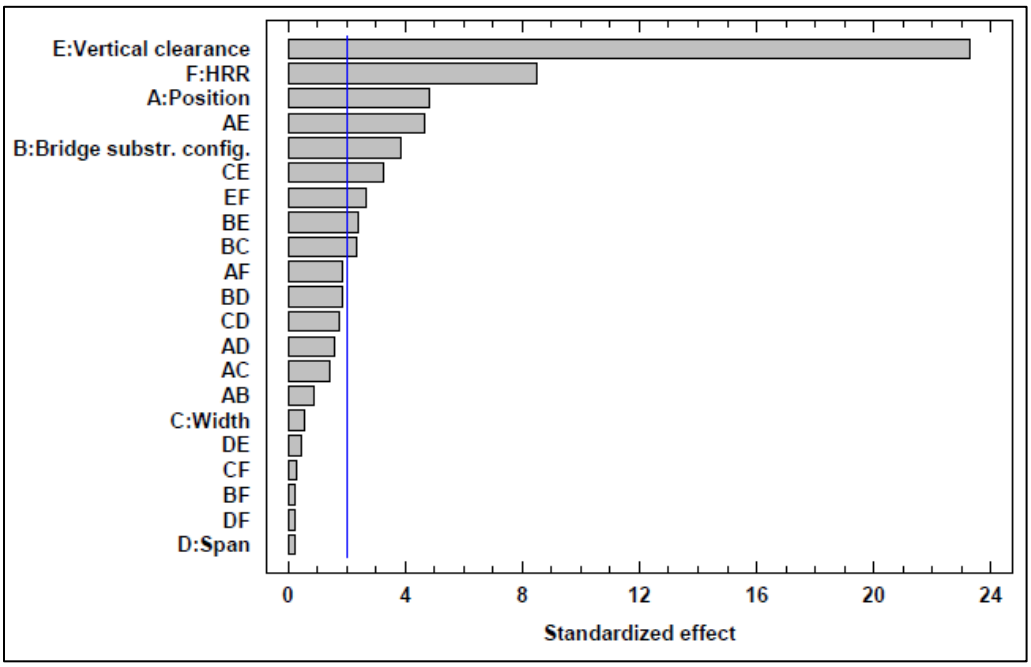

Figure 27. Standardized Pareto chart for bottom flange maximum adiabatic temperatures for all configurations

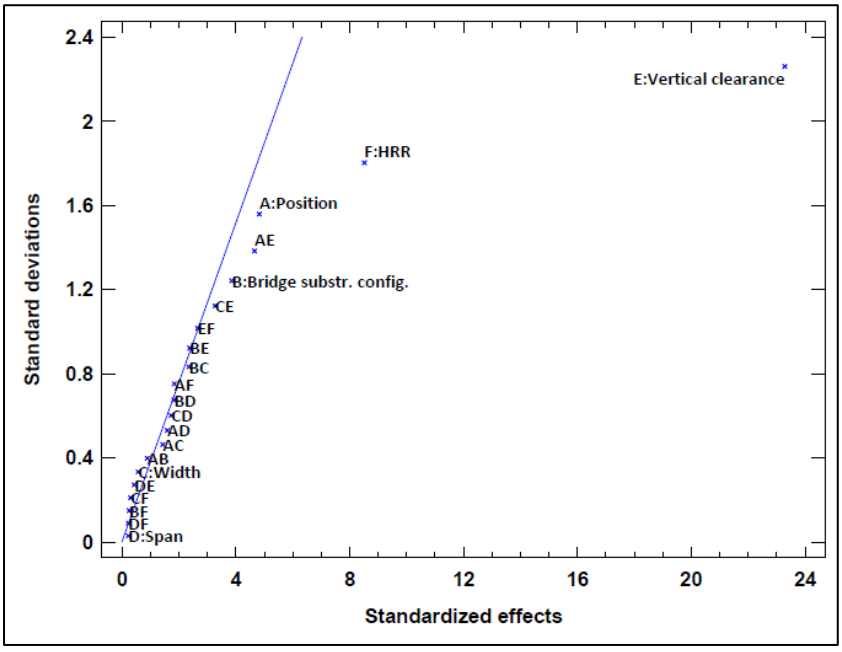

Figure 28. Half-normal probability plot for bottom flange maximum adiabatic temperatures for all configurations

Of the main effects, fire position, bridge substructure configuration, vertical clearance and HRR can be considered statistically significant, whilst both width and span are not. This can be explained due to the nature of the adiabatic temperatures being analysed, as the maximum temperatures of the central girders will occur in the vicinity of the fire, where span and width

have less influence (their significance is greater the further from the source of the fire, as will be shown in the by position analysis).

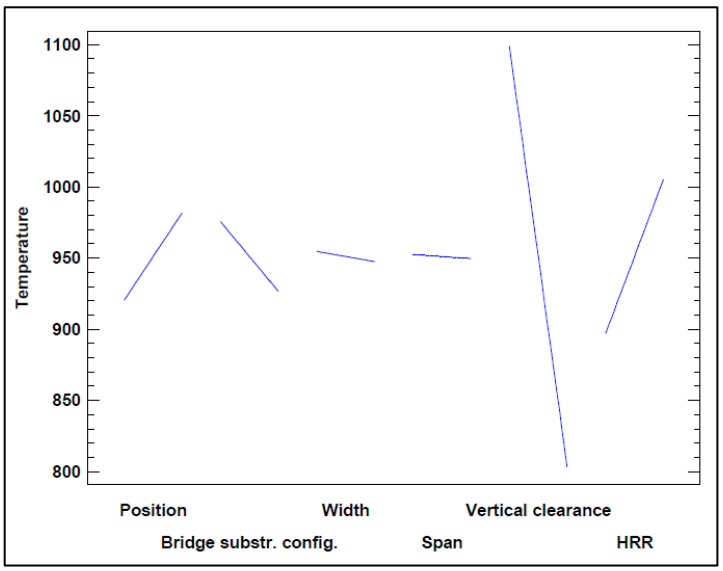

Figure 29. Main effects plot for bottom flange maximum adiabatic temperatures for all configurations

There is one interaction that can be considered as significant as the main effects identified above: fire position and vertical clearance (AE). As stated previously, it is a clear example of the Coandă effect, as the drop in adiabatic temperatures experienced due to a higher vertical clearance is significantly smaller when the fire is located adjacent to abutments/piers than when it is located mid-span, due to the tendency of the flames and/or hot gasses to stay attached to the surface of the abutments or piers and help them reach greater elevation.

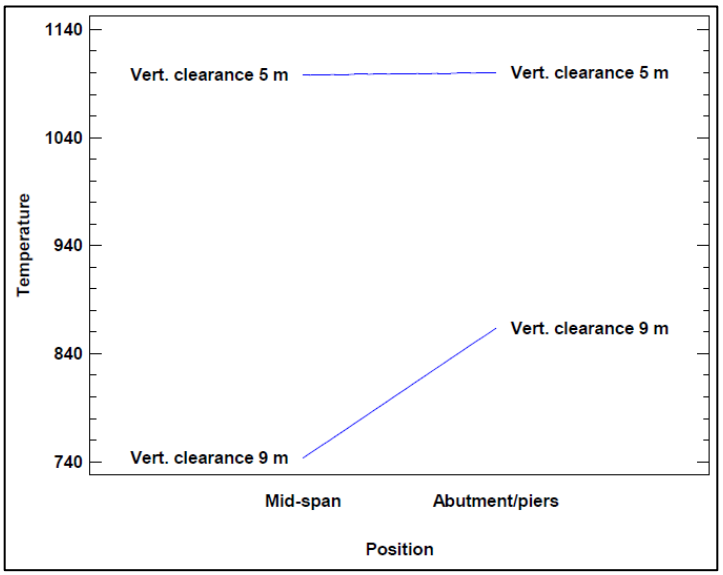

Figure 30. Fire position and vertical clearance interaction plot for bottom flange maximum adiabatic temperatures for all configurations

In Table 19, the ANOVA results for the maximum adiabatic temperatures of the web of the central I-girder are presented, taking into account all sixty-four bridge configurations for the six independent parameters previously defined, with the same residual degrees of freedom as those defined for the bottom flange ANOVA.

WEB TEMPERATURES	Sum of squares	Degrees of freedom	Mean Square	F-ratio	p-value
Main Effects					
A:Position	95500.3	1	95500.3	25.72	**0.0000**
B:Bridge Substructure Config.	6845.29	1	6845.29	1.84	0.1818
C:Width	792.493	1	792.493	0.21	0.6465
D:Span	229.636	1	229.636	0.06	0.8048
E:Vertical Clearance	2513220	1	2513220	676.94	**0.0000**
F:HRR	330652	1	330652	89.06	**0.0000**
Interactions					
AB	22115	1	22115	5.96	**0.0190**
AC	16475.3	1	16475.3	4.44	**0.0412**
AD	1191.89	1	1191.89	0.32	0.5740
AE	112863	1	112863	30.40	**0.0000**
AF	17968.4	1	17968.4	4.84	**0.0334**
BC	9397.61	1	9397.61	2.53	0.1191
BD	1450.94	1	1450.94	0.39	0.5353
BE	61805.1	1	61805.1	16.65	**0.0002**
BF	4473.1	1	4473.1	1.20	0.2786
CD	3002.08	1	3002.08	0.81	0.3737
CE	25587.6	1	25587.6	6.89	**0.0120**
CF	460.263	1	460.263	0.12	0.7265
DE	645.351	1	645.351	0.17	0.6789
DF	12.1017	1	12.1017	0.00	0.9547
EF	16103.3	1	16103.3	4.34	**0.0434**
Residual	155930	42	3712.62		
Total	3.40E+06	63			

Table 19. ANOVA of web maximum adiabatic temperatures for all configurations.

As before, the statistical significance of each of the effects can be presented in graphical form using the Standardized Pareto Chart and the Half Normal Probability Plot:

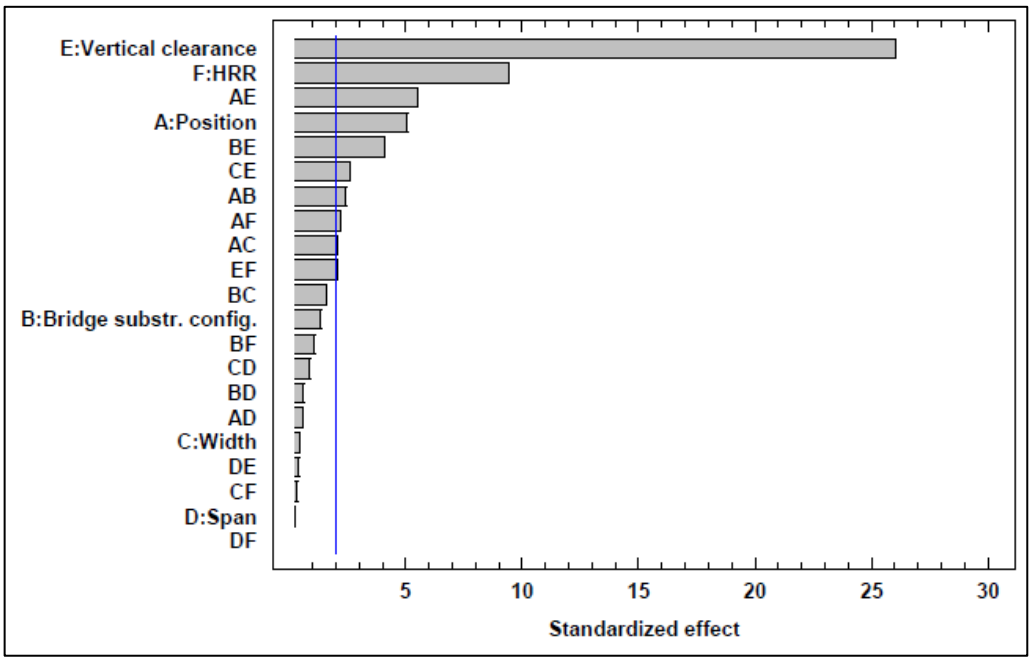

Figure 31. Standardized Pareto chart for web maximum adiabatic temperatures for all configurations

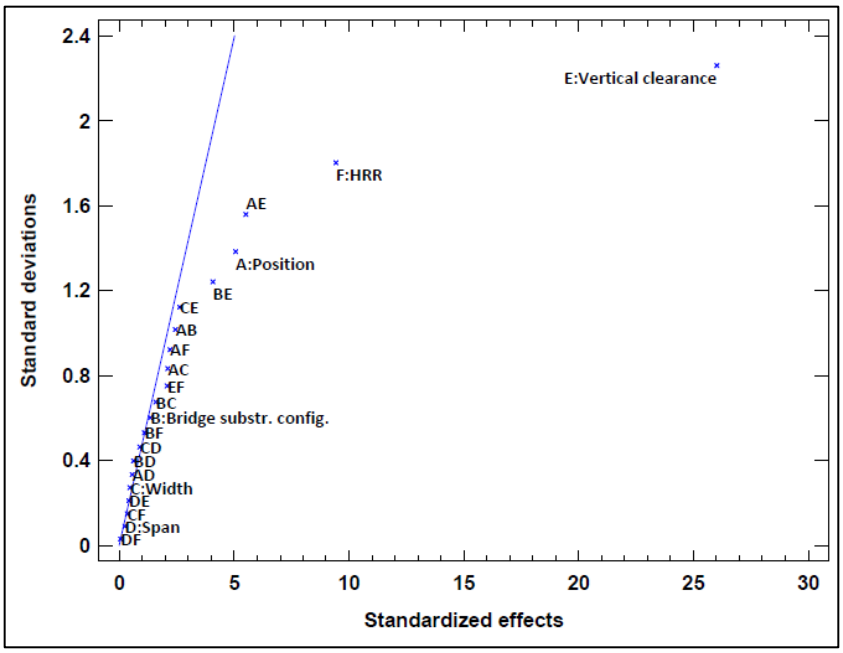

Figure 32. Half-normal probability plot for web maximum adiabatic temperatures for all configurations

Of the main effects, fire position, vertical clearance and HRR can be considered statistically significant, whilst bridge substructure configuration, width and span are not. Once again, the most significant effect is vertical clearance, with the average effect on the mean of maximum adiabatic temperatures between a bridge with a vertical clearance of five metres and 9 metres being approximately -400 ^{o}C.

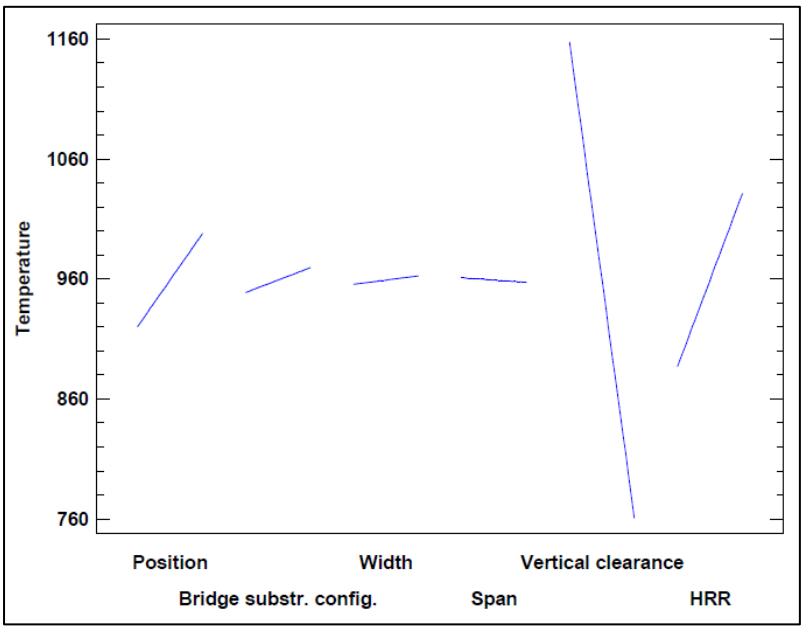

Figure 33. Main effects plot for web maximum adiabatic temperatures for all configurations

The interactions that can be considered statistically significant are fire position and vertical clearance (AE), and fire position and substructure configuration (the latter not being significant in its own right, as was the case for the bottom flange, but only when interacting with changes of vertical clearance).

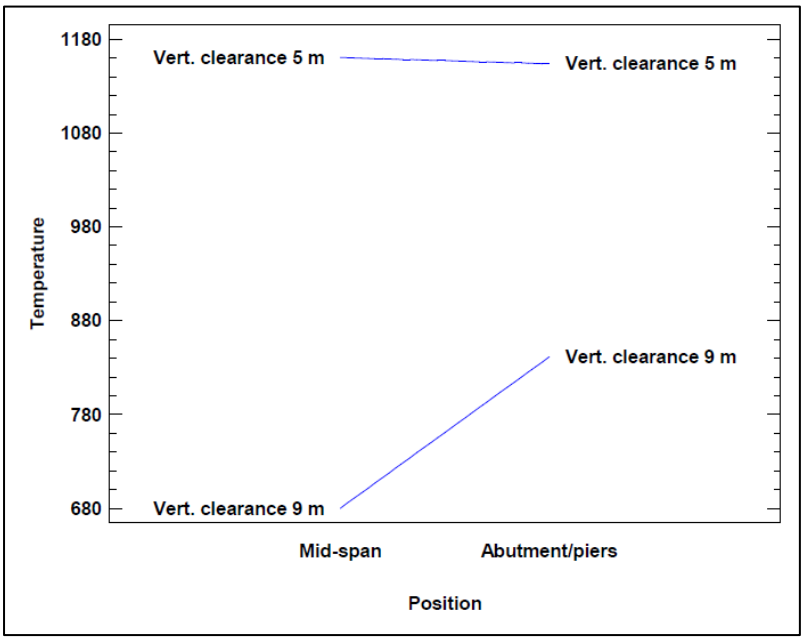

Figure 34. Fire position and vertical clearance interaction plot for web maximum adiabatic temperatures for all configurations

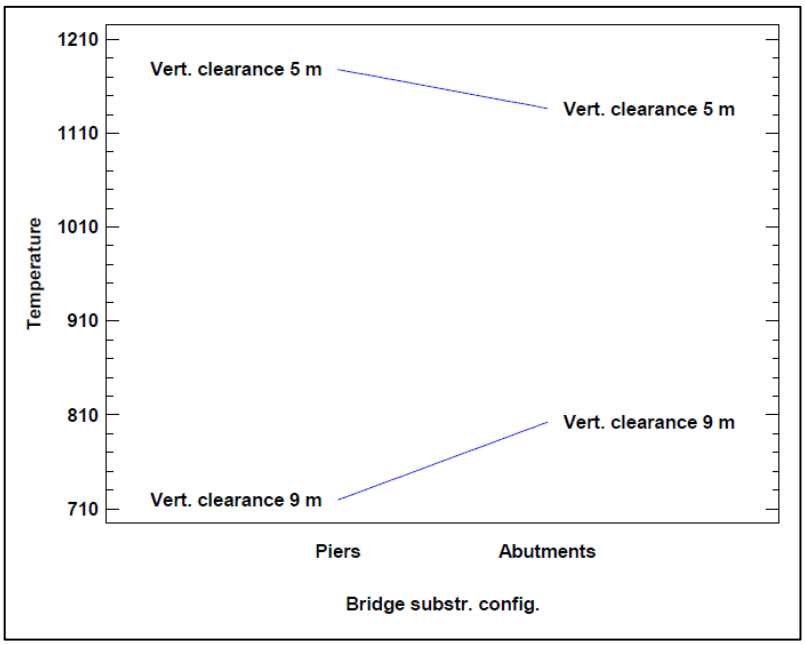

Figure 35. Bridge substructure configuration and vertical clearance interaction plot for web maximum adiabatic temperatures for all configurations

As can be seen in Figure 34, the temperature drop measured for the web due to an increase in vertical clearance from five to nine metres is smaller when the fire position is located adjacent to the bridge substructures (either abutments or piers) compared to when it is locates mid-span, as occurred in Figure 30 for the bottom flange.

In Figure 35, a similar effect can be observed, but in this case the temperature drop experienced by the web is reduced when the bridge substructure is formed by abutments instead of piers, when comparing an increase in vertical clearance from five to nine metres. Once again, this could be explained by the Coandă effect, as this is more significant in the case of an abutment than for piers, due to the larger flat surface of the former.

5.2.2. INDIVIDUAL FIRE LOCATION ANALYSIS

The following ANOVA tests are carried out on two separate subsets of the sixty-four models: one subset of thirty-two models with the fire located adjacent to the abutment or piers and another subset with thirty-two models with the fire located mid-span. As stated previously, the main reason for splitting the models into two subsets is to enable the development of independent fire curves for each fire position scenario.

Although these ANOVA tests use the same maximum adiabatic temperature data as in the global analysis of all models, and therefore in general the significant effects should be similar, some

main effects and interactions could have a greater importance when analysing these two subsets independently.

In the individual fire location analysis, for each subset of thirty-two models, there a total of five parameters and ten interactions (all two-way interactions) being studied, leading to there being sixteen residual degrees of freedom, meaning that the statistical significance of effects can still be determined with a relatively high level of confidence.

i. Fire adjacent to abutment/piers

The ANOVA results for the bottom flange maximum adiabatic temperatures for configurations with the fire located adjacent to an abutment or piers are shown in Table 20. As the position of the fire is now the same for all configurations, the parameter of fire position and its corresponding five interactions are no longer part of the ANOVA, reducing the total number of sources from twenty-one to fifteen.

FLANGE TEMPERATURES	Sum of squares	Degrees of freedom	Mean Square	F-ratio	p-value
Main Effects					
A:Bridge Substructure Config.	28976.7	1	28976.7	13.27	**0.0022**
B:Width	964.044	1	964.044	0.44	0.5159
C:Span	4243.97	1	4243.97	1.94	0.1824
D:Vertical Clearance	446938	1	446938	204.67	**0.0000**
E:HRR	57577.5	1	57577.5	26.37	**0.0001**
Interactions					
AB	41499.4	1	41499.4	19.00	**0.0005**
AC	4027.08	1	4027.08	1.84	0.1933
AD	27477.5	1	27477.5	12.58	**0.0027**
AE	3084.27	1	3084.27	1.41	0.2520
BC	6434.32	1	6434.32	2.95	0.1054
BD	38414.4	1	38414.4	17.59	**0.0007**
BE	258.895	1	258.895	0.12	0.7351
CD	460.561	1	460.561	0.21	0.6522
CE	2.25781	1	2.25781	0.00	0.9747
DE	1787.72	1	1787.72	0.82	0.3790
Residual	34939.4	16	2183.71		
Total	6.97E+05	31			

Table 20. ANOVA of bottom flange maximum adiabatic temperatures for models with fire position located adjacent to an abutment or piers

Of the main effects, bridge substructure configuration, vertical clearance and HRR can be considered statistically significant, whilst both width and span are not, as was obtained in the case of the global analysis for the bottom flange adiabatic temperatures.

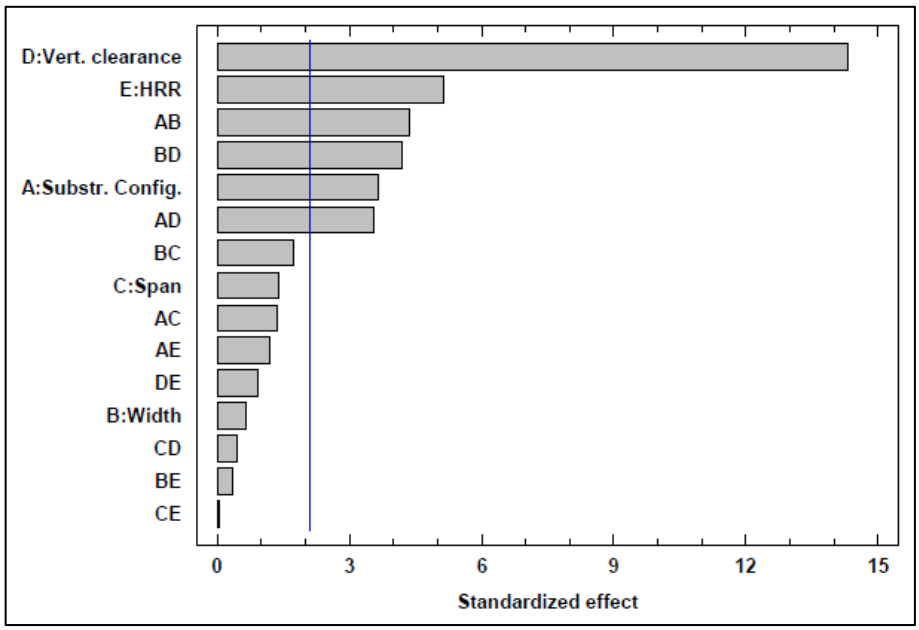

Figure 36. Standardized Pareto chart for bottom flange maximum adiabatic temperatures for models with fire position located adjacent to an abutment or piers

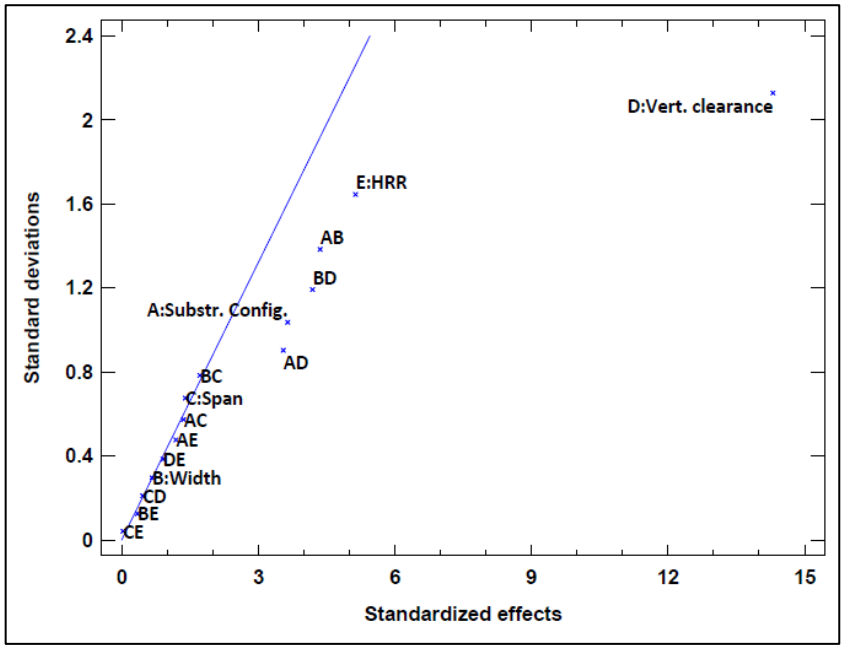

Figure 37. Half-normal probability plot for bottom flange maximum adiabatic temperatures for models with fire position located adjacent to an abutment or piers

As in the case of the global analysis, vertical clearance has the largest effect on bottom flange temperature mean, followed by the Heat Release Rate and the bridge substructure configuration, as can be observed in Figure 38.

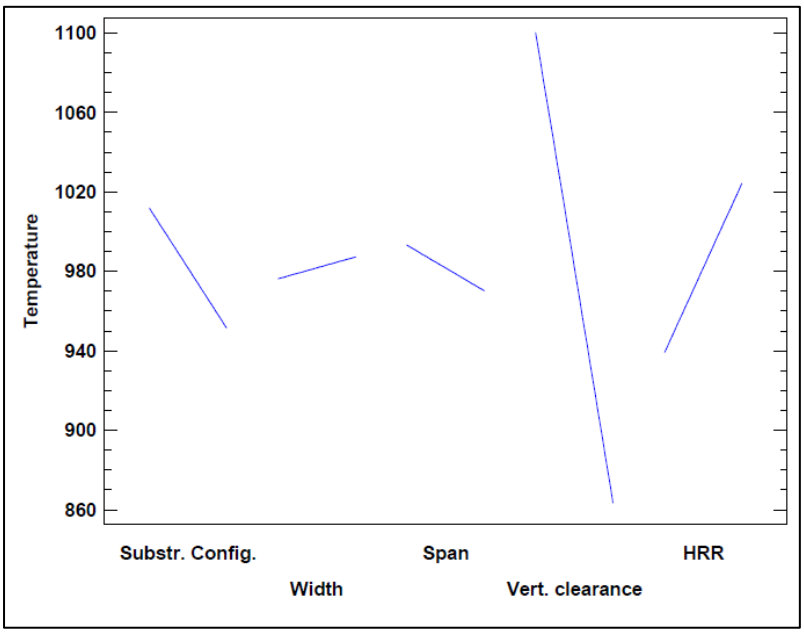

Figure 38. Main effects plot for bottom flange maximum adiabatic temperatures for models with fire position located adjacent to an abutment or piers

The most significant interactions are represented in Figure 39, and are the following: bridge substructure configurations and width (for piers, adiabatic temperatures are hire with a smaller width, whereas for abutments, the opposite is true); vertical clearance and width (when the bridge has a higher width, adiabatic temperatures suffer a smaller reduction in temperatures for a higher vertical clearance); and bridge substructure configurations and vertical clearance (the variation of adiabatic temperatures is smaller for different vertical clearances when the bridge substructures are abutments compared with when they are piers).

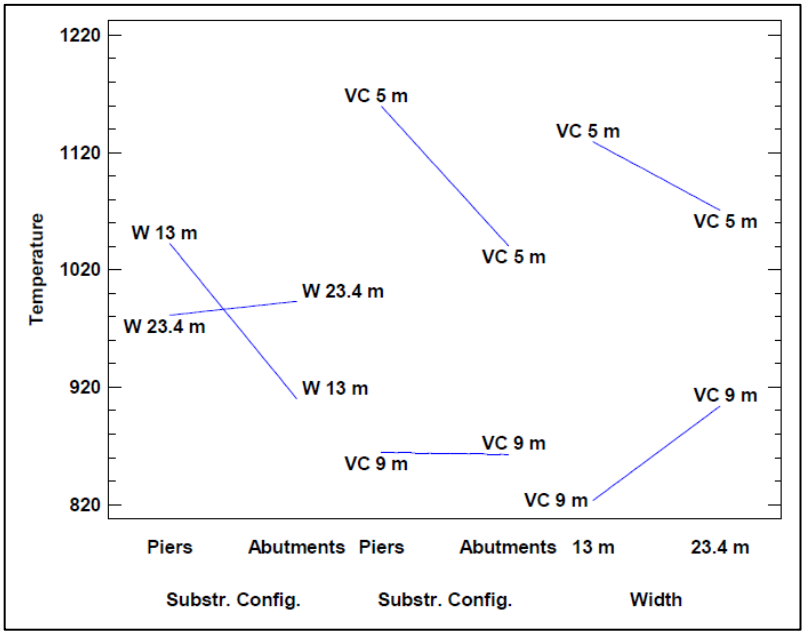

Figure 39. Significant interactions plot for bottom flange maximum adiabatic temperatures for models with fire position located adjacent to an abutment or piers

The ANOVA results for the web maximum adiabatic temperatures for configurations with the fire located adjacent to an abutment or piers are shown in Table 21.

WEB TEMPERATURES	Sum of squares	Degrees of freedom	Mean Square	F-ratio	p-value
Main Effects					
A:Bridge Substructure Config.	26784	1	26784	11.60	**0.0036**
B:Width	12247.3	1	12247.3	5.30	**0.0351**
C:Span	1233.93	1	1233.93	0.53	0.4754
D:Vertical Clearance	780453	1	780453	337.90	**0.0000**
E:HRR	97230.6	1	97230.6	42.10	**0.0000**
Interactions					
AB	27460.5	1	27460.5	11.89	**0.0033**
AC	423.914	1	423.914	0.18	0.6741
AD	127878	1	127878	55.37	**0.0000**
AE	15399.7	1	15399.7	6.67	**0.0201**
BC	1531.12	1	1531.12	0.66	0.4275
BD	38559.3	1	38559.3	16.69	**0.0009**
BE	940.587	1	940.587	0.41	0.5324
CD	146.162	1	146.162	0.06	0.8046
CE	186.583	1	186.583	0.08	0.7799
DE	4223.03	1	4223.03	1.83	0.1951
Residual	36955.2	16	2309.7		
Total	1.17E+06	31			

Table 21. ANOVA of web maximum adiabatic temperatures for models with fire position located adjacent to an abutment or piers

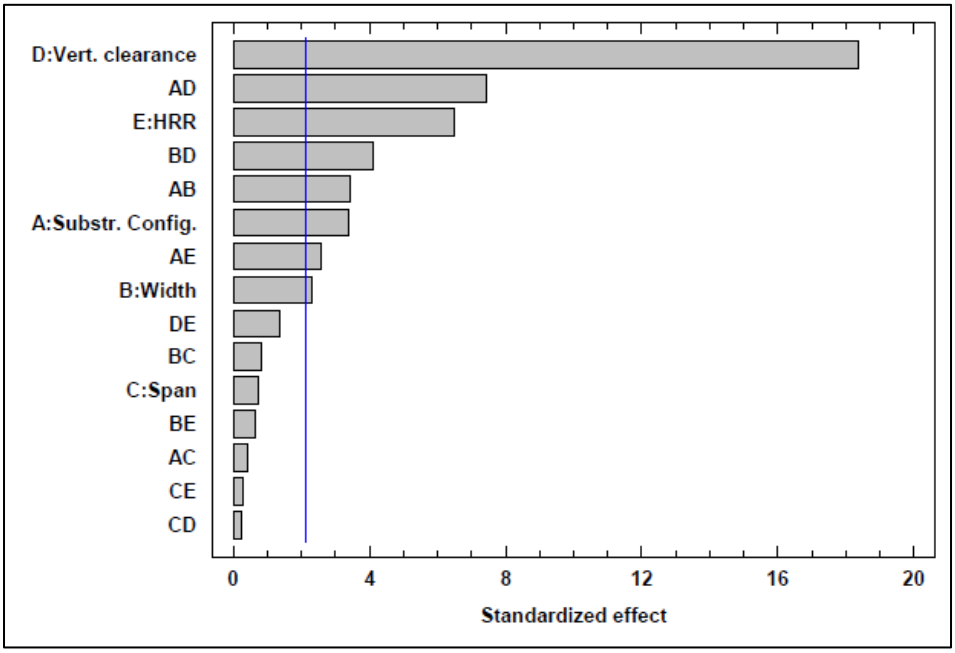

Figure 40. Standardized Pareto chart for web maximum adiabatic temperatures for models with fire position located adjacent to an abutment or piers

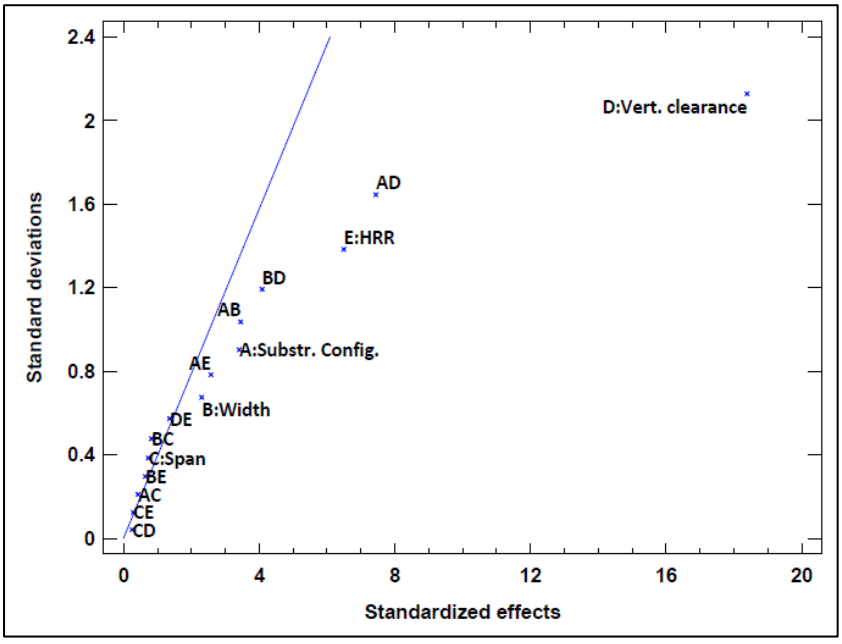

Figure 41. Half-normal probability plot for web maximum adiabatic temperatures for models with fire position located adjacent to an abutment or piers

As can be observed in Table 21, Figure 40 and Figure 41, the most significant main effects are the same as in the case of the bottom flange (bridge substructure configuration, vertical clearance and HRR), with the exception of width, which is deemed statistically significant for the web adiabatic temperatures, although the variation for the parameters two levels is relatively small (approximately thirty-nine degrees Celsius more for the larger width, on average).

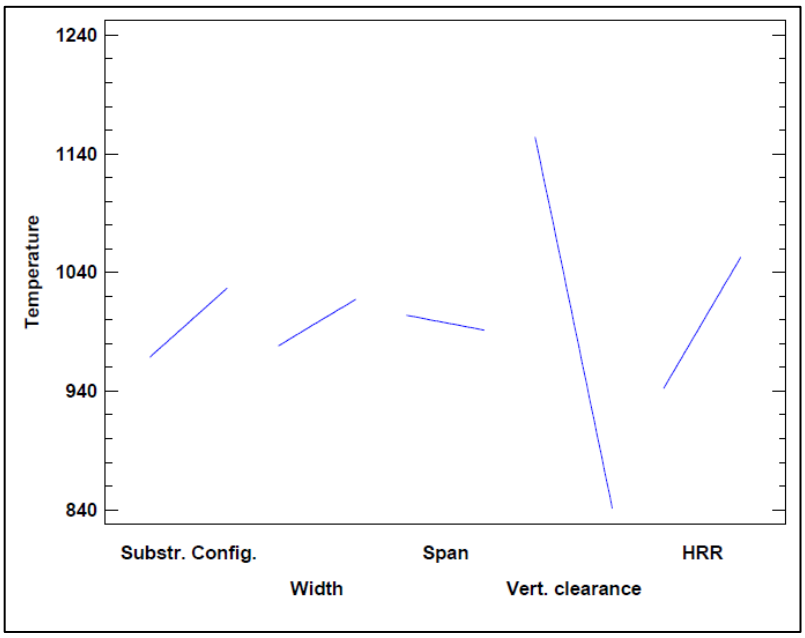

Figure 42. Main effects plot for web maximum adiabatic temperatures for models with fire position located adjacent to an abutment or piers

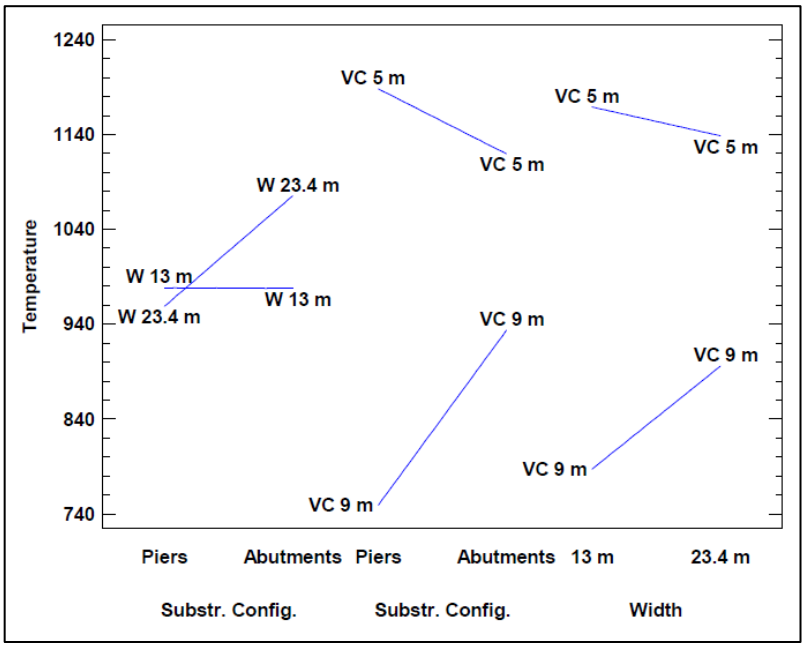

Figure 43. Significant interactions plot for web maximum adiabatic temperatures for models with fire position located adjacent to an abutment or piers

The most significant interactions are represented in Figure 43, and are identical to those obtained for the bottom flange maximum adiabatic temperature ANOVA for configurations with the fire position located adjacent to an abutment or piers.

ii. Fire located mid-span

The ANOVA results for the bottom flange maximum adiabatic temperatures for configurations with the fire located mid-span are shown in Table 22.

FLANGE TEMPERATURES	Sum of squares	Degrees of freedom	Mean Square	F-ratio	p-value
Main Effects					
A:Bridge Substructure Config.	11350.3	1	11350.3	32.60	**0.0000**
B:Width	5156.96	1	5156.96	14.81	**0.0014**
C:Span	2412.87	1	2412.87	6.93	**0.0181**
D:Vertical Clearance	1004820	1	1004820	2885.99	**0.0000**
E:HRR	138129	1	138129	396.73	**0.0000**
Interactions					
AB	1262.41	1	1262.41	3.63	**0.0750**
AC	4556.07	1	4556.07	13.09	**0.0023**
AD	24.5175	1	24.5175	0.07	0.7941
AE	1439.83	1	1439.83	4.14	**0.0589**
BC	1944.85	1	1944.85	5.59	**0.0311**
BD	1492.9	1	1492.9	4.29	**0.0549**
BE	29.5873	1	29.5873	0.08	0.7744
CD	2738.93	1	2738.93	7.87	**0.0127**
CE	307.83	1	307.83	0.88	0.3611
DE	22084.1	1	22084.1	63.43	**0.0000**
Residual	5570.75	16	348.172		
Total	1.20E+06	31			

Table 22. ANOVA of bottom flange maximum adiabatic temperatures for models with fire position located mid-span

According to the ANOVA test, all independent parameters are statistically significant, although as can be observed in Figure 44 and Figure 45, not all parameters have the same effect on the bottom flange's adiabatic temperatures.

As the significance of each parameter is calculated by comparing their variance to that of the residual degrees of freedom, the greater the variation of the mean of adiabatic temperatures between a parameters two levels will lead to a higher statistical significance.

Therefore, as the difference in the mean of adiabatic temperatures for the two levels of vertical clearance (five and nine metres) is the highest (as has been the case for all ANOVA tests performed for maximum adiabatic temperatures), it is logical that the parameter is deemed to have the highest statistical significance.

In the case of the current analysis, bottom flange maximum adiabatic temperatures for models with fire position located mid-span, the main cuantifiable effects can be associated with variations of just two parameters: vertical clearance and HRR.

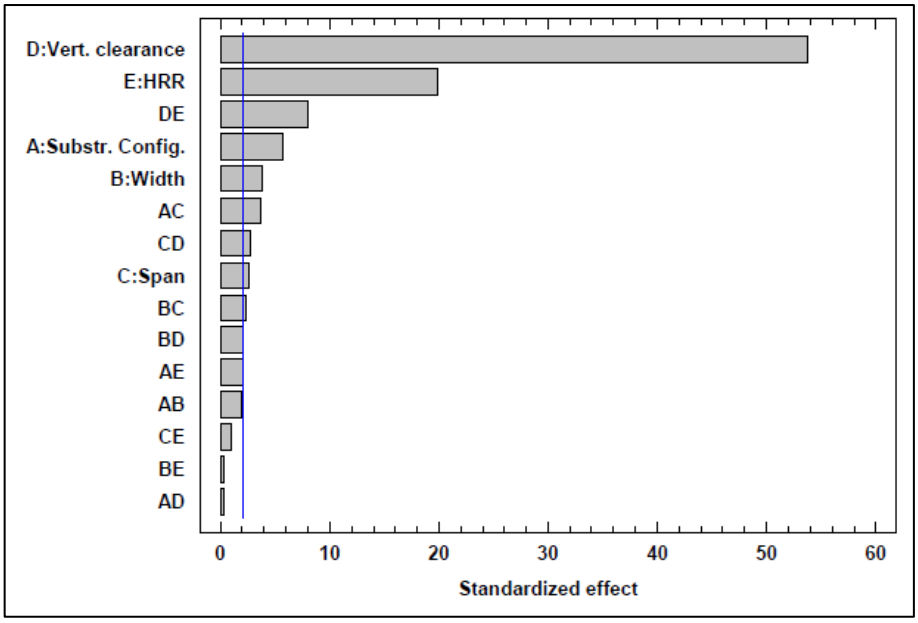

Figure 44. Standardized Pareto chart for bottom flange maximum adiabatic temperatures for models with fire position located mid-span

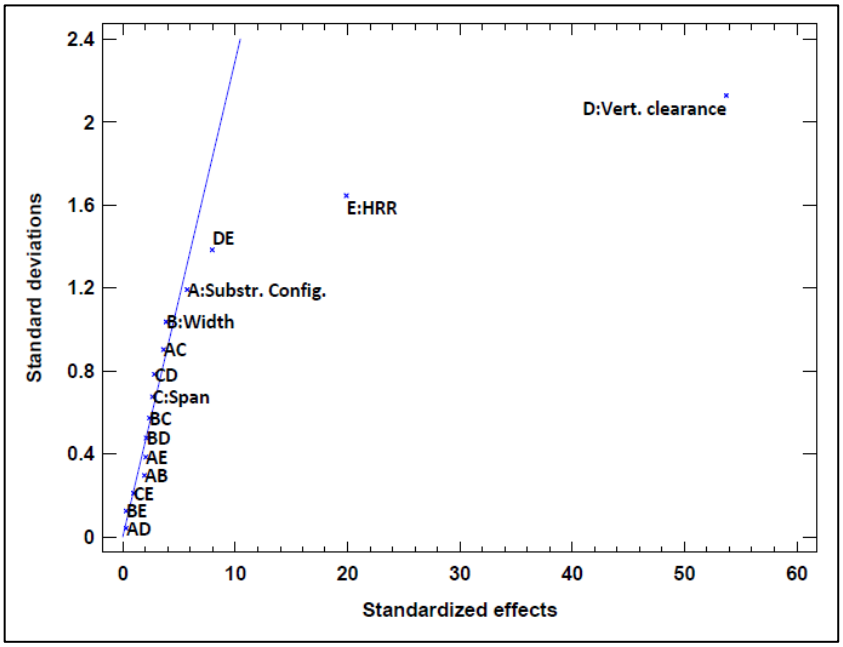

Figure 45. Half-normal probability plot for bottom flange maximum adiabatic temperatures for models with fire position located mid-span

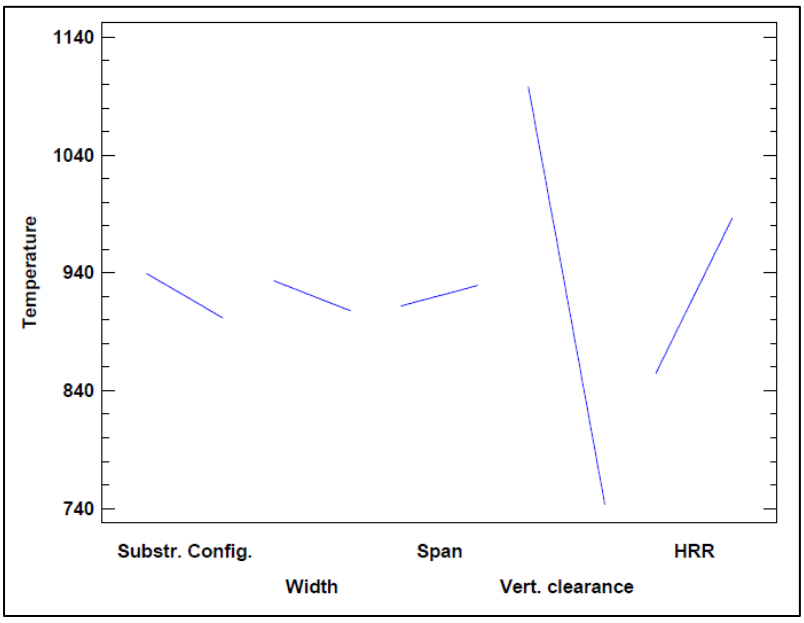

Figure 46. Main effects plot for bottom flange maximum adiabatic temperatures for models with fire position located mid-span

In the case of significant interactions, it is this relationship between the vertical clearance and HRR parameters that has the highest effect on the mean of adiabatic temperatures. As can be observed in Figure 47, for a vertical clearance of five metres, the difference in effects on the mean for the two levels of HRR is lower than that observed for a vertical clearance of nine metres.

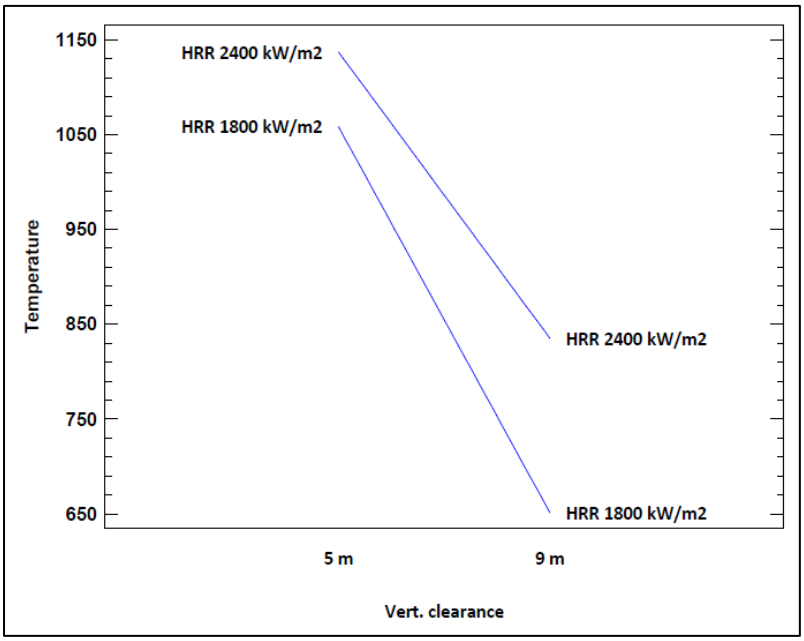

Figure 47. Vertical clearance and HRR interaction plot for bottom flange maximum adiabatic temperatures for models with fire position located mid-span

The ANOVA results for the web maximum adiabatic temperatures for configurations with the fire located mid-span are shown in Table 23Table 22.

WEB TEMPERATURES	Sum of squares	Degrees of freedom	Mean Square	F-ratio	p-value
Main Effects					
A:Bridge Substructure Config.	2176.35	1	2176.35	7.77	**0.0132**
B:Width	5020.52	1	5020.52	17.93	**0.0006**
C:Span	187.598	1	187.598	0.67	0.4251
D:Vertical Clearance	1845630	1	1845630	6590.52	**0.0000**
E:HRR	251390	1	251390	897.68	**0.0000**
Interactions					
AB	818.91	1	818.91	2.92	0.1066
AC	1107.56	1	1107.56	3.95	**0.0641**
AD	36.21	1	36.21	0.13	0.7239
AE	870.905	1	870.905	3.11	**0.0969**
BC	1471.26	1	1471.26	5.25	**0.0358**
BD	891.264	1	891.264	3.18	**0.0934**
BE	0.108112	1	0.108112	0.00	0.9846
CD	2305.54	1	2305.54	8.23	**0.0111**
CE	76.3848	1	76.3848	0.27	0.6086
DE	13105	1	13105	46.80	**0.0000**
Residual	4480.69	16	280.043		
Total	2.13E+06	31			

Table 23. ANOVA of web maximum adiabatic temperatures for models with fire position located mid-span

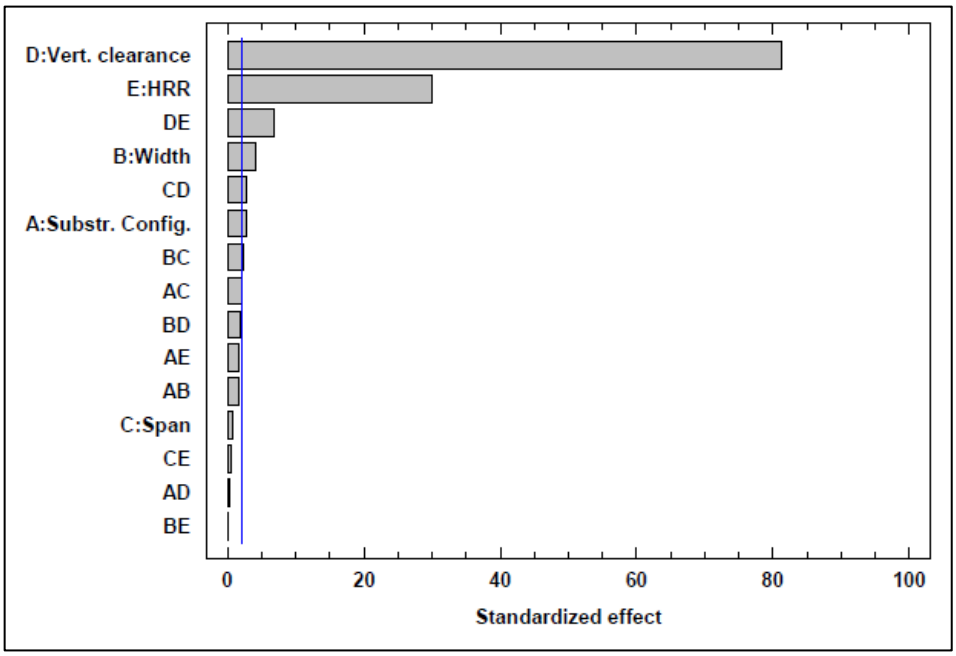

Figure 48. Standardized Pareto chart for web maximum adiabatic temperatures for models with fire position located mid-span

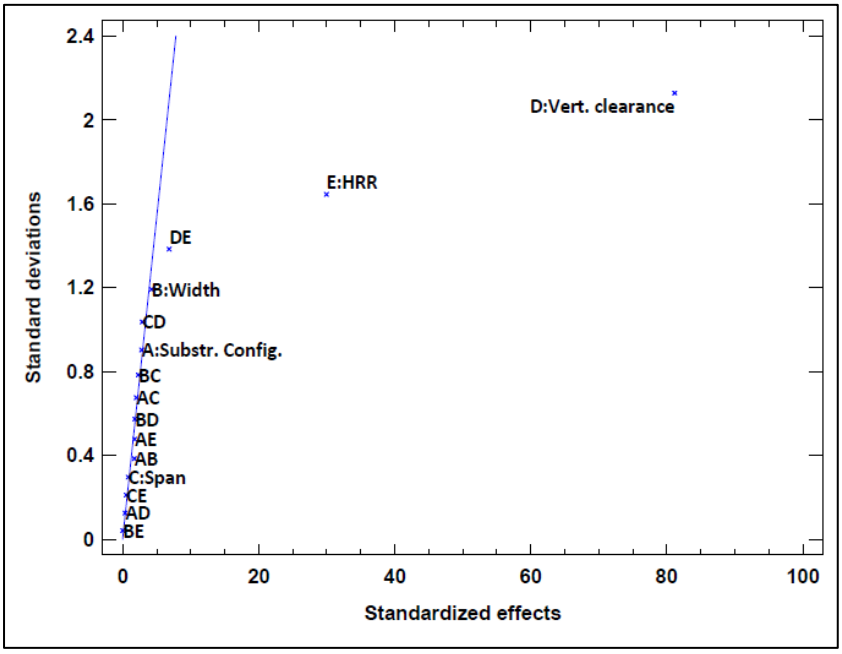

Figure 49. Half-normal probability plot for web maximum adiabatic temperatures for models with fire position located mid-span

The significant main effects for the web maximum adiabatic temperatures are practically the same as for the flange, except in this case, the absolute variations between the two levels of vertical clearance (five and nine metres) are considerably large, with an average difference of approximately four hundred and eighty degrees Celsius.

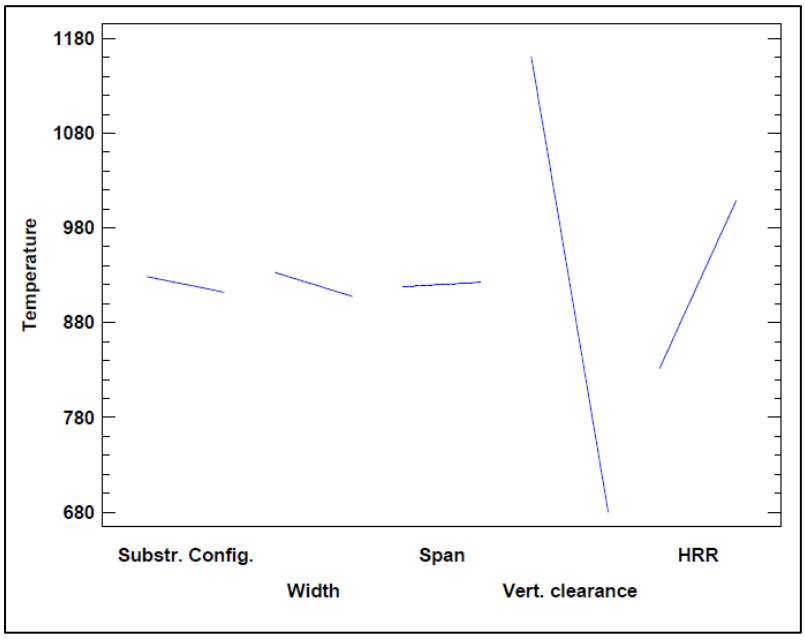

Figure 50. Main effects plot for web maximum adiabatic temperatures for models with fire position located mid-span

The most significant interaction is once again that between vertical clearance and HRR, with the same dynamic as that explained for the maximum flange adiabatic temperatures.

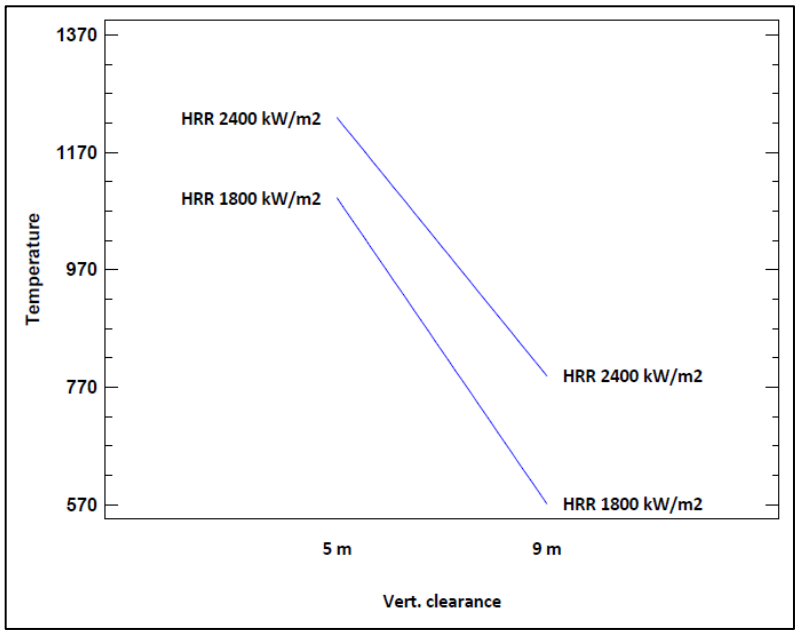

Figure 51. Vertical clearance and HRR interaction plot for web maximum adiabatic temperatures for models with fire position located mid-span

5.3. RELATIVE POSITION TEMPERATURES

The following section provides a summary of the ANOVA tests of the adiabatic temperatures observed for each of the sixty-four bridge configurations analysed, depending on their relative position.

As described in *Section 4. FDS analysis,* the adiabatic temperatures for each configuration have been obtained along the central I-girder, for both the bottom flange and web, every 0.2 metres. In order to determine each parameters significance on adiabatic temperatures depending on their relative position, individual analyses will be carried out for the sensors located at either end of the I-girders (X/L = 0 and X/L = 1) and for the nine deciles that divide the girder/beam into 10 equal parts (X/L = 0.1, X/L = 0.2, X/L = 0.3, X/L = 0.4, X/L = 0.5, X/L = 0.6, X/L = 0.7, X/L = 0.8 and X/L = 0.9). Therefore, due to the positions being defined in relative terms, bridge configurations with different spans can be easily compared and analysed using ANOVA tests.

It should be noted that when the fire position is located adjacent to an abutment or piers, this corresponds to the relative position X/L = 1, whereas when it is located mid-span, the fire position corresponds to relative position X/L = 0.5. The results of the ANOVA tests for these

particular points will be similar to those obtained for the maximum temperature analysis, as depending on fire position, they are associated with the highest adiabatic temperatures (directly above the fire source).

The results for the individual ANOVA tests for each relative position (X/L = 0, …, X/L = 1) and subset (global analysis or individual fire location analyses) can be found in *APPENDIX 2: ANOVA INPUT DATA AND DETAILED RESULTS*APPENDIX 1: FDS average temperatures.

5.3.1. GLOBAL ANALYSIS

In the global analysis, all sixty-four configurations are taken into account, with a total of six parameters and fifteen interactions (all two-way interactions) being studied for each of the defined relative positions (at either end and for the nine deciles).

Table 24 provides a summary of the relative position ANOVA tests for the bottom flange:

FLANGE TEMP.	X/L=0	X/L=0.1	X/L=0.2	X/L=0.3	X/L=0.4	X/L=0.5	X/L=0.6	X/L=0.7	X/L=0.8	X/L=0.9	X/L=1
Main Effects											
A:Position	**0.0049**	**0.0000**	**0.0000**	**0.0000**	**0.0000**	**0.0000**	**0.0000**	0.0587	**0.0000**	**0.0000**	**0.0000**
B:Subst. Config.	**0.0000**	**0.0000**	**0.0000**	**0.0000**	**0.0000**	**0.0000**	**0.0000**	**0.0000**	**0.0000**	**0.0000**	0.1165
C:Width	0.5823	**0.0000**	**0.0000**	**0.0001**	**0.0038**	0.1199	**0.0279**	**0.0067**	**0.0303**	0.1033	0.6013
D:Span	**0.0000**	**0.0000**	**0.0000**	**0.0000**	**0.0000**	**0.0002**	**0.0000**	**0.0000**	**0.0000**	**0.0000**	**0.0000**
E:Vert. Clear.	**0.0000**	**0.0000**	**0.0000**	**0.0000**	**0.0000**	**0.0000**	**0.0000**	**0.0000**	**0.0000**	**0.0000**	**0.0000**
F:HRR	**0.0000**	**0.0000**	**0.0000**	**0.0000**	**0.0000**	**0.0000**	**0.0000**	**0.0000**	**0.0000**	**0.0000**	**0.0000**
Interactions											
AB	**0.0000**	**0.0000**	**0.0000**	**0.0000**	**0.0000**	**0.0000**	**0.0000**	**0.0000**	0.0919	**0.0109**	**0.0000**
AC	**0.0309**	0.1056	0.0868	**0.0148**	**0.0018**	**0.0013**	**0.0023**	0.3085	0.5151	0.6912	0.2054
AD	0.2144	0.3614	0.2178	0.0527	0.2063	**0.0000**	0.5640	0.2546	0.5768	0.9993	**0.0000**
AE	**0.0011**	**0.0447**	0.9680	0.1616	0.6690	**0.0000**	**0.0437**	**0.0100**	**0.0003**	**0.0166**	0.8601
AF	0.0965	0.1291	0.5300	0.8173	0.2471	0.1612	0.3326	0.6635	0.5176	0.9283	0.4183
BC	**0.0009**	0.1848	0.2084	**0.0396**	**0.0399**	0.1414	**0.0267**	**0.0339**	0.3966	0.4078	**0.0005**
BD	**0.0267**	0.2596	0.5801	0.1994	0.0837	0.8162	0.4343	0.9673	0.0895	0.5043	0.2628
BE	**0.0020**	**0.0000**	**0.0000**	**0.0000**	**0.0000**	**0.0018**	**0.0001**	**0.0000**	**0.0001**	0.3318	0.9418
BF	0.5333	0.1528	**0.0357**	**0.0222**	0.0682	0.0866	**0.0280**	**0.0089**	0.1655	0.9067	0.7356
CD	**0.0104**	0.7443	0.7730	0.7637	0.8175	0.8682	0.9802	0.9323	0.8545	0.7264	**0.0132**
CE	**0.0122**	0.0598	0.1202	0.2178	0.1592	0.1122	0.2793	0.1706	0.1246	0.0899	**0.0088**
CF	0.5726	0.3281	0.3455	0.3824	0.4963	0.5452	0.5677	0.4245	0.5649	0.7862	0.9467
DE	0.0875	0.0961	0.1659	0.1082	0.0852	0.7655	**0.0341**	**0.0172**	0.1795	0.1383	0.1273
DF	0.8926	0.9058	0.9019	0.7394	0.4516	0.7055	0.2935	0.5552	0.7224	0.6985	0.5756
EF	0.6926	0.3457	0.2233	0.4056	0.9905	0.2421	0.9392	0.1194	0.1924	0.3571	0.7796

Table 24. Summary of ANOVA tests for the bottom flange relative position adiabatic temperatures for all configurations.

The results of the eleven individual ANOVA tests show that all six parameters studied can be considered to have a significant effect on the bottom flanges adiabatic temperatures for any of the relative positions studied, with one exception: the bridges width.

The ANOVA tests for relative positions corresponding with mid-span and either end show that width does not appear to have a significant effect on the bottom flange adiabatic temperatures. This result is coherent with those obtained in the maximum temperature analysis, where it was determined that width did not have a significant effect on the maximum adiabatic temperatures.

In general, the most significant interactions are those between fire position and the bridges substructure configuration, fire position and vertical clearance, and width and vertical clearance, although depending on the relative position, other interactions can be considered significant.

In Table 25, a summary of the relative position ANOVA tests for the web is provided:

WEB TEMP.	X/L=0	X/L=0.1	X/L=0.2	X/L=0.3	X/L=0.4	X/L=0.5	X/L=0.6	X/L=0.7	X/L=0.8	X/L=0.9	X/L=1
Main Effects											
A:Position	0.0000	0.0000	0.0000	0.0000	0.0000	0.0000	0.0000	0.2567	0.0000	0.0000	0.0000
B:Subst. Config.	0.0000	0.0000	0.0000	0.0000	0.0000	0.0000	0.0000	0.0000	0.0000	0.0000	0.0190
C:Width	0.0032	0.0012	0.0030	0.0152	0.0965	0.3172	0.3014	0.1389	0.0831	0.0886	0.1914
D:Span	0.0000	0.0000	0.0000	0.0000	0.0000	0.0002	0.0000	0.0000	0.0000	0.0000	0.0009
E:Vert. Clear.	0.0000	0.0000	0.0000	0.0000	0.0000	0.0000	0.0000	0.0000	0.0000	0.0000	0.0000
F:HRR	0.0000	0.0000	0.0000	0.0000	0.0000	0.0000	0.0000	0.0000	0.0000	0.0000	0.0000
Interactions											
AB	0.0000	0.0000	0.0000	0.0000	0.0000	0.0000	0.0000	0.0000	0.0000	0.0000	0.2879
AC	0.0420	0.0309	0.0180	0.0068	0.0030	0.0037	0.0039	0.0184	0.0857	0.2051	0.3166
AD	0.1021	0.1951	0.1919	0.0936	0.0106	0.0001	0.2648	0.8796	0.9952	0.1700	0.0074
AE	0.0000	0.0000	0.0000	0.0000	0.0000	0.0000	0.0000	0.0001	0.0050	0.1284	0.8679
AF	0.0295	0.0229	0.0171	0.0070	0.0031	0.0156	0.0138	0.1094	0.4529	0.6878	0.5578
BC	0.1039	0.0638	0.0624	0.0765	0.1415	0.2424	0.1549	0.0734	0.0578	0.0570	0.0566
BD	0.8729	0.3828	0.3765	0.3841	0.4538	0.9094	0.8693	0.6990	0.2823	0.3133	0.7875
BE	0.0253	0.0002	0.0003	0.0024	0.0363	0.1674	0.2454	0.4280	0.9214	0.1052	0.0067
BF	0.9995	0.4952	0.4017	0.4031	0.4542	0.5689	0.8729	0.7502	0.3920	0.1763	0.2195
CD	0.7151	0.8579	0.8301	0.7681	0.7516	0.7461	0.7239	0.7500	0.7385	0.6562	0.4570
CE	0.0054	0.0056	0.0055	0.0048	0.0030	0.0036	0.0026	0.0029	0.0054	0.0181	0.0289
CF	0.3710	0.3828	0.4119	0.4211	0.4422	0.4874	0.5216	0.5725	0.6360	0.7161	0.7477
DE	0.0297	0.0299	0.0378	0.0545	0.1772	0.8237	0.3734	0.2669	0.3025	0.3502	0.2688
DF	0.9536	0.8550	0.8483	0.8521	0.8862	0.8281	0.8069	0.7450	0.8346	0.9277	0.7926
EF	0.5791	0.3346	0.2870	0.4204	0.9125	0.3294	0.9077	0.4024	0.3696	0.6326	0.8549

Table 25. Summary of ANOVA tests for the web relative position adiabatic temperatures for all configurations.

As in the case of the bottom flange ANOVA tests, all six parameters studied have a significant effect on the adiabatic temperatures measured for each of the eleven relative positions, with the exception of width in those relative positions associated with the maximum temperatures (mid-span and adjacent to abutments). This does not mean that width is not relevant to the adiabatic temperatures, as it is involved in numerous interactions with other parameters, such as position, and in the case of the web especially, vertical clearance.

This last interaction is considered significant for every relative position, and is probably related to the influence of these two parameters (width and vertical clearance) on the size of the body of air under the bridge, as well as the potential entry of air, which controls the build-up of heat and smoke under the superstructure

5.3.2. INDIVIDUAL FIRE LOCATION ANALYSIS

The following relative position ANOVA tests are carried out on two separate subsets of the sixty-four models: one subset of thirty-two models with the fire located adjacent to the abutment or piers and another subset with thirty-two models with the fire located mid-span. As stated previously, the main reason for splitting the models into two subsets is to enable the development of independent fire curves for each fire position scenario.

These ANOVA tests use the same relative position adiabatic temperature data as in the global analysis of all models, and therefore in general the significant effects should be similar, some main effects and interactions could have a greater importance when analysing these two subsets independently.

In the individual fire location analysis, for each subset of thirty-two models, there a total of five parameters and ten interactions (all two-way interactions) being studied, as the fire location parameter and its five corresponding interactions with each of the other parameters no longer have two levels due to the segregation of the models.

i. Fire adjacent to abutment/piers

A summary of the ANOVA results for the relative position adiabatic temperatures for configurations with the fire located adjacent to an abutment or piers are shown in Table 26 for the bottom flange and in Table 27 for the web.

As the position of the fire is now the same for all configurations, the parameter of fire position and its corresponding five interactions are no longer part of the ANOVA, reducing the total number of sources from twenty-one to fifteen.

FLANGE TEMP.	X/L=0	X/L=0.1	X/L=0.2	X/L=0.3	X/L=0.4	X/L=0.5	X/L=0.6	X/L=0.7	X/L=0.8	X/L=0.9	X/L=1
Main Effects											
A:Substr. Config.	0.0000	0.0000	0.0000	0.0000	0.0000	0.0000	0.0000	0.0000	0.0000	0.0066	0.0022
B:Width	0.0963	0.0033	0.0029	0.0010	0.0002	0.0001	0.0006	0.0252	0.2391	0.2649	0.5159
C:Span	0.0001	0.0001	0.0000	0.0000	0.0000	0.0000	0.0000	0.0000	0.0000	0.0000	0.1824
D:Vert. Clear.	0.0000	0.0000	0.0000	0.0000	0.0000	0.0000	0.0000	0.0000	0.0000	0.0000	0.0000
E:HRR	0.0100	0.0021	0.0006	0.0002	0.0000	0.0000	0.0000	0.0000	0.0000	0.0000	0.0001
Interactions											
AB	0.0152	0.1826	0.2090	0.0754	0.0092	0.0014	0.0026	0.0436	0.2438	0.1736	0.0005
AC	0.7204	0.2160	0.2312	0.1288	0.0351	0.0166	0.1346	0.6695	0.1365	0.2746	0.1933
AD	0.0914	0.0017	0.0002	0.0000	0.0000	0.0000	0.0000	0.0015	0.5949	0.0040	0.0027
AE	0.7176	0.3700	0.1489	0.0787	0.0374	0.0186	0.0162	0.0448	0.4543	0.4003	0.2520
BC	0.2725	0.9519	0.9690	0.9431	0.7734	0.4614	0.3586	0.4438	0.7951	0.9948	0.1054
BD	0.0107	0.0199	0.0267	0.0381	0.0463	0.0353	0.0191	0.0045	0.0019	0.0013	0.0007
BE	0.3839	0.3252	0.3491	0.3286	0.3437	0.3204	0.3281	0.4063	0.5632	0.7252	0.7351
CD	0.3479	0.5364	0.4472	0.4782	0.2911	0.1121	0.0949	0.0868	0.3321	0.1991	0.6522
CE	0.9906	0.9441	0.9572	0.9436	0.7513	0.6984	0.9906	0.9441	0.9572	0.9436	0.7513
DE	0.6213	0.8683	0.7259	0.4889	0.3081	0.2189	0.6213	0.8683	0.7259	0.4889	0.3081

Table 26. Summary of ANOVA tests for the bottom flange relative position adiabatic temperatures for for models with fire position located adjacent to an abutment or piers.

WEB TEMP.	X/L=0	X/L=0.1	X/L=0.2	X/L=0.3	X/L=0.4	X/L=0.5	X/L=0.6	X/L=0.7	X/L=0.8	X/L=0.9	X/L=1
Main Effects											
A:Subst. Config.	0.0000	0.0000	0.0000	0.0000	0.0000	0.0000	0.0000	0.0000	0.0000	0.0000	0.0035
B:Width	0.0123	0.0080	0.0082	0.0088	0.0116	0.0185	0.0300	0.0376	0.0401	0.0207	0.0365
C:Span	0.0001	0.0001	0.0000	0.0000	0.0000	0.0001	0.0002	0.0012	0.0006	0.0158	0.4702
D:Vert. Clear.	0.0000	0.0000	0.0000	0.0000	0.0000	0.0000	0.0000	0.0000	0.0000	0.0000	0.0000
E:HRR	0.0018	0.0004	0.0001	0.0001	0.0000	0.0000	0.0000	0.0000	0.0000	0.0000	0.0000
Interactions											
AB	0.1383	0.1196	0.1041	0.0784	0.0607	0.0582	0.0645	0.0644	0.0495	0.0114	0.0033
AC	0.2835	0.2778	0.2702	0.2712	0.2922	0.4012	0.6705	0.9183	0.3100	0.1739	0.6670
AD	0.2632	0.0229	0.0145	0.0185	0.0382	0.1168	0.3877	0.8843	0.1021	0.0002	0.0000
AE	0.9862	0.6907	0.5550	0.5420	0.6339	0.8387	0.8545	0.4931	0.1637	0.0135	0.0216
BC	0.9234	0.9803	0.9674	0.9431	0.8690	0.7820	0.7828	0.8717	0.9922	0.7894	0.4229
BD	0.0115	0.0098	0.0085	0.0070	0.0051	0.0036	0.0026	0.0020	0.0017	0.0008	0.0009
BE	0.3211	0.3392	0.3567	0.3604	0.3681	0.3893	0.4166	0.4644	0.5219	0.5345	0.5359
CD	0.3051	0.3295	0.2821	0.2405	0.2157	0.2664	0.4213	0.5865	0.7272	0.8530	0.7891
CE	0.9315	0.9991	0.9867	0.9453	0.8934	0.9009	0.9422	0.9721	0.8597	0.6673	0.7955
DE	0.8452	0.8399	0.6292	0.4982	0.4297	0.4210	0.4509	0.5187	0.6689	0.8700	0.1864

Table 27. Summary of ANOVA tests for the web relative position adiabatic temperatures for for models with fire position located adjacent to an abutment or piers.

In the case of the bottom flange adiabatic temperatures, all five parameters have a significant effect on the adiabatic temperatures for the majority of the relative positions. In the case of the bridges width, the ANOVA tests for relative positions near the fire source (X/L = 0.8 to X/L = 1) indicate that the parameter is not statistically significant, as is also the case for the effect of the bridges span on adiabatic temperatures in the immediate vicinity of the fire (X/L = 1). It is logical that these parameters have greater significance the further we are from the fire source, as the temperatures of these relative positions depend more on the absolute distance to the fire, as well as the ventilation conditions.

For the web adiabatic temperatures, it has been determined that width does have a significant effect for all relative positions. This is due to the fact that the gasses/smoke in contact with the web are confined in between neighbouring I-girders, and therefore, the greater the width, the more I-girders present, and the more difficult it is for the gasses/smoke in contact with the central I-girder to escape, causing an increased build-up in adiabatic temperatures.

ii. Fire located mid-span

In Table 28 and Table 29, a summary of the ANOVA results for the relative position adiabatic temperatures for models with the fire located mid span are shown, for the bottom flange and web respectively.

FLANGE TEMP.	X/L=0	X/L=0.1	X/L=0.2	X/L=0.3	X/L=0.4	X/L=0.5	X/L=0.6	X/L=0.7	X/L=0.8	X/L=0.9	X/L=1
Main Effects											
A:Substr. Config.	**0.0000**	**0.0000**	**0.0000**	**0.0000**	0.1312	**0.0004**	**0.0000**	**0.0000**	**0.0000**	**0.0000**	**0.0000**
B:Width	0.0786	**0.0001**	**0.0000**	**0.0022**	0.4066	**0.0019**	**0.0191**	**0.0073**	**0.0000**	**0.0001**	**0.0369**
C:Span	**0.0000**	**0.0000**	**0.0000**	**0.0000**	**0.0000**	0.1813	**0.0000**	**0.0000**	**0.0000**	**0.0000**	**0.0000**
D:Vert. Clear.	**0.0000**	**0.0000**	**0.0000**	**0.0000**	**0.0000**	**0.0000**	**0.0000**	**0.0000**	**0.0000**	**0.0000**	**0.0000**
E:HRR	**0.0000**	**0.0000**	**0.0000**	**0.0000**	**0.0000**	**0.0000**	**0.0000**	**0.0000**	**0.0000**	**0.0000**	**0.0000**
Interactions											
AB	**0.0051**	0.7641	0.7105	0.0548	0.5573	0.1094	0.9579	0.1305	0.7527	0.7787	**0.0062**
AC	**0.0000**	0.9437	**0.0336**	0.7903	0.2319	**0.0005**	0.2292	0.3250	**0.0054**	0.7871	0.3810
AD	**0.0007**	**0.0000**	**0.0000**	**0.0000**	**0.0012**	0.8542	**0.0006**	**0.0000**	**0.0000**	**0.0000**	**0.0002**
AE	0.4608	0.0500	**0.0050**	**0.0056**	0.0609	0.0922	**0.0108**	**0.0031**	**0.0009**	**0.0082**	0.4062
BC	**0.0010**	0.2098	0.2019	0.1492	**0.0145**	**0.0468**	**0.0034**	0.0914	0.1328	0.0946	**0.0010**
BD	0.4548	0.1903	**0.0219**	**0.0120**	0.7801	0.0763	**0.0056**	**0.0009**	**0.0018**	0.0575	0.3953
BE	0.7620	0.8086	0.7462	0.9298	0.9070	0.6987	0.6812	0.6509	0.3925	0.6999	0.7489
CD	**0.0422**	**0.0014**	**0.0110**	**0.0006**	**0.0000**	**0.0490**	**0.0000**	**0.0028**	**0.0057**	**0.0011**	**0.0050**
CE	0.7492	0.8547	0.7644	0.2725	**0.0035**	0.4757	**0.0001**	0.1065	0.5732	0.2743	0.1627
DE	0.0941	**0.0017**	**0.0018**	0.3441	**0.0003**	**0.0000**	**0.0005**	**0.0300**	**0.0001**	**0.0002**	0.0620

Table 28. Summary of ANOVA tests for the bottom flange relative position adiabatic temperatures for for models with fire position located mid-span.

WEB TEMP.	X/L=0	X/L=0.1	X/L=0.2	X/L=0.3	X/L=0.4	X/L=0.5	X/L=0.6	X/L=0.7	X/L=0.8	X/L=0.9	X/L=1
Main Effects											
A:Subst. Config.	**0.0471**	**0.0000**	**0.0000**	**0.0142**	**0.0440**	**0.0265**	0.0791	**0.0000**	**0.0000**	**0.0000**	**0.0001**
B:Width	**0.0471**	**0.0229**	0.1640	0.5105	**0.0059**	**0.0006**	**0.0002**	**0.0122**	0.9575	0.0903	0.2538
C:Span	**0.0000**	**0.0000**	**0.0000**	**0.0000**	**0.0000**	0.6686	**0.0000**	**0.0000**	**0.0000**	**0.0000**	**0.0000**
D:Vert. Clear.	**0.0000**	**0.0000**	**0.0000**	**0.0000**	**0.0000**	**0.0000**	**0.0000**	**0.0000**	**0.0000**	**0.0000**	**0.0000**
E:HRR	**0.0000**	**0.0000**	**0.0000**	**0.0000**	**0.0000**	**0.0000**	**0.0000**	**0.0000**	**0.0000**	**0.0000**	**0.0000**
Interactions											
AB	0.3797	0.1674	0.2008	0.6164	0.3559	0.1147	0.2264	0.5584	0.0745	**0.0483**	0.1676
AC	**0.0023**	0.4862	0.4846	0.5339	0.4676	**0.0355**	**0.0198**	0.0931	0.0841	0.1724	0.7311
AD	**0.0001**	**0.0000**	**0.0000**	**0.0019**	0.3025	0.6508	0.0644	**0.0000**	**0.0000**	**0.0000**	**0.0000**
AE	0.9487	0.2309	0.2390	0.2448	0.1520	0.1085	0.1419	0.0988	0.0563	0.0541	0.6570
BC	0.2654	0.4203	0.2938	0.1412	0.0601	**0.0392**	**0.0111**	**0.0134**	**0.0333**	**0.0368**	**0.0248**
BD	0.2408	0.5103	0.5575	0.4400	0.1051	0.1021	0.5534	0.7069	0.8251	0.7577	0.2084
BE	0.8550	0.8558	0.8230	0.8764	0.9611	0.9660	0.7339	0.6123	0.7732	0.9471	0.9957
CD	**0.0001**	**0.0001**	**0.0002**	**0.0017**	0.2421	**0.0135**	0.3777	**0.0015**	**0.0001**	**0.0000**	**0.0000**
CE	0.5691	0.4635	0.4619	0.6013	0.9028	0.6287	0.3935	**0.0475**	**0.0237**	**0.0138**	**0.0083**
DE	**0.0069**	**0.0058**	**0.0175**	0.4325	**0.0029**	**0.0000**	**0.0179**	0.1265	**0.0011**	**0.0003**	**0.0011**

Table 29. Summary of ANOVA tests for the web relative position adiabatic temperatures for for models with fire position located mid-span.

For both the bottom flange and web adiabatic temperature located over the fire source (X/L = 0.5), all parameters are considered significant, except the bridges span. For the rest of relative positions, the span does have a significant effect on the measured temperatures, as the absolute distance between adjacent deciles is entirely dependent on the bridges span (2.4 metres in the case of bridges with a span of 24 metres, and 1.6 metres for bridges of 16 metres).

The span also has an influence when considering its interactions with other parameters, especially in the case of its interaction with vertical clearance, which is deemed to be statistically significant for practically all relative positions of both the bottom flange and web. When comparing bridges with different vertical clearances, the drop in temperatures between a bridge with a vertical clearance of nine metres compared to a bridge with five metres is lower when the bridge has a span of sixteen metres versus when the span is of twenty-four metres.

This shows, that although the parameters studied might not always be significant when compared independently, they can have a significant influence on adiabatic temperatures when studied as a combination with other parameters.

6. DEVELOPMENT OF FIRE CURVES

In this section, a proposal for design fire curves will be developed, taking into account the results of the ANOVA tests presented in *Section 5. Statistical analysis of the influence of different parameters on the adiabatic temperatures generated in I-girder bridge fires*, using multiple linear regression (MLR) models.

These MLR models are used to predict the adiabatic temperatures using a linear function of the independent parameters defined in this report, for both the maximum and relative position adiabatic temperatures, and the global and individual fire location analyses.

The accuracy of each regression model is verified using the coefficient of determination (R^2), which indicates the proportion of the dependent variable (adiabatic temperatures) that is predictable from the independent parameters (and interactions), and by plotting the observed and predicted temperatures in order to graphically check if the model can be considered a "good fit".

In order to simplify the regression prediction models, an iterative calculation contrasting the of number of parameters and interactions versus the coefficient of determination (R^2) for each calculation is carried out. Where parameters or interactions are identified that have little effect on the overall coefficient of determination, they are removed from that predictive regression model, even if found to have been to be "significant" in the corresponding ANOVA test.

In the case of the relative position adiabatic temperatures, each MLR predictive model will be associated with one point of the design fire curve, and the representation of all eleven points (either end of the bridges superstructure and the nine intermediary deciles) will define this curve. Each fire curve will be associated with either the bottom flange or the web, and for one of the scenarios considered: global analysis or individual fire position analyses

At the end of the section, the design fire curves will be contrasted with the adiabatic temperatures of three test models, which did not form part of the initial sixty-four FDS models used to develop the MLR models.

6.1. MULTIPLE LINEAR REGRESSION

Multiple linear regression models analyse the possible relation between the variation of a dependent variable (such as adiabatic temperatures) and the value of independent parameters/factors (in the case only one parameter is studied, then a linear regression model is sufficient), proposing a predictive model that fits the observed data, with the following structure:

$$Y = \beta_0 + \beta_1 \cdot x_1 + \cdots + \beta_i \cdot x_i + \beta_j \cdot x_m \cdot x_n + \cdots + \beta_k \cdot x_r \cdot x_s$$

where m, n, r and s belong to [1, i].

This equation defines the multiple linear regression models used in this report, where Y is the dependent variable (adiabatic temperatures), x_1 to x_i are the independent parameters, β_0 is the model constant and β_1 to β_k are the partial regression coefficients, responsible for describing the effect of each independent parameter on the dependent variable.

As can be observed, this particular equation includes interactions between parameters, with their own individual partial regression coefficients. Therefore, an interactions relationship with the mean is considered linear, and therefore modifies the linear relationship between its individual independent parameters and the dependent variable (amplifying or diminishing its effect).

6.1.1. MODEL ESTIMATION

The estimation of the optimum model constant (β_0) and partial regression coefficients (β_1, …, β_k) has been carried out using Statgraphics Centurion 18, using both the *Multiple Regression* and *Regression Model Selection* modules.

The method used for estimating the optimum coefficients is intrinsically related with the Analysis of Variance (ANOVA) method, by comparing the sum of squares of each parameter to the residual sum of squares.

i. Multiple Regression module

The *Multiple Regression* module allows the fitting of the model to be carried out using various techniques: Ordinary Least Squares, Forward Stepwise Selection, Backwards Stepwise Selection and other optimization methods.

The Ordinary Least Squares method includes all independent parameters (defined by the user) in the model, determining the optimum partial regression coefficients for each, whilsth the stepwise selection methods add or remove (for the forwards and backwords methods respectively) independent parameters from the model based on their significance on the variance of the dependant variable (using the ANOVA technique).

For the following report, the independent parameters and interactions defined for each MLR model are those obtained for each individual ANOVA test carried out in Section 5, including maximum and relative position temperatures, and for the global and individual fire location analyses.

The Backwards Stepwise Selection method has been used to perform the fitting of the models, removing parameters and interactions that are deemed to be nonsignificant. The reason for additional parameters being removed after their significance had already been tested using the ANOVA tests is due the iterative nature of this calculation, as each removal increases the residual degrees of freedom, and allows a more precise determination of the significance each parameter to be achieved, which can lead to additional parameters being removed.

ii. Regression Model Selection module

The Regression Model Selection module calculates MLR models for all the possible combinations of independent parameters (and interactions) defined and provides a summary of the best models based on the models with the best fit (measured using the adjusted R^2 coefficient).

The best models for each number of independent parameters can be plotted, allowing the user to determine the optimum number of coefficients to include in the MLR model, based on the drop in the adjusted R^2 coefficient.

This report uses the first module to obtain an initial MLR model, and then contrasts this with the second module, to determine if any additional independent parameters or interactions can be

remover in order to simplify the associated equation without causing a significant drop in the predictive capability of the model (principle of parsimony).

6.1.2. HIERARCHY PRINCIPLE

In this report it should be noted that some MLR models are nonhierarchical, meaning that the inclusion of an interaction between two independent parameters in the regression model does not mean that those independent parameters have to be included in the model as main effects.

This contravenes the "*Hierarchy Principle*" [5, 6], which states that the exclusion of main effects included in higher-order interactions alters the meaning of these interactions, and therefore they should not be excluded, even if these main effects are deemed to be statistically insignificant (based on the F-test or associated P-value).

However, according to Montgomery et al. [7], "leaving highly insignificant terms in the model for the sake of hierarchy can increase standard errors and result in poor prediction. Parsimony in empirical modelling is often an important virtue", and as the main objective for this report is the development of design fire curves that offer the best prediction of adiabatic temperatures compared to the FDS models analysed, the hierarchical principle has not been applied.

6.1.3. COEFFICIENT OF MULTIPLE DETERMINATION (R^2)

The coefficient of multiple determination, also known as the R^2 coefficient, is used to determine the predictive capability or "fit" of the model for the observed data (used to determine the MLR partial regression coefficients).

It can be calculated determining the relation between the sum of the sum of squares associated with each independent parameter/interaction (or using the complementary residual sum of squares) and the total sum of squares of the dependant variable:

$$R^2 = \frac{SS_{parameters}}{SS_{total}} = 1 - \frac{SS_{residual}}{SS_{total}}$$

As the more parameters or interactions that are included in the model would lead to a higher R^2 coefficient, which could lead to nonsignificant parameters being included in the model, the adjusted R^2 coefficient is generally used, which takes into account the relation of the number of residual degrees of freedom and the total degrees of freedom:

$$\bar{R}^2 = 1 - \frac{SS_{residual}/df_{res}}{SS_{total}/df_{total}}$$

$$\bar{R}^2 = 1 - (1 - R^2) \cdot \frac{n-1}{n-p-1}$$

where p is the total number independent parameters and interactions in the MLR model (not including the constant term) and n is the total size of the sample (either 32 or 64 depending on the analysis).

6.1.4. INDIVIDUAL MLR MODEL VALIDATION

Although the adjusted R^2 coefficient is a good measure of the global predictive accuracy of an MLR model, it does not analyse the presence of anomalous results associated with the comparison of predicted and observed values of the dependant variable.

Using the multiple linear regression equation obtained for each individual model, the observed and predicted values for the dependant variable (in this case adiabatic temperatures) are represented on a scatterplot, allowing the goodness of fit to be checked graphically. The closer the points are to the X = y line, the better the fit.

The deviation of the predicted values from the experimental data is easier to see if the former are represented versus the studentized residuals, allowing unusual residuals to be identified, which could be down to an over-simplified model, or anomalous data.

6.1.5. MLR MODEL RESULTS

The results for the individual multiple linear regression models, for both the maximum and relative position adiabatic temperatures (X/L = 0, …, X/L = 1), and each subset (global analysis or individual fire location analyses) can be found in *APPENDIX 3: Multiple regression analysis results.* In the case of the global analysis for the relative position adiabatic temperatures, a further reduction of independent parameters/interactions was carried out, and their results are provided separately.

In order to demonstrate the methodology followed for carrying out the multiple linear regression model estimations, the MLR model associated with the bottom flange maximum adiabatic temperatures of models with fire position located mid-span is presented hereafter.

i. ANOVA results

The full ANOVA results for the bottom flange maximum adiabatic temperatures of models with fire position located mid-span are shown in Table 22.

The independent parameters and interactions determined to be statistically significant will be used as the basis for developing the multiple linear regression model. They were the following: bridge substructure configuration (A); width (B), span (C), vertical clearance (D); HRR (E); AB; AC; AE; BC; BD; CD and DE (five main effects and six interacions).

ii. MLR model - Backwards Stepwise Regression

Whilst the initial parameters were admitted with a P-value of less than 0.1 (in order to not prematurely eliminate potential significant effects from the model), Statgraphics Centurion 18 Backwards Stepwise Regression method performs an iterative ANOVA test to eliminate the remaining nonsignificant main effects and/or interactions (P-value more than 0.05). The following script shows the steps of this analysis, with the corresponding adjusted R^2 coefficient for each iteration:

"Stepwise regression
Method: backward selection
P-to-enter: 0.05
P-to-remove: 0.05

Step 0:
12 variables in the model. 19 d.f. for error.
R-squared = 99.51% Adjusted R-squared = 99.20% MSE = 312.247

Step 1:
Removing variable Span with P7-to-remove =0.909813
11 variables in the model. 20 d.f. for error.
R-squared = 99.51% Adjusted R-squared = 99.24% MSE = 296.84

Step 2:
*Removing variable Bridge Substructure Configuration*Width with P7-to-remove =0.0524177*
10 variables in the model. 21 d.f. for error.
R-squared = 99.40% Adjusted R-squared = 99.12% MSE = 342.819

Step 3:
*Removing variable Bridge Substructure Configuration*HRR with P7-to-remove =0.0531226*
9 variables in the model. 22 d.f. for error.
R-squared = 99.28% Adjusted R-squared = 98.99% MSE = 392.684

Step 4:
*Removing variable Width*Vertical Clearance with P7-to-remove =0.0640564*
8 variables in the model. 23 d.f. for error.
R-squared = 99.16% Adjusted R-squared = 98.87% MSE = 440.519

Step 5:
Removing variable HRR with P7-to-remove =0.0643144
7 variables in the model. 24 d.f. for error.
R-squared = 99.02% Adjusted R-squared = 98.73% MSE = 491.481

Final model selected."

Therefore, the fitted model has a total of seven independent parameters (three main effects and four interactions), with an adjusted R^2 coefficient of 98.73%. The estimation of the optimum model constant (β_0) and partial regression coefficients (β_i) allow us to obtain the model equation:

$$Max.Temp.Bot.Flange = 1604.01 - 157.685 \cdot Bridge\ Substructure\ Configuration - 10.1718 \cdot Width - 133.763 \cdot Vertical\ Clearance + 6.00092 \cdot Bridge\ Substructure\ Configuration \cdot Span + 0.386526 \cdot Width \cdot Span - 1.12597 \cdot Span \cdot Vertical\ Clearance + 0.0322291 \cdot Vertical\ Clearance \cdot HRR$$

iii. MLR model - Regression Model Selection module

The Regression Model Selection module carries out a "brute force calculation" of all possible combinations of the seven main effects and interactions determined in the Backwards Stepwise Regression method to determine the best adjusted R^2 coefficient for each number of parameters.

MSE	R^2	adjusted R^2	Parameters
491.48	99.02	98.73	BSC, VC, HRR, BSCxWidth, BSCxSpan,VCxHRR
575.05	98.81	98.52	BSC, VC, HRR, BSCxWidth, BSCxSpan, BSCxHRR,VCxHRR
616.92	98.67	98.41	BSC, VC, BSCxWidth, BSCxSpan,VCxHRR
677.49	98.48	98.25	VC, BSCxWidth, BSCxSpan,VCxHRR
848.85	98.02	97.81	VC, BSCxWidth, VCxHRR
1377.64	96.68	96.45	VC, VCxHRR
6616.7	83.50	82.95	VC

Table 30. Regression Model Selection for bottom flange maximum adiabatic temperatures of models with fire position located mid-span

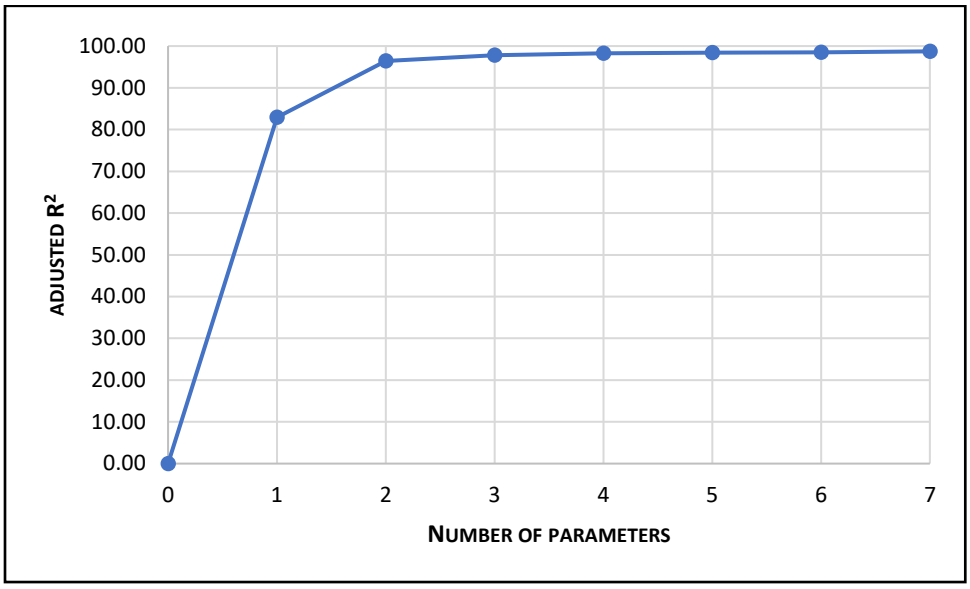

Figure 52. Regression Model Selection plot for bottom flange maximum adiabatic temperatures of models with fire position located mid-span

The analysis suggests that the bottom flange maximum adiabatic temperatures of models with fire position located mid-span only require two parameters for a very good fit of the maximum temperatures, as the ANOVA test suggested, due to the relative significance of vertical clearance and HRR (see Figure 44).

Either way, the model obtained with seven parameters will be used to show how to carry out the individual model validation.

iv. Individual model validation

The individual model validation is carried out by comparing the observed adiabatic temperatures in the FDS simulations to the predicted adiabatic temperatures obtained using the multiple linear regression.

These temperatures are provided in Table 31, whilst Figure 53 represents the data on a scatterplot, allowing the goodness of fit to be checked graphically. The closer the points are to the X = Y line, the better the fit. In this case, the predicted model can be considered a very good fit for almost all the configurations.

Figure 53 includes the confidence intervals corresponding to an error of 20%, based on the value of the observed temperatures, in order to better appreciate the deviation of predicted temperatures.

Model	Substructure Config.	Width	Span	Vert. Clear.	HRR	CFD Temp.	Pred. Temp.
3	Piers	23.4 m	24 m	5 m	2400 kW/m2	1137.6 ºC	1165.9 ºC
4	Piers	23.4 m	24 m	5 m	1800 kW/m2	1083.3 ºC	1069.2 ºC
7	Piers	23.4 m	24 m	9 m	2400 kW/m2	836.0 ºC	832.1 ºC
8	Piers	23.4 m	24 m	9 m	1800 kW/m2	664.8 ºC	658.1 ºC
11	Piers	23.4 m	16 m	5 m	2400 kW/m2	1145.3 ºC	1138.6 ºC
12	Piers	23.4 m	16 m	5 m	1800 kW/m2	1074.5 ºC	1041.9 ºC
15	Piers	23.4 m	16 m	9 m	2400 kW/m2	841.6 ºC	840.8 ºC
16	Piers	23.4 m	16 m	9 m	1800 kW/m2	680.5 ºC	666.8 ºC
19	Piers	13.0 m	24 m	5 m	2400 kW/m2	1153.2 ºC	1175.2 ºC
20	Piers	13.0 m	24 m	5 m	1800 kW/m2	1097.1 ºC	1078.5 ºC
23	Piers	13.0 m	24 m	9 m	2400 kW/m2	844.6 ºC	841.4 ºC
24	Piers	13.0 m	24 m	9 m	1800 kW/m2	672.3 ºC	667.4 ºC
27	Piers	13.0 m	16 m	5 m	2400 kW/m2	1156.6 ºC	1180.0 ºC
28	Piers	13.0 m	16 m	5 m	1800 kW/m2	1092.0 ºC	1083.3 ºC
31	Piers	13.0 m	16 m	9 m	2400 kW/m2	872.0 ºC	882.3 ºC
32	Piers	13.0 m	16 m	9 m	1800 kW/m2	678.6 ºC	708.3 ºC
35	Abutments	23.4 m	24 m	5 m	2400 kW/m2	1148.6 ºC	1152.2 ºC
36	Abutments	23.4 m	24 m	5 m	1800 kW/m2	1059.3 ºC	1055.5 ºC
39	Abutments	23.4 m	24 m	9 m	2400 kW/m2	828.1 ºC	818.5 ºC
40	Abutments	23.4 m	24 m	9 m	1800 kW/m2	636.8 ºC	644.4 ºC
43	Abutments	23.4 m	16 m	5 m	2400 kW/m2	1052.4 ºC	1076.9 ºC
44	Abutments	23.4 m	16 m	5 m	1800 kW/m2	924.6 ºC	980.2 ºC
47	Abutments	23.4 m	16 m	9 m	2400 kW/m2	806.4 ºC	779.2 ºC
48	Abutments	23.4 m	16 m	9 m	1800 kW/m2	605.5 ºC	605.1 ºC
51	Abutments	13.0 m	24 m	5 m	2400 kW/m2	1165.5 ºC	1161.5 ºC
52	Abutments	13.0 m	24 m	5 m	1800 kW/m2	1080.8 ºC	1064.8 ºC
55	Abutments	13.0 m	24 m	9 m	2400 kW/m2	821.0 ºC	827.8 ºC
56	Abutments	13.0 m	24 m	9 m	1800 kW/m2	638.5 ºC	653.7 ºC
59	Abutments	13.0 m	16 m	5 m	2400 kW/m2	1138.2 ºC	1118.4 ºC
60	Abutments	13.0 m	16 m	5 m	1800 kW/m2	1054.8 ºC	1021.7 ºC
63	Abutments	13.0 m	16 m	9 m	2400 kW/m2	832.7 ºC	820.6 ºC
64	Abutments	13.0 m	16 m	9 m	1800 kW/m2	633.9 ºC	646.6 ºC

Table 31. Predicted adiabatic temperatures for bottom flange maximum adiabatic temperatures of models with fire position located mid-span

Figure 54 shows the studentized residuals of the adiabatic temperatures of each model. In this case, only one unusual residual is detected, corresponding to Model 44. Overall, the MLR model can be concluded to be a very good fit to the observed data.

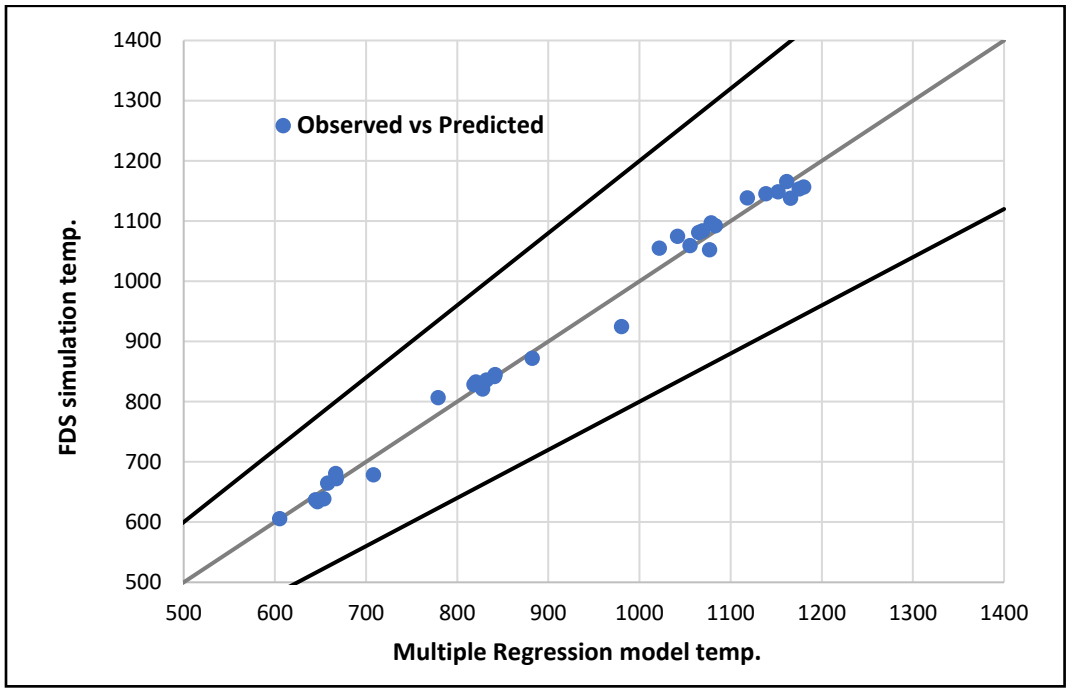

Figure 53. Measured vs predicted adiabatic temperatures for bottom flange maximum adiabatic temperatures of models with fire position located mid-span

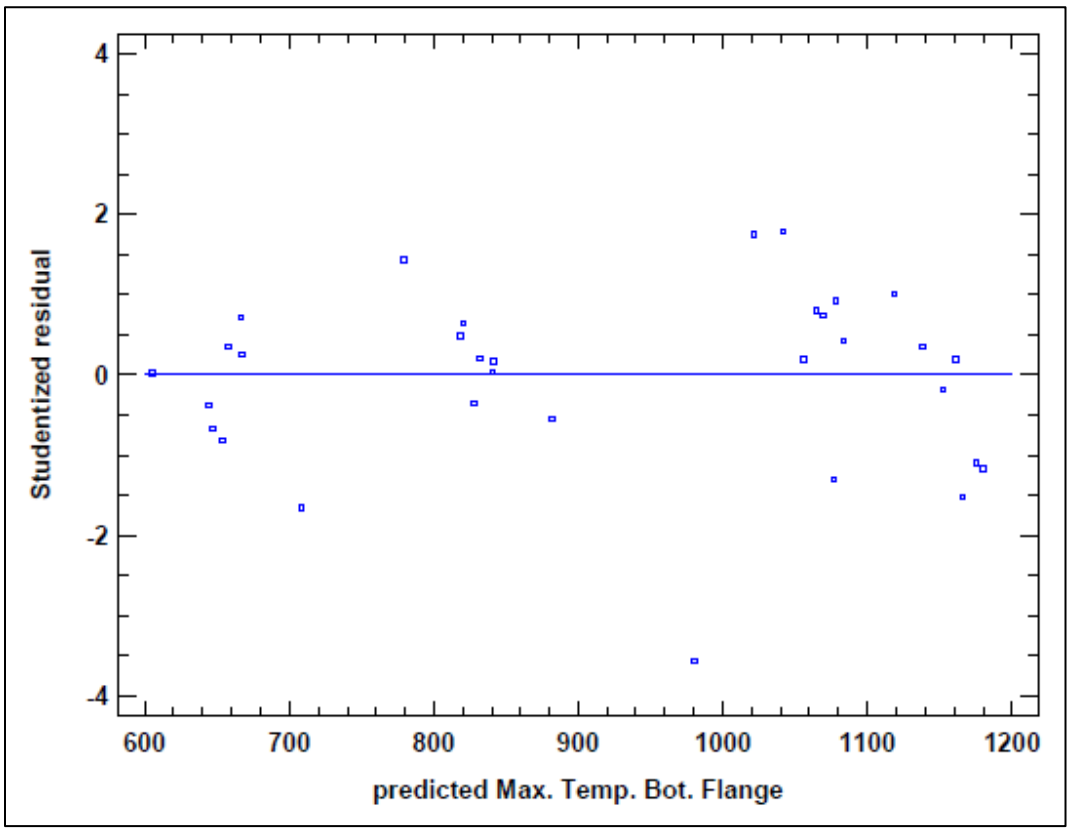

Figure 54. Studentized residuals of predicted adiabatic temperatures for bottom flange maximum adiabatic temperatures of models with fire position located mid-span

6.2. FIRE CURVES

The fitted multiple linear regression models obtained for each relative position, for both the bottom flange and web, depending on the analysis performed (global or individual fire location analyses), can be used to determine design fire curves capable of predicting the adiabatic temperatures of a bridge's superstructure.

The full results of these proposed fire curves can be found in *APPENDIX 4: Design Fire Curves,* and are provided both in graphical format (as a comparison of the sixty-four FDS model adiabatic temperatures and the predicted adiabatic temperatures for bridges with said configurations) and in matrix form, which allows the partial regression coefficients and model constant to be viewed for each relative position.

BOTTOM FLANGE FIRE CURVE	X/L=0	X/L=0.1	X/L=0.2	X/L=0.3	X/L=0.4	X/L=0.5	X/L=0.6	X/L=0.7	X/L=0.8	X/L=0.9	X/L=1
Constant	788.203	470.456	525.964	692.326	744.810	1069.090	1012.620	824.589	519.012	675.654	876.399
Position	-333.104	-176.759	-196.894	-349.192	-545.484	-852.511	-451.065	-151.301	0	159.005	272.857
Bridge Substructure Config.	0	395.226	251.123	0	203.650	131.744	0	0	284.412	85.756	0
Width	0	5.145	5.017	0	0	0	0	0	2.216	0	0
Span	-16.785	-12.530	-12.813	-12.626	-14.022	0	-24.529	-21.039	-12.382	-11.893	-19.387
Vertical Clearance	-49.485	-31.253	-22.861	-19.158	-23.281	-76.142	-51.601	-46.443	-32.075	-56.541	-59.731
HRR	0.147	0.159	0.116	0.097	0.177	0.188	0.131	0.113	0.161	0.190	0.161
Position - Bridge Substructure Config.	240.348	240.701	254.489	287.198	322.696	310.459	210.165	119.275	0	0	-160.500
Position - Width	0	0	0	4.925	7.481	6.775	5.233	0	0	0	0
Position - Span	0	0	0	0	0	-15.709	0	0	0	0	16.507
Position - Vertical Clearance	24.486	0	0	0	0	57.658	10.245	10.860	15.953	17.584	0
Position - HRR	0	0	0	0	0	0	0	0	0	0	0
Bridge Substructure Config. - Width	5.500	0	0	4.866	0	0	0	4.110	0	0	5.512
Bridge Substructure Config. - Span	7.755	0	0	0	0	0	0	0	0	0	0
Bridge Substructure Config. - Vertical Clearance	-23.437	-40.122	-46.768	-40.045	-29.965	-23.272	-21.255	-26.360	-23.012	0	0
Bridge Substructure Config. - HRR	0	0	0.082	0.118	0	0	0.083	0.088	0	0	0
Width - Span	0	0	0	0	0	0	0	0	0	0	0
Width - Vertical Clearance	0	0	0	0	0	0	0	0	0	0	0
Width - HRR	0	0	0	0	0	0	0	0	0	0	0
Span - Vertical Clearance	0	0	0	0	0	0	1.349	1.248	0	0	0
Span - HRR	0	0	0	0	0	0	0	0	0	0	0
Vertical Clearance - HRR	0	0	0	0	0	0	0	0	0	0	0

Table 32. Design fire curve for bottom flange adiabatic temperatures

6.2.1. INITIAL VALIDATION

In order to perform an initial validation test of the proposed design fire curves, three more FDS models (not considered in the development of the multiple linear regression models) are calculated, allowing the observed fire curve adiabatic temperatures along the bottom flange and web of the central I-girder to be compared to those predicted by the different fire curve models.

The values of the parameters proposed for the test models are shown in TABLE. As parameters such as width, span and vertical clearance are considered continuous variables (as is HRR, but

the values have been maintained as either 1800 or 2400 kW/m^2), meaning they can adopt values between the two defined levels defined in the design of experiments of the current report, as well as certain values outside of these levels, although the applicable limits will have to be determined by performing a thorough validation with multiple tests for each parameter.

Model	Position	Bridge Substructure Configuration	Width	Span	Vertical Clearance	HRR
Test 1	Abutment	Piers	13.0 m	20.0 m	7.0 m	2400 kW/m2
Test 2	Abutment	Abutments	18.0 m	13.0 m	8.0 m	1800 kW/m2
Test 3	Mid-span	Abutments	18.0 m	18.0 m	6.0 m	2400 kW/m2

Table 33. Bridge configuration for test models

The results of the adiabatic temperatures for the FDS models and the corresponding design fire curves (for each of the three types designed depending on the data subset and number of independent parameters) are compared in the following figures, for both the bottom flange and web adiabatic temperatures:

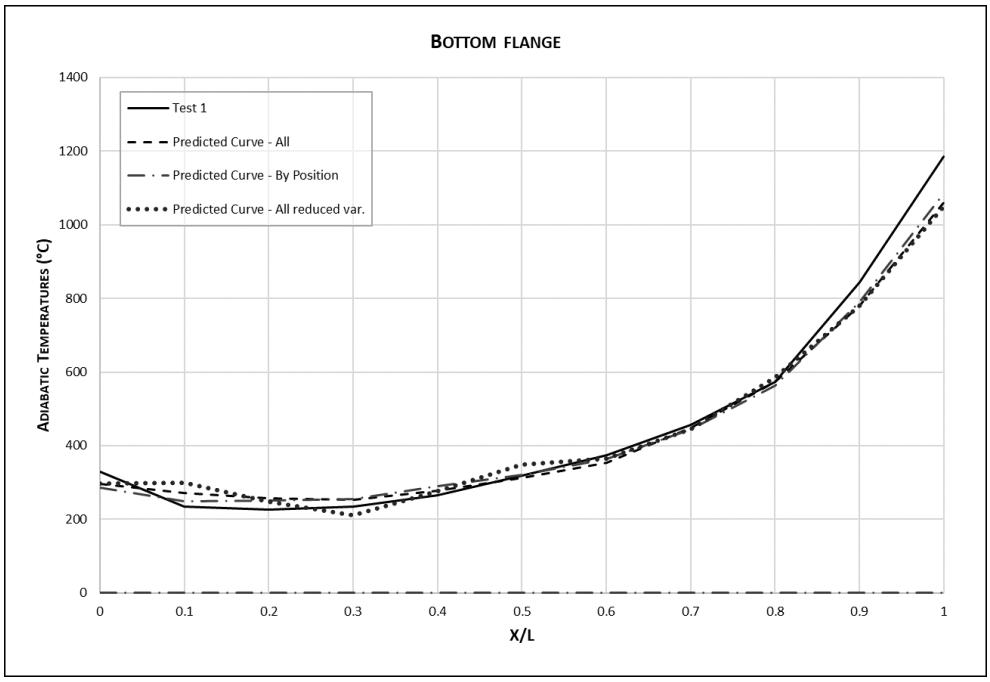

Figure 55. Design fire curve comparison for the bottom flange of test model 1

The fit of the design fire curves for the first test model is very good, with the errors between the measured adiabatic temperatures in the FDS model and those predicted being relatively small (maximum deviations of around 10%), and comparable with those obtained for initial sixty-four models.

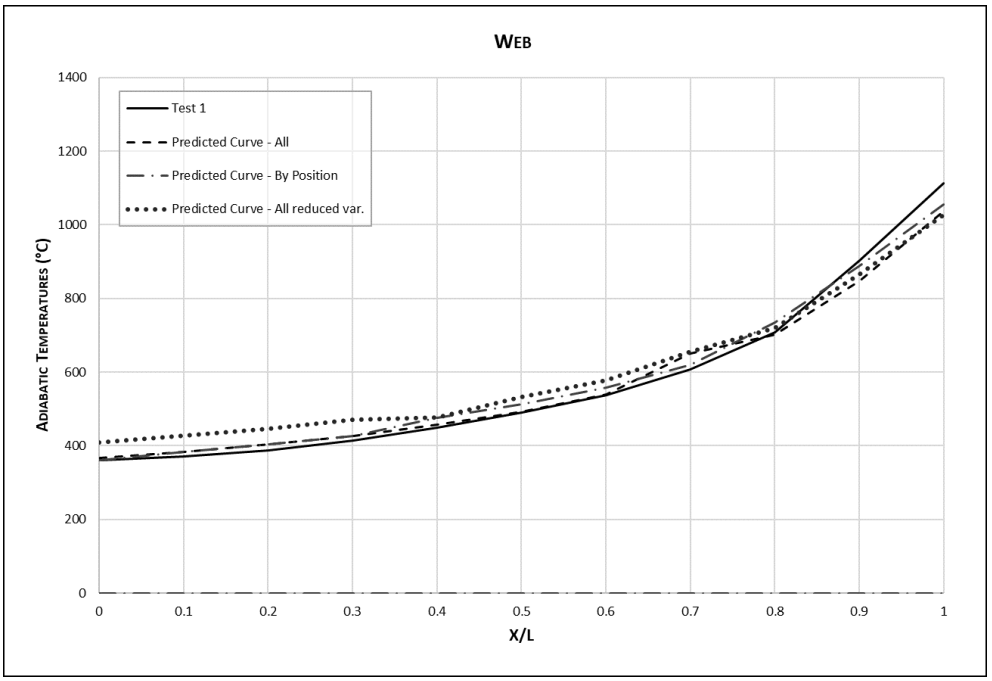

Figure 56. Design fire curve comparison for the web of test model 1

In the case of the web predictions, the prediction virtually matches the results obtained in the FDS analysis, with a small deviation being observed for the maximum temperature located adjacent to the abutment.

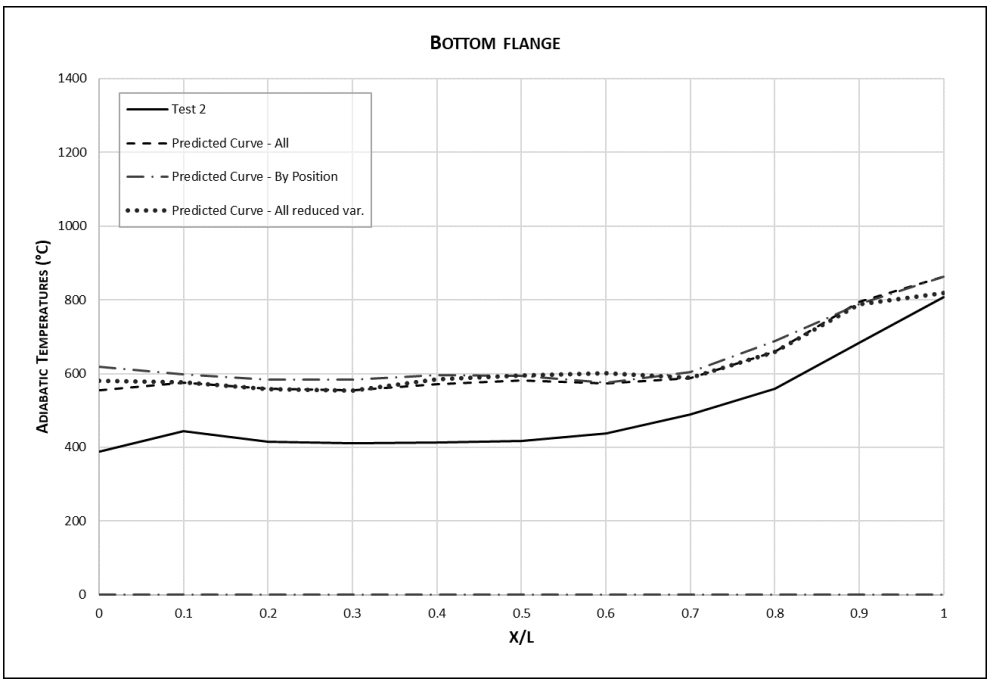

Figure 57. Design fire curve comparison for the bottom flange of test model 2

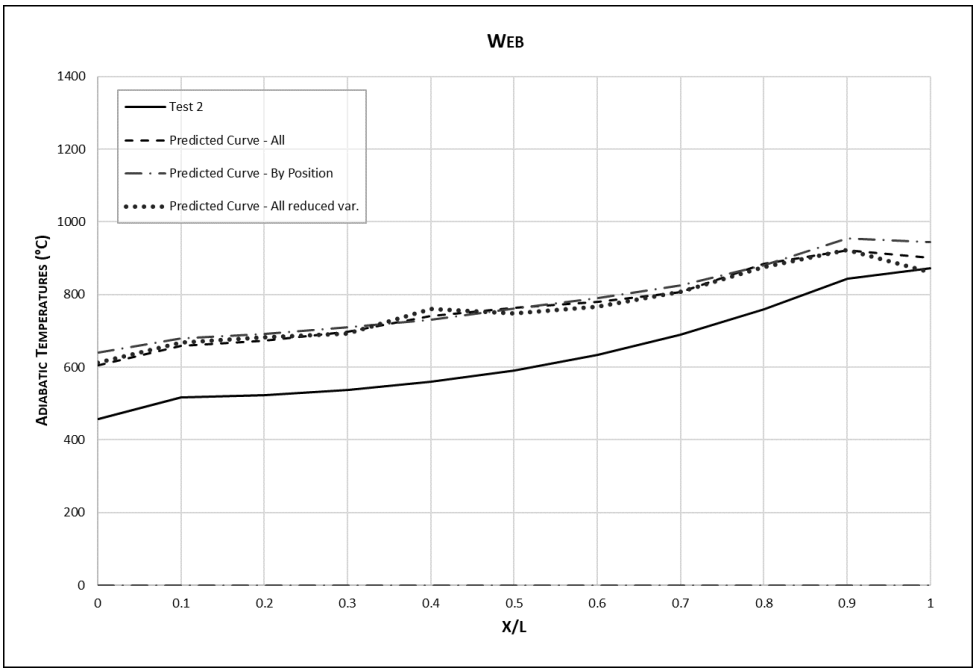

Figure 58. Design fire curve comparison for the web of test model 2

In the case of test model 2, the maximum temperature is correctly predicted, but for the rest of positions, there is a tendency to overestimate the adiabatic temperatures by up to 200 ^{o}C. The overestimation observed has been determined to relate to the influence of the width on bridges with reduced spans, and as in most cases this interaction was considered nonsignificant, it was not included in the prediction equations.

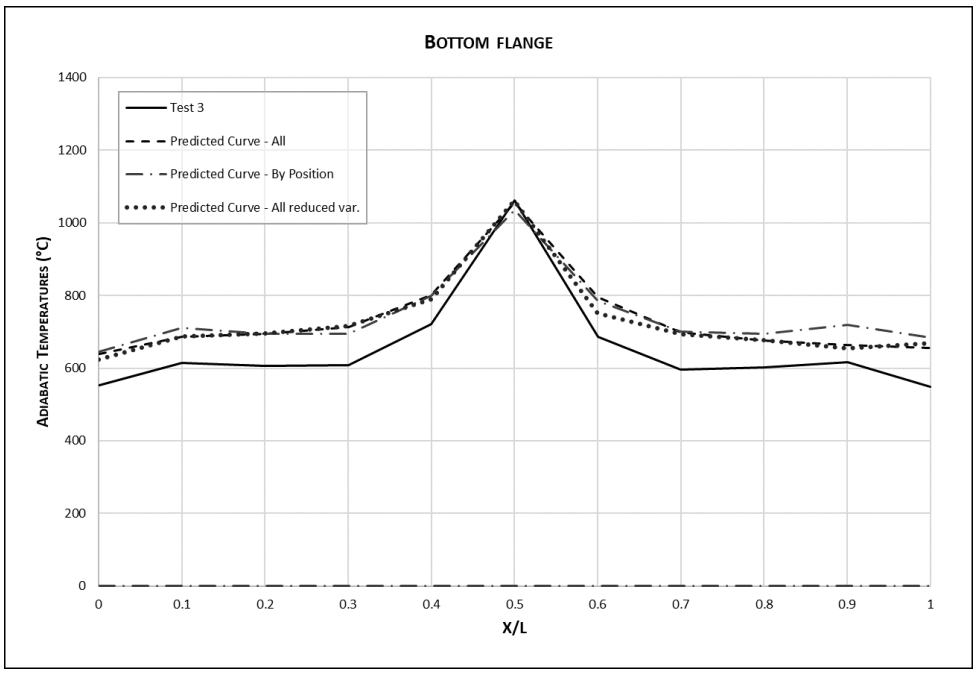

Figure 59. Design fire curve comparison for the bottom flange of test model 3

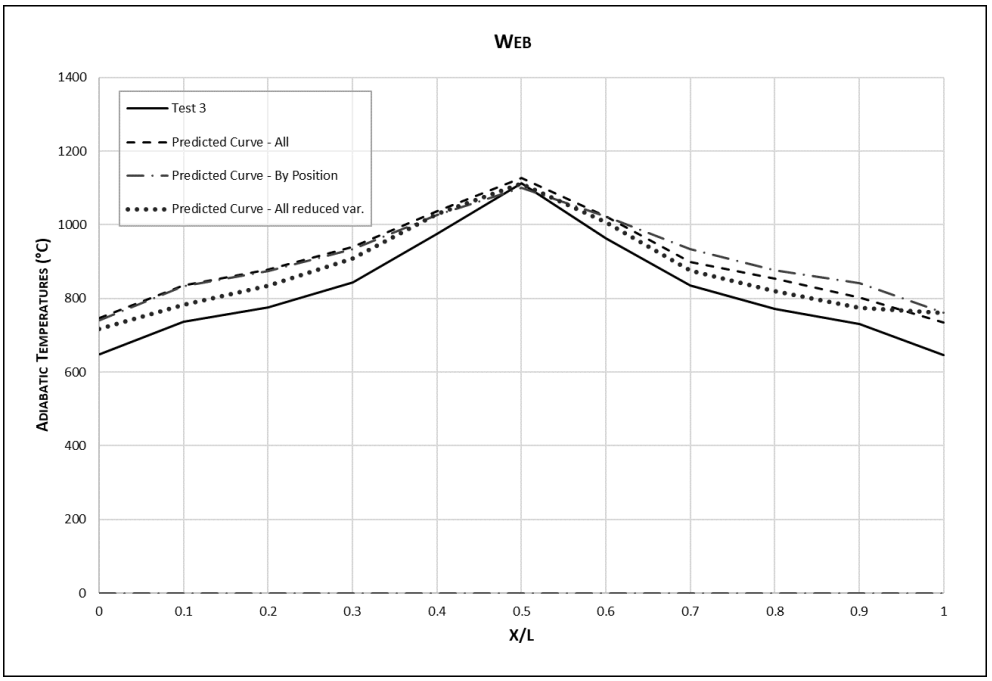

Figure 60. Design fire curve comparison for the web of test model 3

The prediction for test model 3 is an overall good fit, with the maximum temperatures once again being predicted with a high level of accuracy (deviations of under 2%), whilst the deviation for the rest of positions is at maximum 15%.

The analysis of the three test models shows that the further from the fire location a relative position is, the more complicated it is to accurately predict its adiabatic temperatures as a function of the studied parameters and interactions. This is due to the high number of parameters and interactions than can be considered significant for these positions (generally, width and span, and their respective interactions, are more significant further away from the fire source).

Even so, in general, the design fire curves offer a reasonable approximation to the measured fire curve, and with the appropriate factor of safety applied, they could be guaranteed to be an upper bound estimation.

In the following section, the design fire curves will be applied to an existing overpass on U.S. Route 1, in Trenton, New Jersey, U.S.A., comparing not only the accuracy of the fire curves, but also the effect of possible deviations on the thermomechanical response of the bridge's superstructure.

7. CASE STUDY OF AN OVERPASS ON U.S. ROUTE 1

7.1. DESCRIPTION

In this section, the design fire curves developed using multiple linear regression models will be applied to an existing bridge on U.S. Route 1, in Trenton, New Jersey, U.S.A., comparing the adiabatic temperatures obtained with those measured in the corresponding FDS models developed for the present case study.

The selected bridge is an overpass that allows Broad St. to cross over U.S. Route 1 in the city of Trenton (NJ, USA), and is located approximately seven hundred metres northbound of the Delaware River Joint Toll Bridge.

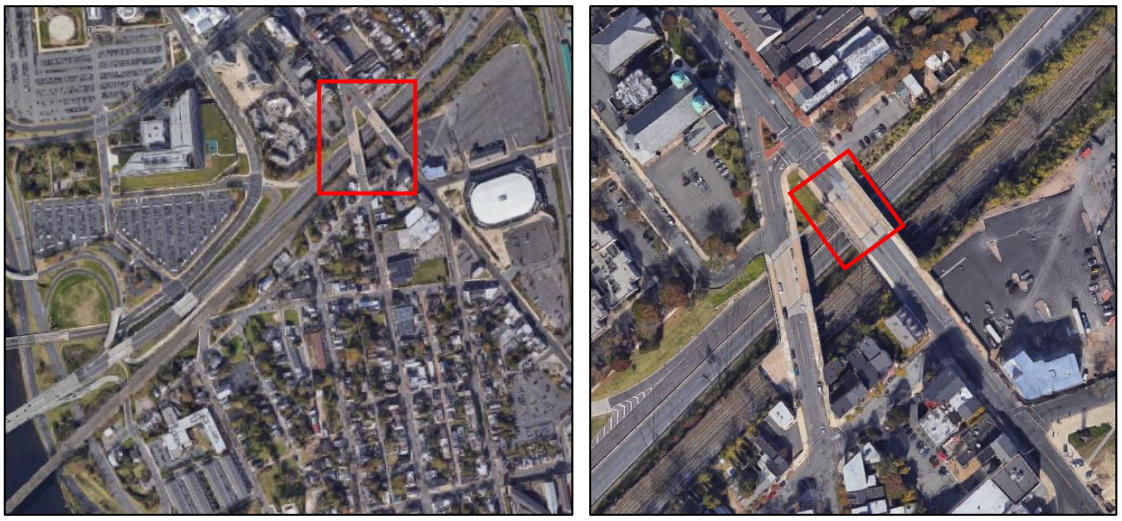

Figure 61. Location of selected bridge on U.S. Route 1, in Trenton, New Jersey, U.S.A. Source: Google Maps.

The overpass carries four lanes of traffic (two in each direction) and two pedestrian walkways, with a further four lanes of traffic passing underneath the bridge.

According to National Bridge Inventory (NBI) summary report from 2018 [8], the bridge has a main span of 23.4 metres (77 ft), a width of 21.8 metres (71.5 ft) and a vertical clearance of 5.18 metres (17 ft). It was built in 1952 and is privately owned by the State Toll Authority.

Figure 62. Southbound view of bridge from U.S. Route 1. Source: Google Street View

The superstructure is composed of steel I-girders, with a separation of approximately 2 metres (6.5 ft) between each girder (measured between axes). There are a total of five diaphragms/cross beams, located at either end of the span and at the three longitudinal quartiles, with a separation of 5.75 metres (18.9 ft).

Figure 63. Northbound view of bridge from U.S. Route 1. Source: Google Street View

The superstructure supports a concrete deck with a width of 0.2 metres (0.66 ft). The deck is not connected to the steel I-girders, and therefore this cannot be considered a composite bridge. The bridges substructures are two vertical concrete abutments at either end of the superstructure, on which the I-girders are simply supported.

Figure 64. Superstructure of bridge.

The I-girder and diaphragm cross sections have been estimated based on the observed dimensions, the bridges span and the design recommendations published by the *Federal Highway Administration* (FHWA) in 1982, with the title "*Standard plans for Highway Bridges: Volume II (Structural Steel Superstructures)*" [9]. This document includes designs of different types of bridges based on their span length and configuration, providing the dimensions of the I-girder beams and concrete deck, as well as the necessary reinforcement.

The dimensions and properties of the I-girders and diaphragm cross sections have been based on the profiles defined in the *American Institute of Steel Construction* (AISC) catalogue [10]. In the case of the I-girders, they have been defined as W-shape beams (W33x291), whilst the diaphragms/cross-beams are considered to be C-shape beams (C15x50).

In both cases, the material is considered to be ASTM A36 steel, with a minimum yield strength of 250 MPa (36,000 psi).

7.2. FDS MODELS

In this case study, the bridges dimensions (vertical clearance, span and width) as well as the bridge substructure configuration (abutments) are all defined parameters, and therefore the only parameters that can be varied to study different fire scenarios are those related to the fire position (adjacent to an abutment or mid-span), as shown in Figure 65, and the Heat Release Rate.

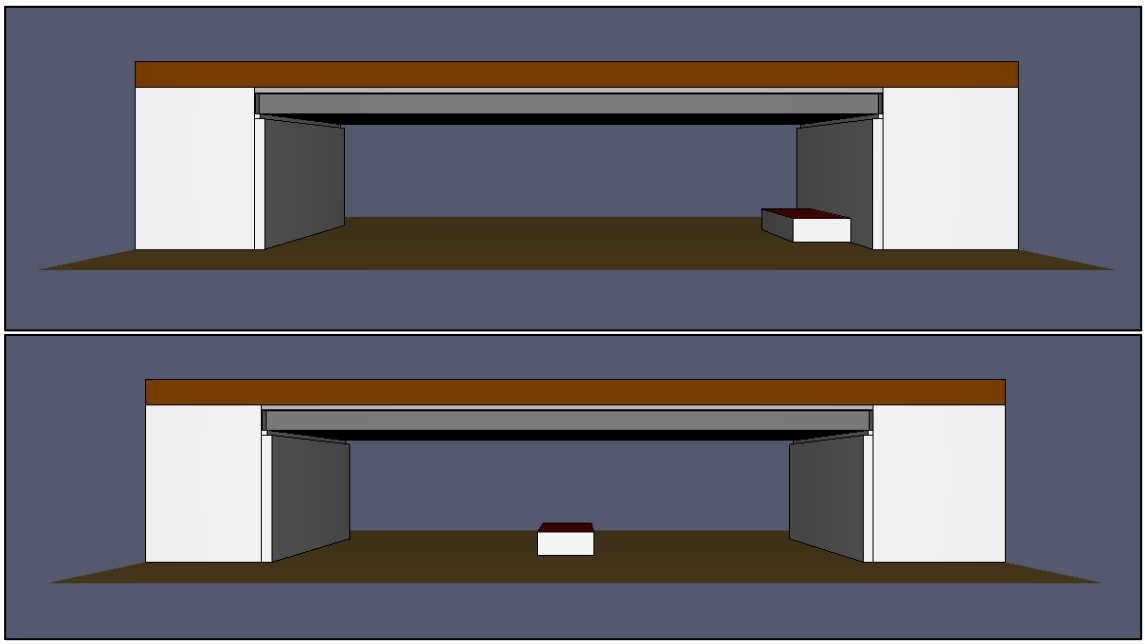

Figure 65. Fire position located adjacent to abutment (top) and mid-span (bottom).

Although the FDS models used to develop the design fire curves did not include diaphragms, in this case, in order to study the effects of these cross beams on the bridges adiabatic temperatures, two different groups of configurations will be analysed: bridges without diaphragms and bridges with diaphragms (Figure 66).

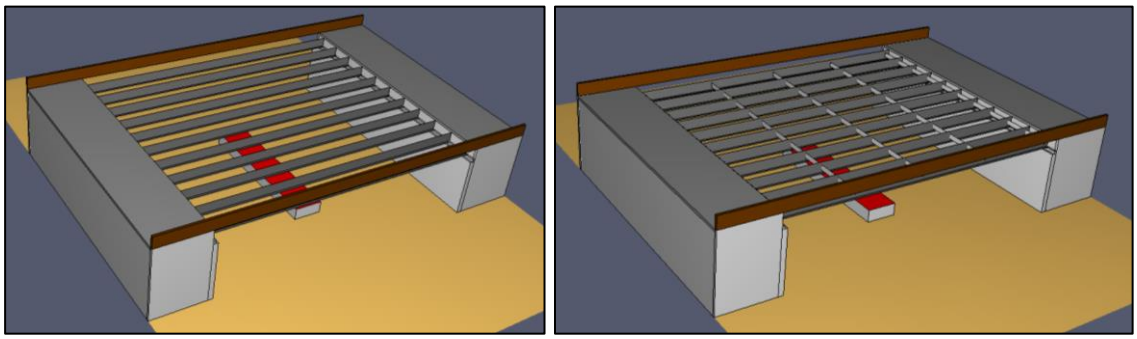

Figure 66. Bridge superstructure configuration: with diaphragms (left) and without diaphragms (right).

The configuration of the models, including the definition of the control volumes, mesh, geometry, material properties (adiabatic superstructure, nonadiabatic substructure), fire source, combustion model and sensors is described in detail in *Section 4 FDS analysis.*

In Table 34, the fire scenario configurations to be analysed are defined, including the values of each of the independent parameters, which will be used to obtain the respective design fire curves in Section 7.3.

Model	Position	Bridge Substructure Configuration	Width	Span	Vertical Clearance	HRR	Diaphragms
1a	Abument	Abutments	21.8 m	23.4 m	5.2 m	2400 kW/m2	No
2a	Mid-span	Abutments	21.8 m	23.4 m	5.2 m	2400 kW/m2	No
3a	Abument	Abutments	21.8 m	23.4 m	5.2 m	1800 kW/m2	No
4a	Mid-span	Abutments	21.8 m	23.4 m	5.2 m	1800 kW/m2	No
1b	Abument	Abutments	21.8 m	23.4 m	5.2 m	2400 kW/m2	Yes
2b	Mid-span	Abutments	21.8 m	23.4 m	5.2 m	2400 kW/m2	Yes
3b	Abument	Abutments	21.8 m	23.4 m	5.2 m	1800 kW/m2	Yes
4b	Mid-span	Abutments	21.8 m	23.4 m	5.2 m	1800 kW/m2	Yes

Table 34. FDS model configurations for the case study.

7.3. DESIGN FIRE CURVE AND FDS MODEL COMPARISON

In the following figures, the design fire curves obtained for the corresponding values of the independent parameters (Table 34) are compared to the adiabatic temperatures measured in each of the eight FDS analyses.

As stated previously, the design fire curves do not discriminate between bridges based on the presence of diaphragms, and therefore each design fire curve is compared to both corresponding FDS models (with or without diaphragms).

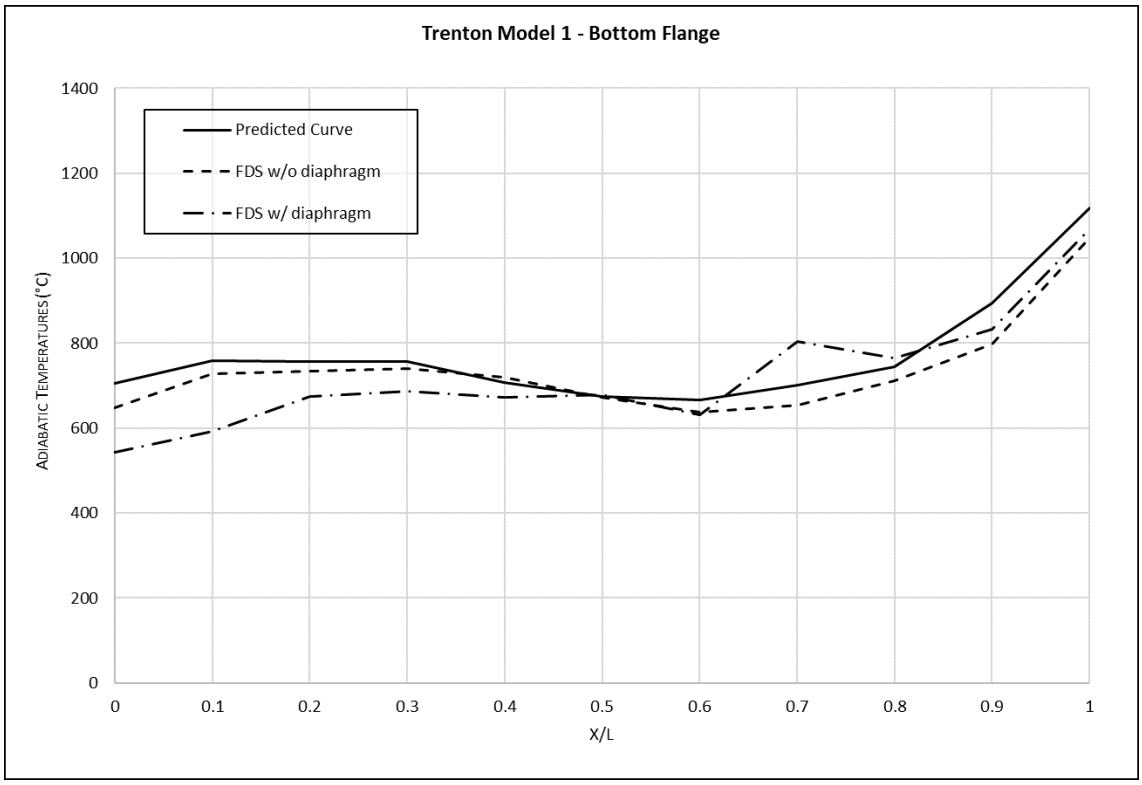

Figure 67. Design fire curve comparison for the bottom flange of case study model 1

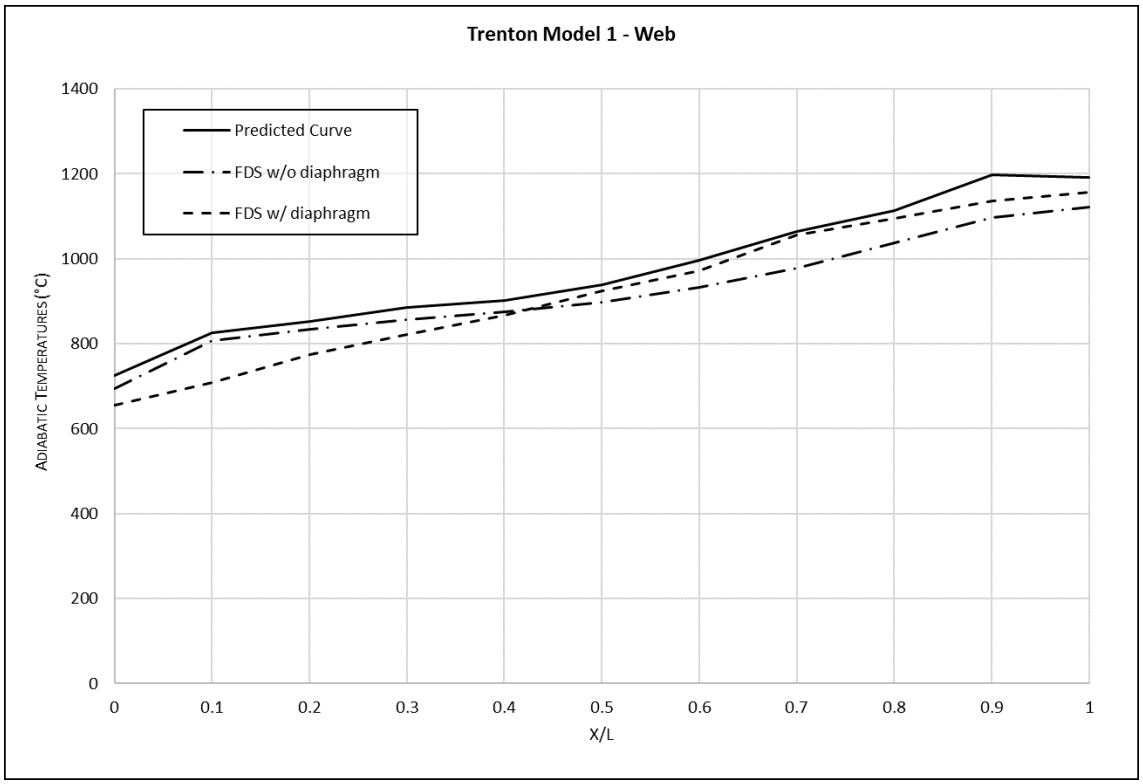

Figure 68. Design fire curve comparison for the web of case study model 1

In the case of the bottom flange design fire curve, when compared to the FDS model without diaphragms (1a), the prediction can be considered a very good fit, with both curves following a near parallel trajectory, with a slight overestimation of the design fire curve (approximately 50^{o}C). For the web adiabatic temperatures, also in the case of the FDS model without diaphragms (1a), the prediction also a very good fit, again with a generalised overestimation of approximately 75^{o}C.

Whilst in the case of the web the presence of diaphragms does not seem to have significantly altered the adiabatic temperature distribution, the same can not be said for the bottom flange, where there is a clear build up in temperatures around the position of the diaphragm located at XL=0.75 (nearest to the fire source). The diaphragms also contribute to a steeper fall in temperatures for the subsequent diaphragms (with respect to the fire source).

Therefore, it appears that the diaphragms cause a build up of hot gases/smoke near the fire source, as they are an additional obstacle for air/gas circulation, confining these into the area around the fire source. This is also the reason adiabatic temperatures are lower on the opposite end of the bridge, as the diaphragms make the propagation of hot gases/smoke from one end to the other more difficult.

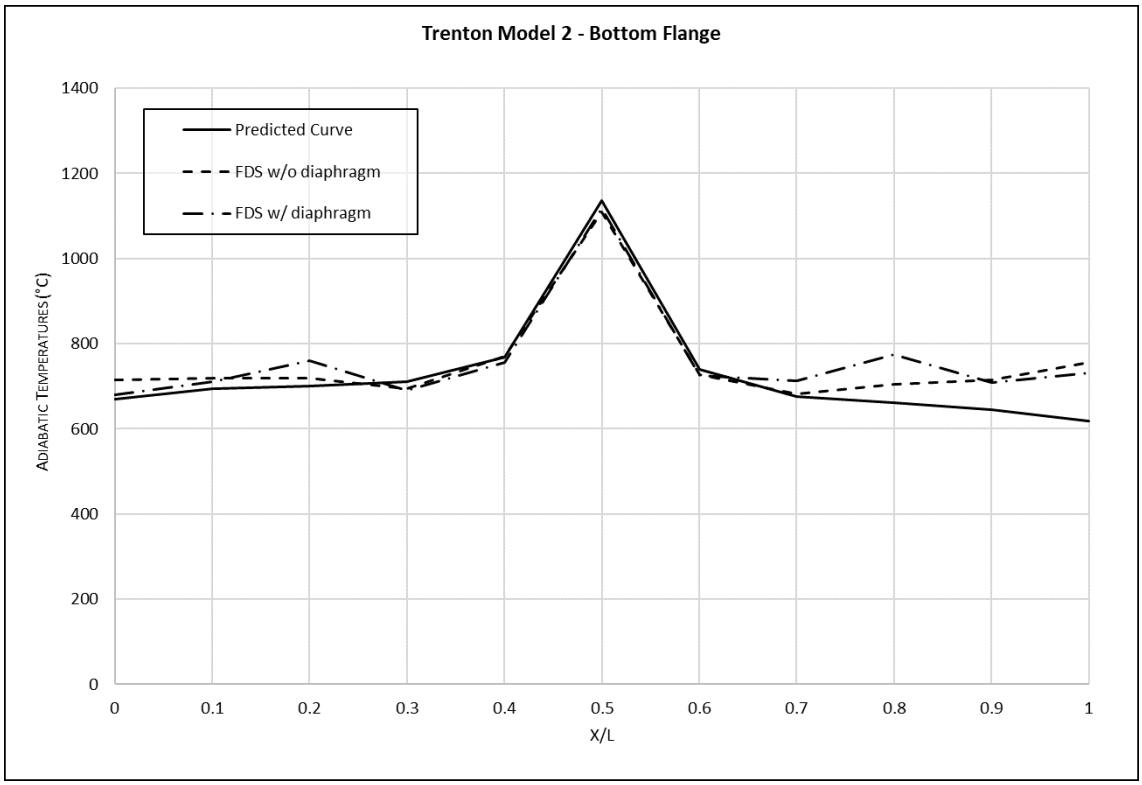

Figure 69. Design fire curve comparison for the bottom flange of case study model 2

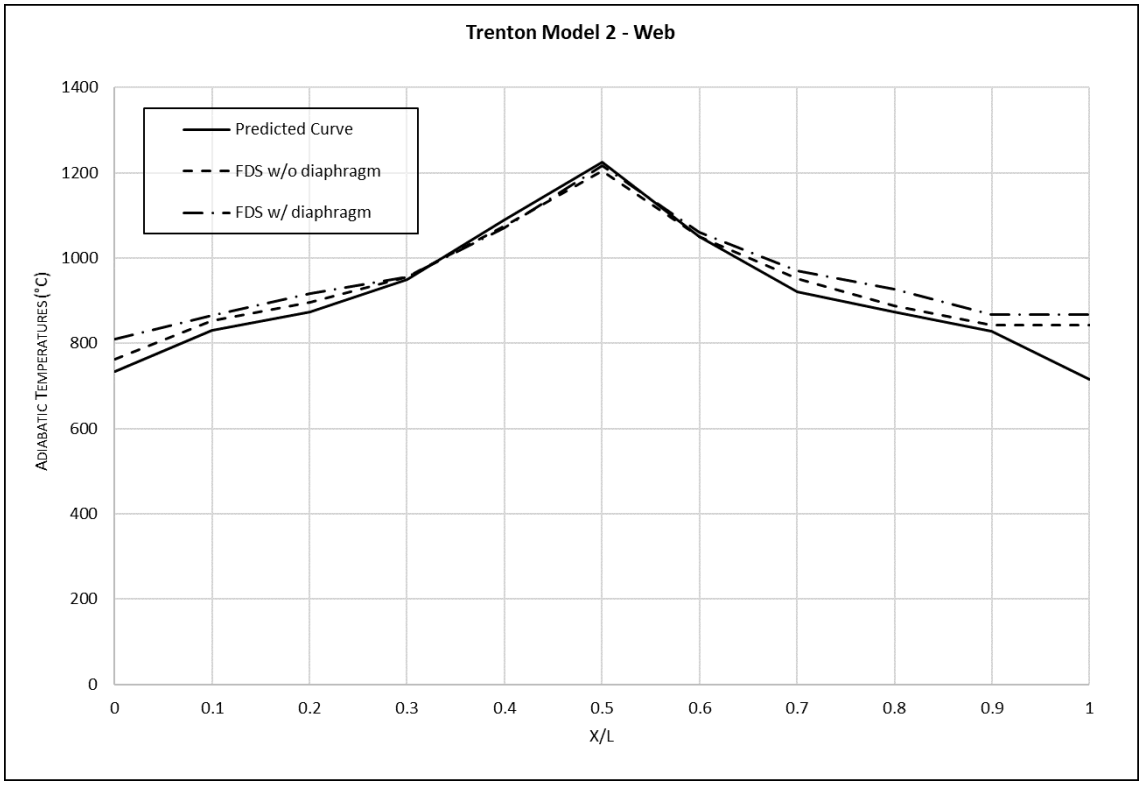

Figure 70. Design fire curve comparison for the web of case study model 2

Once again, the accuracy of the prediction of the design fire curves for the bottom flange and web adiabatic temperatures of model 2 is very high. In the case of the maximum temperatures, the prediction is practically identical to that measured in both FDS models, with a slight underestimation occurring as we near either abutment.

In this case, a similar effect is observed to that of model 1: a build-up of adiabatic temperatures in the vicinity of the diaphragms on either side of the fire source (X/L = 0.25 and X/L = 0.75) for the bottom flange, whilst the effect is virtually non-existent for the web temperatures.

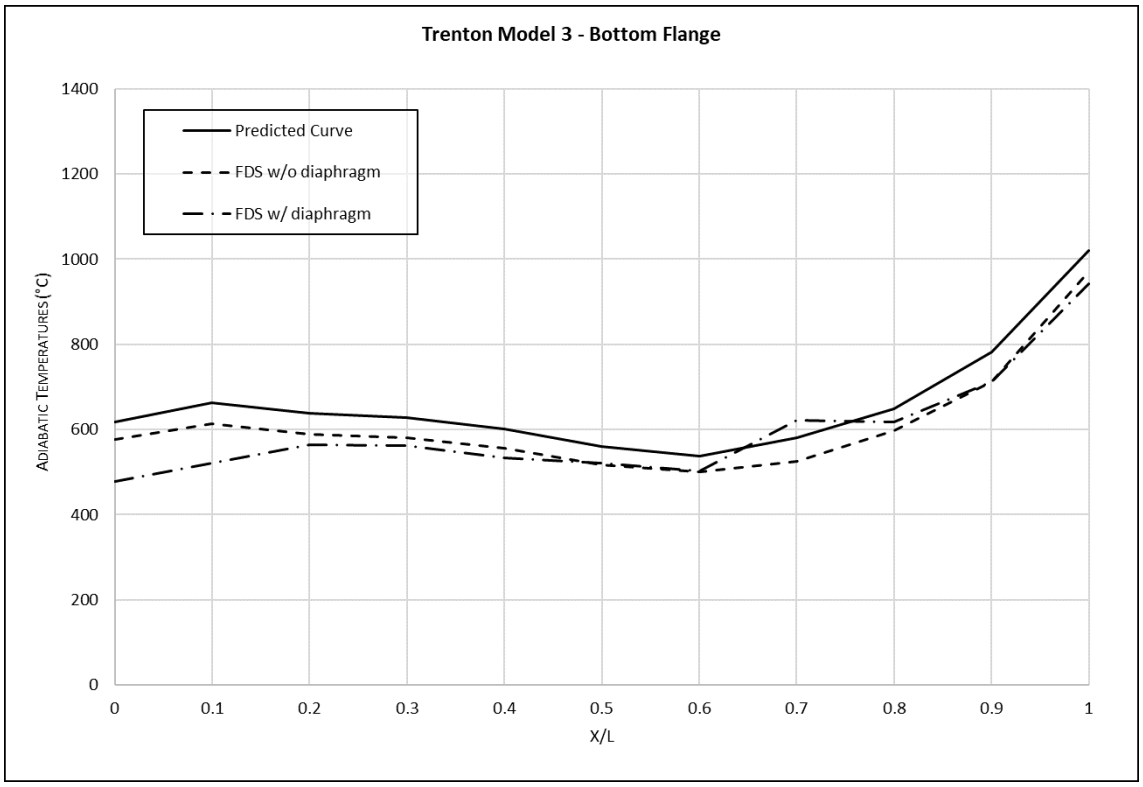

Figure 71. Design fire curve comparison for the bottom flange of case study model 3

In the case of models 3 and 4 (see Figure 71, Figure 72, Figure 73 and Figure 74), the comparison of the design fire curves and FDS models adiabatic temperatures are practically identical to those described for models 1 and two, with an overall reduction in temperatures associated with the lower Heat Release Rate assigned for these cases.

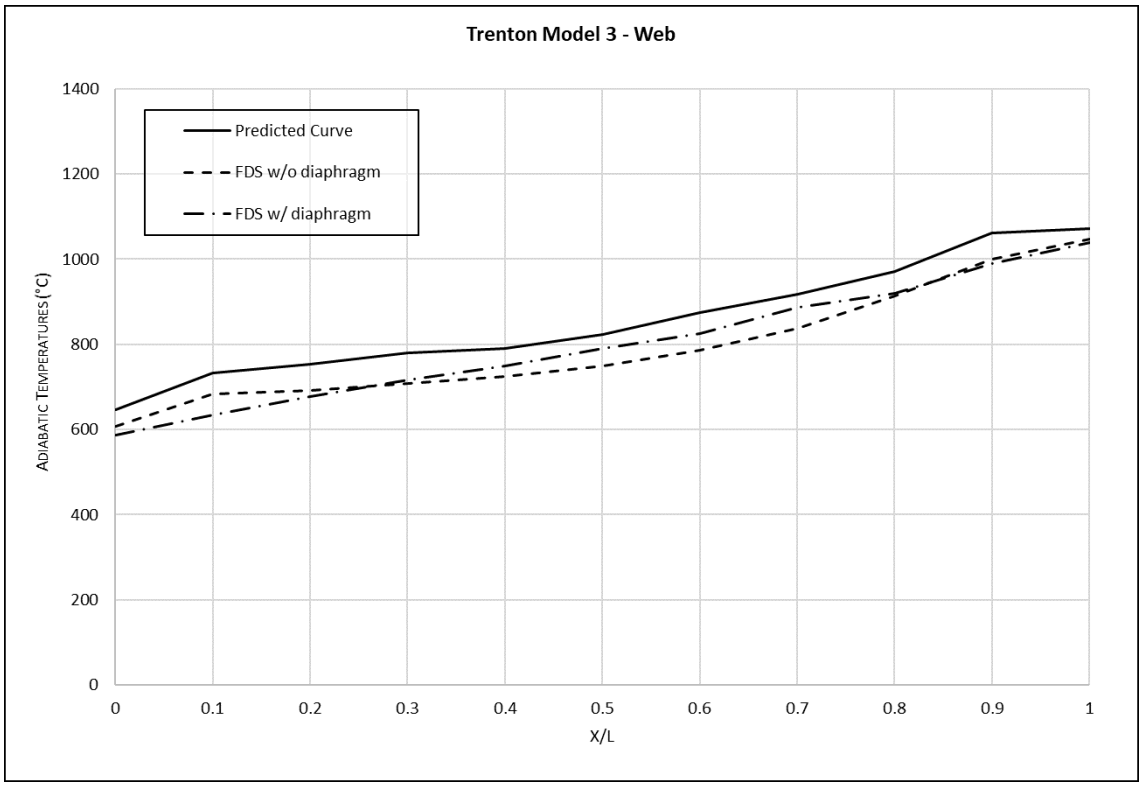

Figure 72. Design fire curve comparison for the web of case study model 3

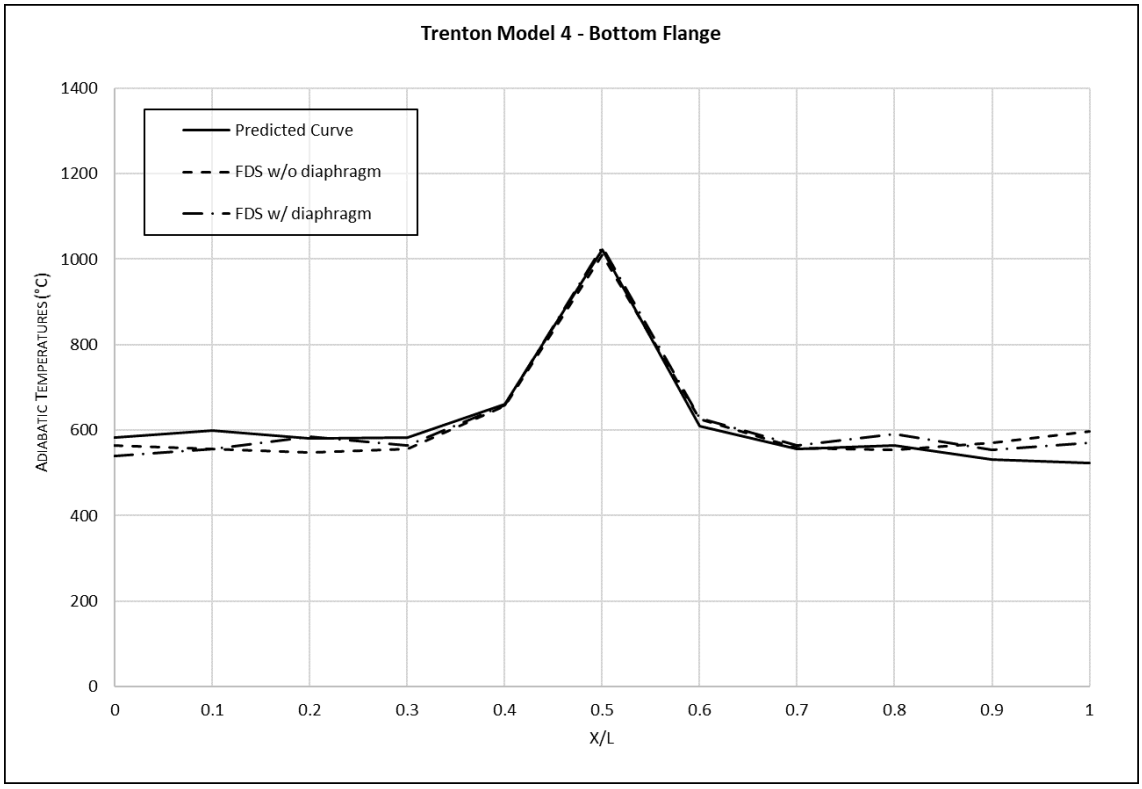

Figure 73. Design fire curve comparison for the bottom flange of case study model 4

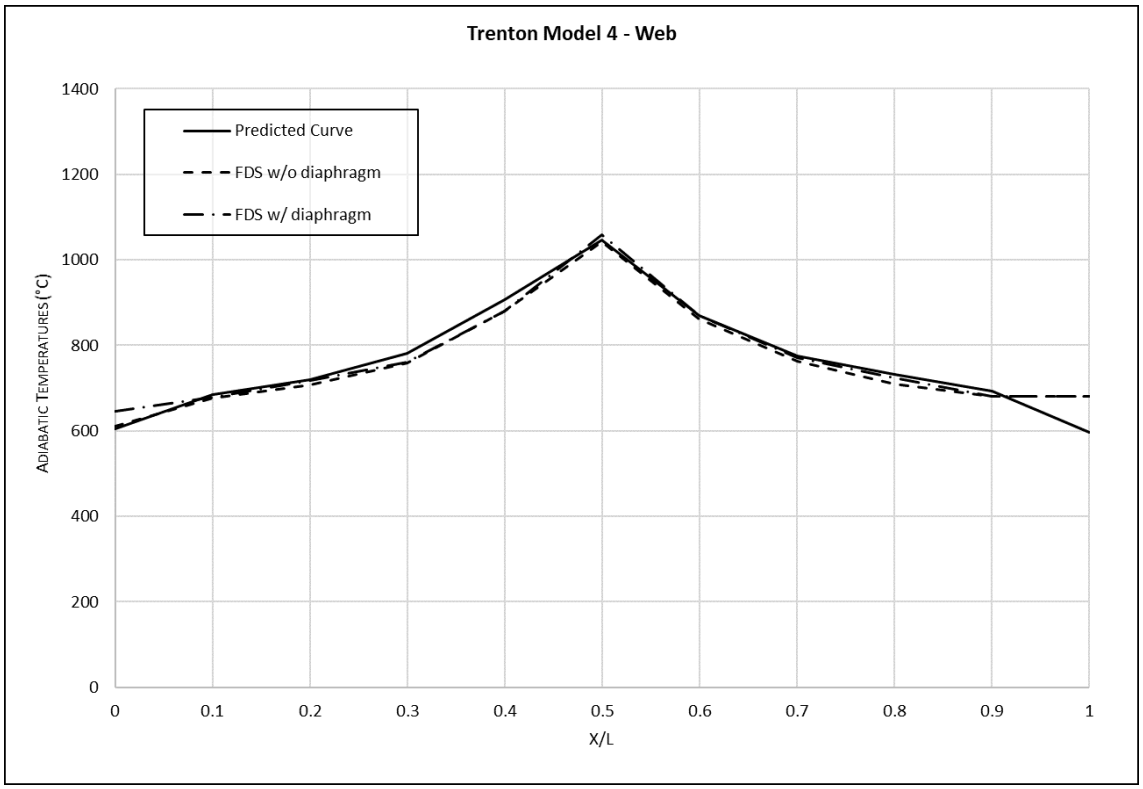

Figure 74. Design fire curve comparison for the web of case study model 4

Due to the similar nature of the adiabatic temperature curves between models with different Heat Release Rates, only models 1 and 2 (corresponding with the higher HRR, 2400 kW/m^2) will be studied using a thermomechanical analysis.

In order to determine the effect of the adiabatic temperature difference between the design fire curves and the FDS models on the thermomechanical response of the bridges central I-girder, the following section will carry out a comparison using the different temperature curves for models 1 and 2.

7.4. THERMOMECHANICAL ANALYSIS

In order to validate the design fire curves obtained from the statistical analysis, *this section* compares the thermomechanical response of an overpass on US Route 1 in Trenton, New Jersey, U.S.A. for the adiabatic temperatures obtained from an FDS analysis and those predicted by the design fire curves.

7.4.1. DESCRIPTION

The thermomechanical response of the bridge is obtained with SAFIR, version 2019.a.2, a computer program specifically written for modelling the behaviour of structures subjected to fire, for which the *Instituto de Ciencia y Tecnología del Hormigón (ICITECH)* of the *Universitat Politècnica de València* has a license.

Developed using the FORTRAN programming language, the software allows both two and three-dimensional models, using the finite element method (FEM) to find approximate solutions for very complex partial differential equations.

SAFIR is capable of obtaining the temperature field of the defined cross sections as a function of time, and additionally, the mechanical response of the structure at high temperatures takes into account thermal expansion and the reduction in strength and stiffness of the materials. This temperature field is not uniform in the whole structure, and it varies throughout the fire, and for that reason a transient analysis is carried out.

The program has predefined temperature curves, based on international codes, but also allows user to define their own time-temperature curves.

The response is calculated in two steps: the first, performs the heat transfer analysis, using the adiabatic temperatures from either the FDS model or the fire design curves, to obtain the temperature evolution of the I-girder beam taking into account the materials thermal conductivity properties; the second, uses the results of the heat transfer analysis to perform an iterative mechanical analysis, using the modified material properties for each time step corresponding with the calculated temperatures.

Due to the difficulty of working directly with the FORTRAN programming language that SAFIR uses, the models are defined using the GiD pre-processor (v14.1.0d), which allows FEM models to be defined using an initiative graphical user interface. GiD generates the necessary files for the SAFIR calculations and can then be used to view the results of the thermomechanical analyses.

7.4.2. SAFIR MODELS

The cross section of the bridges I-girders (W33x291) are defined in GiD, and the material is defined as ASTM A36 steel with a minimum yield strength of 250 MPa, a Poisson's ratio 0.3 and a Young modulus of 210.000 MPa.

The program includes the predefined steel models based on EN 1993-1-2, which includes the definition of steels specific heat, thermal conductivity, thermal expansion and constitutive equations.

In Figure 75, the assigned thermal frontier constraints and cross section discretization are shown. Each frontier constraint corresponds to either the predicted/measure bottom flange (green) or web (red) adiabatic temperatures.

These frontiers are is where heat will be exchanged between the cross section and the defined adiabatic temperatures. The top flange's upper side is considered to be an adiabatic surface, as it is shielded from the fire by the concrete deck.

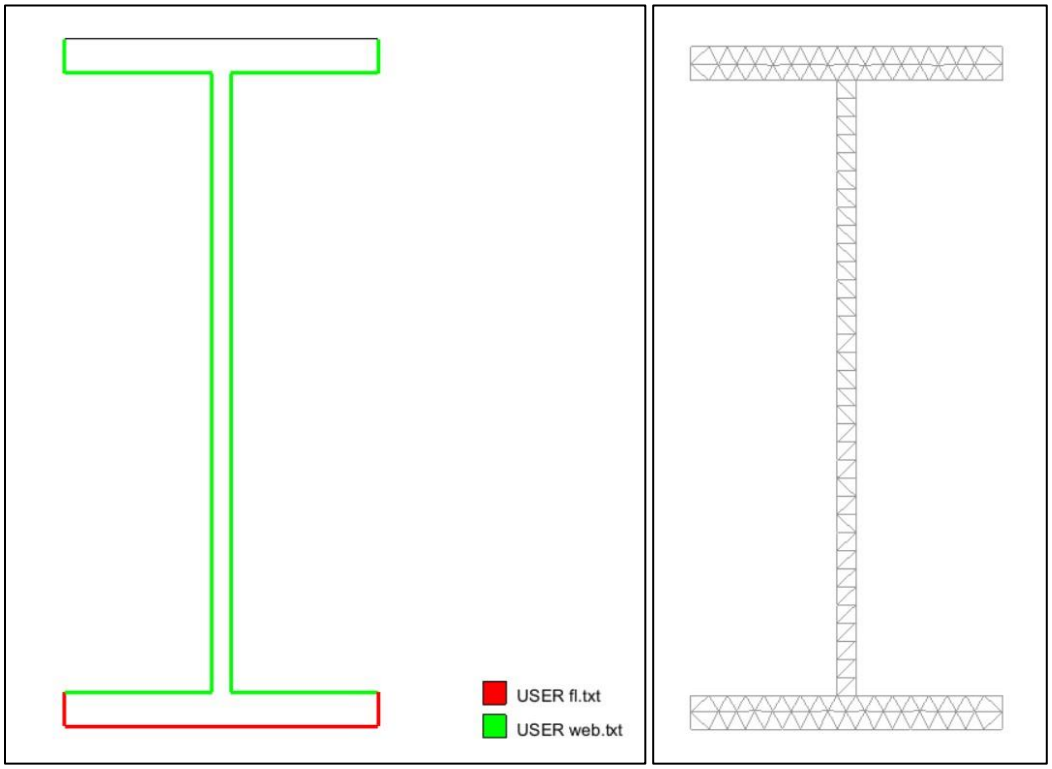

Figure 75. Cross-section frontier constraints and mesh discretization.

The adiabatic temperatures applied to the frontier constraints are considered to reach their maximum temperatures in ten seconds, following a linear increase during this period. After, these temperatures are considered constant for the duration of the analysis.

This temperature curve is used in the heat transfer analysis, based on the adiabatic temperatures from either the FDS model or the fire design curves, to obtain the temperature evolution of the I-girder beam taking into account the materials thermal conductivity properties.

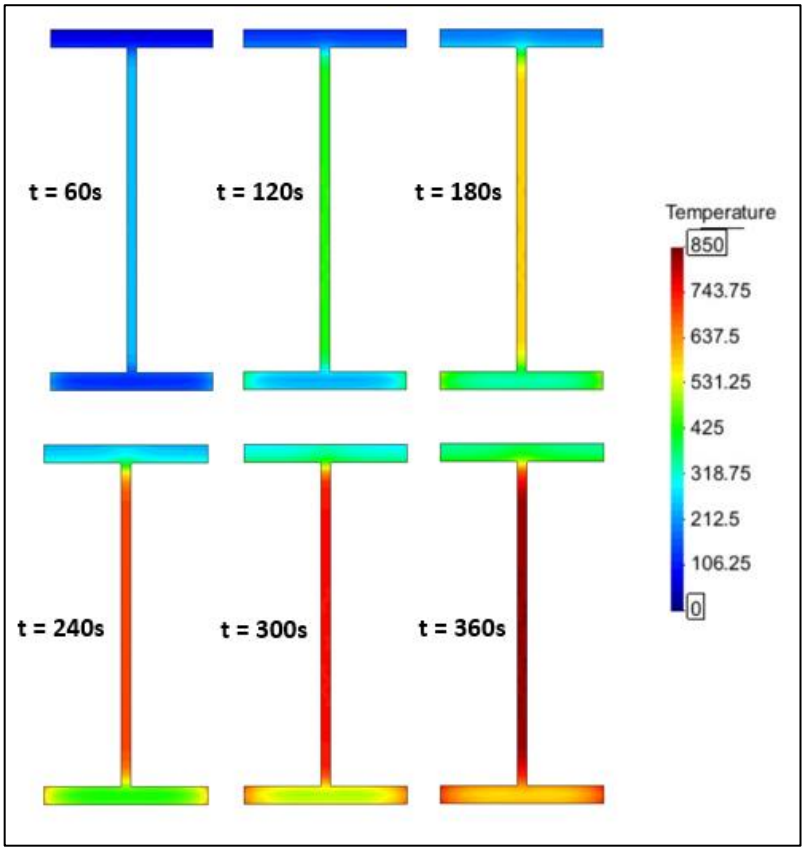

Figure 76. Example of the heat transfer analysis for model 1 at X/L = 1.

Once each of the individual heat transfer analyses has been carried out (one for each relative position, a total of eleven each for the bottom flange and web, meaning a total of 22 analyses per model), they are defined onto the longitudinal I-girder model, depending on their relative position.

As can be seen in Figure 77, a total of eleven different heat transfer models are defined for each mechanical model, with the adiabatic temperatures of X/L = 0 and X/L= 1 being applied to 1/20L at either end, and the remaining adiabatic temperatures, X/L = 0.1 through to X/L = 0.9, being applied to 1/10L of the model, centred on their corresponding relative positions.

Figure 77. Definition of individual heat transfer models for each of the relative positions of the fire curve.

The loads considered during the mechanical analysis are the following:

- Dead weight of the I-girder beam: 4.25 kN/m
- Dead weight of the concrete deck, considering the separation between adjacent I-girders (2 metres): 10 kN/m
- Dead weight of the road pavement: 3.22 kN/m

The live loads corresponding to traffic and other temporary loads have not been included in the analysis, as according to Peris-Sayol et al. [1] , they do not have a significant effect on the mechanical response of the structure during a fire and they are unlikely to be present during one.

Finally, the mechanical model constraints are defined as follows:

- Fix: both supports have their x and y movements constrained.
- Free: both supports have their y movements constrained, whilst only has the x movement constrained, allowing the free thermal expansion of the model.

Although Peris-Sayol et al. concludes that the actual behaviour of the longitudinal I-girders is neither fixed or free, due to the thermal expansion of the I-girders, which causes them to reach the abutments, constraining further expansion, the current reports objective is to compare the relative effect of the design fire curves to the temperatures measured in the FDS analyses, and therefore the fix and free scenarios are considered sufficient.

7.5. RESULTS

The following figures show the mechanical response of the I-girder during the different fire scenarios considered (calculated from their corresponding heat transfer analysis, which is used to determine the material properties of the I-girders during the fire).

In Figure 78 and Figure 79, the mid-span deflection of model 1 and 2 are plotted, depending on whether the temperatures considered were from the FDS analysis or the design fire curves, and for the two support constraint scenarios defined above (fixed or free horizontal expansion).

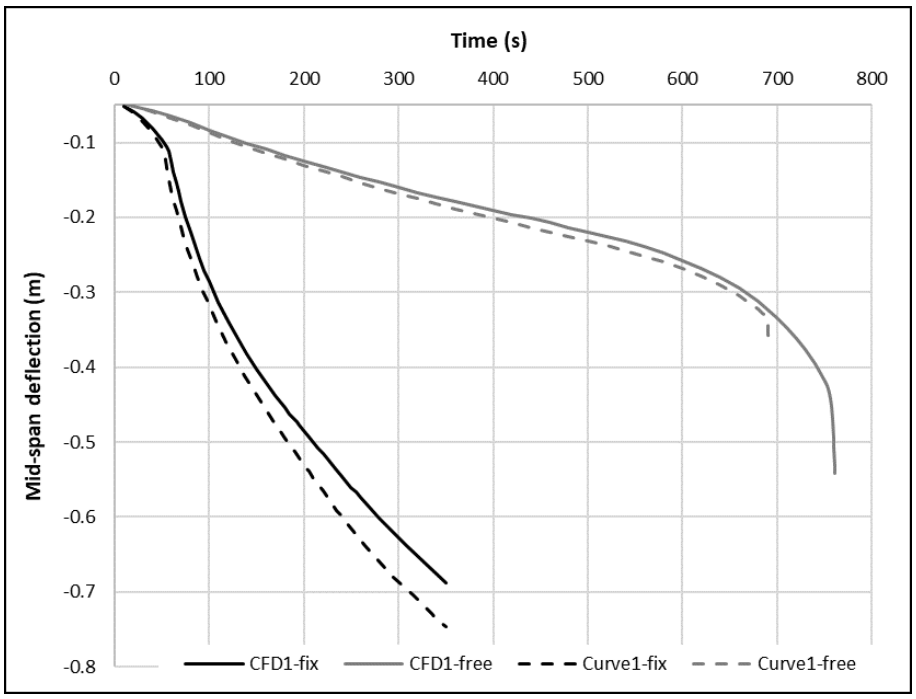

Figure 78. Mid-span deflection for the thermomechanical analyses of model 1, for the different fire (FDS or design fire curve) and constraint (fixed or free thermal expansion) scenarios.

As can be seen, in the case of a free longitudinal thermal expansion, deflection linearly increases until the section reaches its minimum yield strength, after which the deflection rapidly increases.

The models with thermal expansion impeded (fixed), reach the minimum yield strength a lot faster, as the tension produced by this impeded dilatation causes a faster increase in the I-girders deflection.

Finally, when comparing the models that use adiabatic temperatures obtained from the FDS analyses to those obtained from the design fire curves, it can be observed that the mechanical response is practically identical in both cases. The slightly higher adiabatic temperatures

predicted by the design fire curves cause very little difference to the structural response of the I-girder.

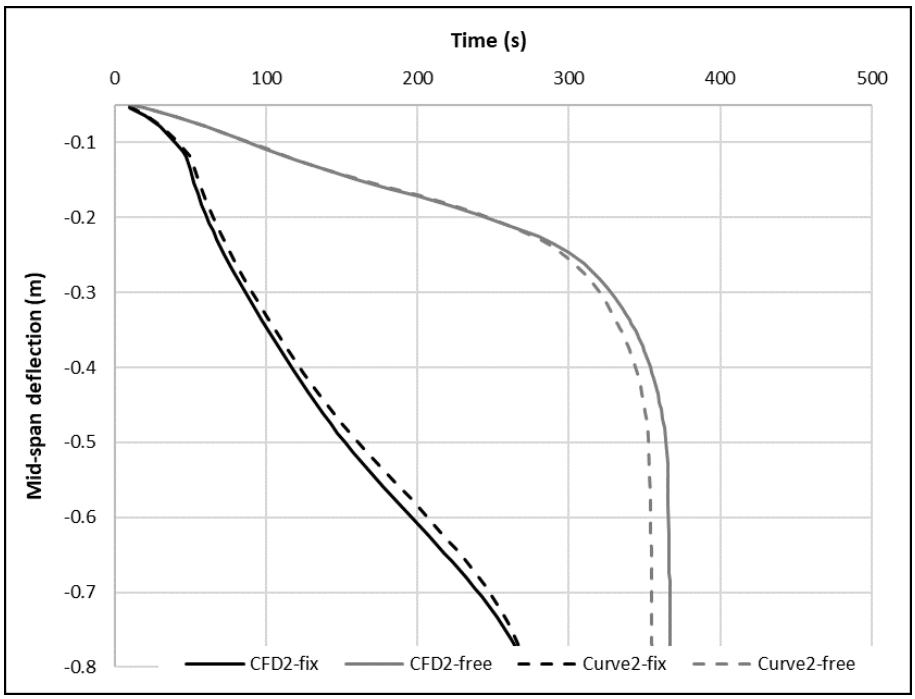

Figure 79. Mid-span deflection for the thermomechanical analyses of model 2, for the different fire (FDS or design fire curve) and constraint (fixed or free thermal expansion) scenarios.

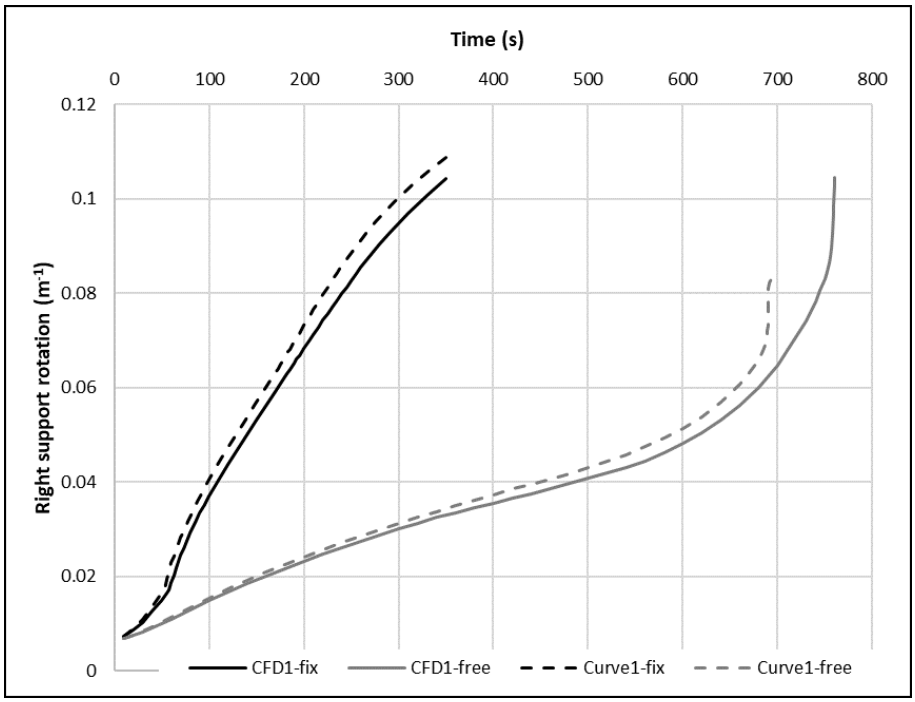

Figure 80. Support rotation for the thermomechanical analyses of model 1, for the different fire (FDS or design fire curve) and constraint (fixed or free thermal expansion) scenarios.

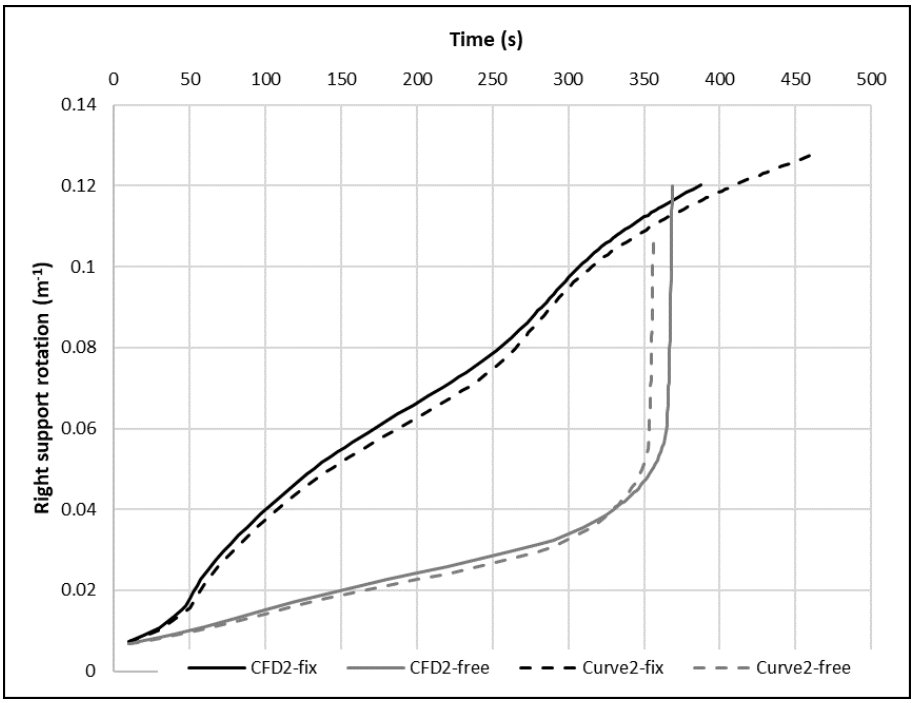

Figure 81. Support rotation for the thermomechanical analyses of model 2, for the different fire (FDS or design fire curve) and constraint (fixed or free thermal expansion) scenarios.

The results for the rotation of the right support are shown in Figure 80 and Figure 81, for the adiabatic temperatures measured from the FDS analysis or predicted using the design fire curves, and for the two support constraint scenarios defined above (fixed or free horizontal expansion.

In the case of models with longitudinal expansion fixed, the rotation increases a lot quicker than those that consider this movement not to be impeded, with a similar behaviour of that observed for the mid-span deflection occurring in each case.

Finally, once again the differences observed between the models pertaining to the FDS adiabatic temperatures and the design fire curves are virtually insignificant, with each pair of models reaching similar rotations at virtually the same time.

It appears that small differences observed in the prediction of adiabatic temperatures using the design fire curves are attenuated even more when comparing the results of the mechanical analysis, and therefore, with the possible application of a factor of safety, the design fire curves can be considered as an acceptable substitute for FDS models when analysing girder bridges.

8. CONCLUSIONS

This report has developed a proposal of design fire curves for I-girder bridges, based on an analytical approach of first studying the significance of different parameters influence on adiabatic temperatures, and then using multiple linear regression techniques to obtain predictive equations for these temperatures, based on the relative position studied, as a function of the analysed independent parameters.

The adiabatic temperatures used to carry out this statistical analysis have been obtained in a total of sixty-four FDS analyses. In these analyses, the bridges superstructure was defined using adiabatic surfaces, meaning that the temperatures obtained are independent of the type of superstructure analysed (steel, concrete, composite, etc.), and therefore, they can be used to perform a thermomechanical analysis of a bridges superstructure, for both steel or concrete girders (or other material types).

Therefore, the design fire curves proposed have wide applications, and are not just limited to steel superstructures like the one used to validate the model. Some remaining questions that require further work are proposing methods for estimating adiabatic temperatures on non-central I-girder beams, determining the influence of other parameters not included in the main analysis, and proposing strategies and passive measures to counteract the effects of bridge fires.

9. REFERENCES

[1] Peris-Sayol G, Payá-Zaforteza I, Alós-Moya J, Hospitaler-Pérez A. (2015). *"Analysis of the influence of geometric, modeling and environmental parameters on the fire response of steel bridges subjected to realistic fire scenarios"*. Computers & Structures, Volume 158, (1 October 2015), Pages 333–345. DOI:10.1016/j.compstruc.2015.06.003

[2] K. McGrattan, S. Hostikka, R. McDermott, J. Floyd, C. Weinschenk y K. Overholt, *"Fire Dynamics Simulator: Technical reference guide Volume 3: Validation"* NIST Special Publication 1018-3, Gaitherburg, Maryland, USA, 2016.

[3] J. Alós-Moya, I. Payá-Zaforteza, M. Garlock, E. Loma-Ossorio, D. Schiffner y A. Hospitaler, *"Analysis of a bridge failure due to fire using computational fluid dynamics and finite element models"* Engineering Structures, vol. 68, pp. 96-110, 2014.

[4] U. Wickström, D. Dat Duthinh y K. McGrattan, *"Adiabatic Surface Temperature for Calculating Heat Transfer to Fire Exposed Structures"* de Interflam, 2007.

[5] Peixoto, Julio L. "*Hierarchical Variable Selection in Polynomial Regression Models."* The American Statistician, vol. 41, no. 4, 1987, pp. 311–313. JSTOR, www.jstor.org/stable/2684752.

[6] Peixoto, Julio L. *"A Property of Well-Formulated Polynomial Regression Models."* The American Statistician, vol. 44, no. 1, 1990, pp. 26–30. JSTOR, www.jstor.org/stable/2684952.

[7] Montgomery, D. C., Myers, R. H., Carter, W. H. and Vining, G. G. (2005), "*The Hierarchy Principle in Designed Industrial Experiments*." Qual. Reliab. Engng. Int., 21: 197-201. doi:10.1002/qre.615

[8] Bridge Summary Report (2018) - Structure Number 3300027 - National Bridge Inventory (NBI) - https://infobridge.fhwa.dot.gov/Data/BridgeDetail/20860373

[9] American Association of State Highway and Transportation Officials (AASHTO), LRFD Bridge design specifications, Washington D.C, Estados Unidos: AASHTO, 2012.

[10] American Institute of Steel Construction, 13th Edition AISC Steel Construction Manual, Estados Unidos: AISC, 2005.

[11] Romero-Villafranca, R., Zúnica-Ramajo, L.R. (2005) *"Métodos estadísticos en ingeniería"*. Editorial UPV. Ref. editorial: 637